SYNTHESIS AND RADIOIODINATION OF NICOTINIC ACID ANALOGUES

A. MANSOURI*, H. ALI*, D.GUILLOTEAU** and J.E. VAN LIER*****

*Laboratoire des Radiopharmaceutiques, C.D.T.N.
2, Bd Frantz Fanon, BP 1017 Alger-gare, Algerie.
**Laboratoire de Biophysique Médicale, U316, 2 Bis,
Bd Tonnellé, 37042 Tours Cedex, France.
***Département de Médecine Nucleaire et Radiobiologie,
Université de Sherbrooke, Québec, J1H 5N4, Canada.

The aim of the present work is the synthesis and the identification of radioiodinated nicotinic acid analogues capable to cross the blood-brain barrier for a possible brain imaging.

The 5 - bromonicotinic acid was synthesized analogously,to the method described by Bachman and Micucci.The 5 - bromonicotinic acid was acylated with thionyl chloride and the product obtained was reacted with the appropriate amine to give 5 - bromonicotinic acid alkyl amide. However the subsequent reduction step, using 1M borane - dimethylsulfide, gave 5 - bromonicotinic acid alkylamine according to the method of Brown and Helm with slight modifications.

After purification, high performance liquid chromatography (HPLC) was performed on μbondapack C-18 (25 x 0,94cm) column. The compounds were eluted with acetate buffer / methanol (80:20) at a flow rate of 1ml / min. and were detected at 254 nm. The Melting point, IR, UV-visible and mass spectral data were used to confirm the structure of these compounds.

Radioiodination and identification of the labelled compounds were done according to the procedures reported for 5 - [^{125}I] iodonicotine via a halogen exchange method modified from Hawkins et al, and Carlsen and Andresen. The radiochemical yields of these compounds

are determined by thin layer chromatography (TLC) using different solvant systems.

The biodistribution of these radioiodinated compounds will be realised on animals in the future.

REFERENCES

1 - M.A. GHAFFARI,H. ALI, J. ROUSSEAU and J.E. Van LIER - 7 th international symposium on radiopharmaceutical chemistry, Groningen, The Netherlands, 4 - 8 july, 1 (1988)
2 - G.B. BACHMAN and D.D. MICUCCI - J. Am. Chem. Soc. 70 : 2381 (1984)
3 - J.Thompson WAYNE and John GAUDINO - J. Org. Chem. 49 : 5237 (1984)
4- H.C. BROWN and P. HELM - J. Org. Chem. 38 : 912 (1973)
5 - S.M. CHAN,G.P. BASMADJIAN, D.F. MARTEN,S.A. SADEK, R.A.MARGARIAN,J.R. GRUNDER and R.D. ICE - J.Label. Compds. Radiopharm. 20 : 1017 (1983)
6 - S.M. CHAN,G.P. BASMADJIAN,D.F. MARTEN,S.A. SADEK, R.A. MARGARIAN,and J.R. GRUNDER - J. Label. Compds. Radiopharm. 23 : 647 (1986)
7 - L. HAWKINS,A. ELLIOTT,R. SHIELDS,K. HERMAN,P. HORTON,W. LITTLE and C. UMBERS - Eur. J. Nucl. Med. 7 : 58 (1982),
8 - L. CARLSEN and K. ANDRESEN - Eur. J. Nucl. Med. 7 : 280 (1982)

Scheme 2 : Radioiodination of 5-bromonicotinic acid analogues with 125-Iodine.

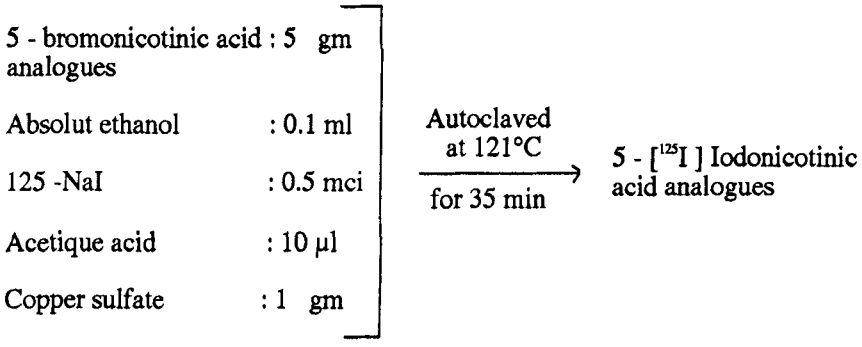

Scheme 1 : Synthesis of 5 - bromoniconitic acid analogues

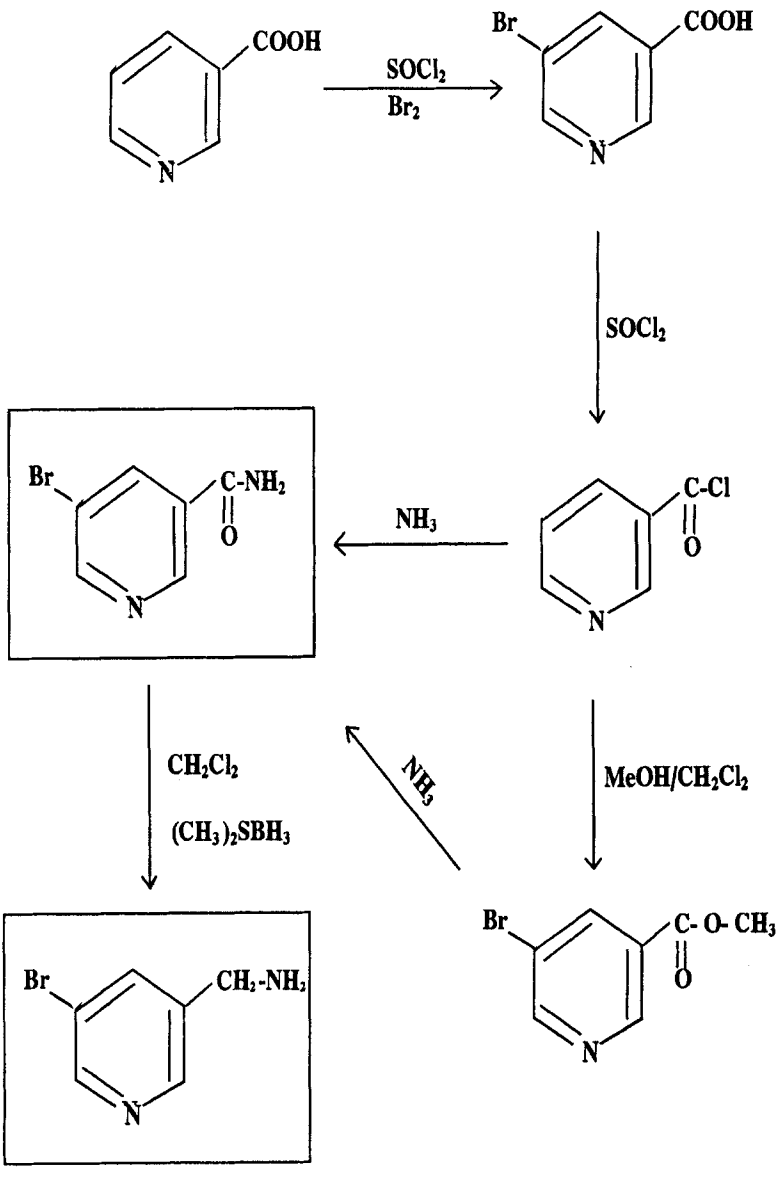

Regional Distribution of (-)-[^{11}C]Methamphetamine and (-)-3,4-Methylenedioxy-[^{11}C]Methamphetamine in a Monkey Brain: Comparison with Cocaine.

Shiue C-Y., Shiue G.G., Cornish^{+} K.G., O'Rourke^{+} M.F., and Sunderland J.J.
Center for Metabolic Imaging, Creighton University, Omaha, Nebraska 68108. $^{+}$ University of Nebraska Medical Center, Omaha, Nebraska 68198.

Cocaine, amphetamine and its analogs are the most commonly abused drugs. Although cocaine has been thoroughly studied with PET,[1-3] little is known about the pharmacokinetics and the pharmacodynamics of amphetamine and its analogs in the human brain. In order to study and compare the pharmacokinetics of amphetamine and its analogs with cocaine in the brain,we have synthesized (-)-[^{11}C]methamphetamine (2) and (-)-3,4-methylenedioxy-[^{11}C]methamphetamine (Ecstasy) (4) and compared their brain uptakes and metabolism in a monkey brain with PET. Carbon-11 labeled 2 and 4 were synthesized by methylation of (-)-amphetamine (1) and MDA (3) respectively with [^{11}C]H_3I in DMF-DMSO (4:1) at 135° C for 2 minutes followed by purification with HPLC (Phenomenex Ultremex 5 silica column, 10x250 mm, CH_3OH : NH_4NO_3 aq. buffer, 98.75:1.25, PH 9.3, 7.5 ml/min) in 40-60% yield in a synthesis time of 30 minutes from EOB (Scheme 1). Following i.v. administration, both 2 and 4 were distributed homogeneously to monkey striatum, cerebellum, cortex and temporal lobe (Figures 1 and 2). While the retention of radioactivity in these brain regions remained constant throughout the study for 2, it was washed out slowly from monkey brain for 4. Figures 1 and 2 also showed that the half-life of either 2 or 4 in monkey brain was longer than that of [^{11}]cocaine (Fig. 3). Peripheral metabolism of 4 was more rapid than that of 2. At 30 min. post-injection of 4, only 6% of radioactivity in the plasma remained as the parent compound. These results suggest that the uptakes of both 2 and 4 in a monkey brain are probably not receptor mediated. Rather, blood flow or other transport mechanism may play a role in their uptakes.

1. Volkow, N.D., Mullani, N., Gould, K.L., Alder, S. and Krajewski, K. Br. J. Psychiatry. 152. 641-648 (1988).
2. Volkow, N.D., Fowler, J.S., Wolf, A.P., et al Am. J. Psychiatry. 147. 719-724 (1990).
3. Fowler, J.S., Volkow, N.D., Wolf, A.P., et al. Synapse. 4. 371-377 (1989).

Scheme 1. Synthesis of (-)-[^{11}C]Methamphetamine (2) and (-)-3,4-methylenedioxy[^{11}C]Methamphetamine (4)

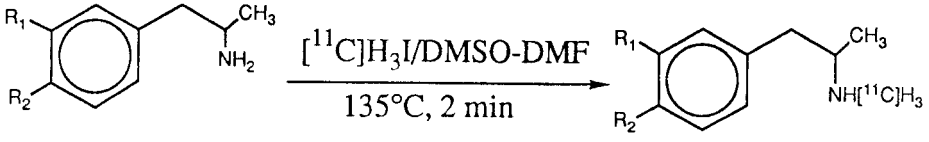

1). R_1=R_2= H
3). R_1, R_2= OCH_2O

2). R_1=R_2= H
4). R_1, R_2= OCH_2O

Fig. 1. [^{11}C]Methamphetamine uptake in Macaca Multta

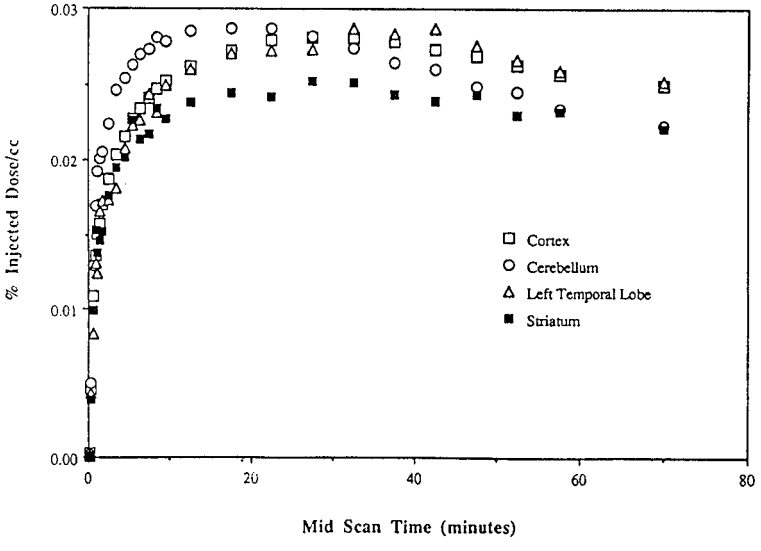

Fig. 2. [^{11}C]Ecstasy Uptake in Macaca Multta

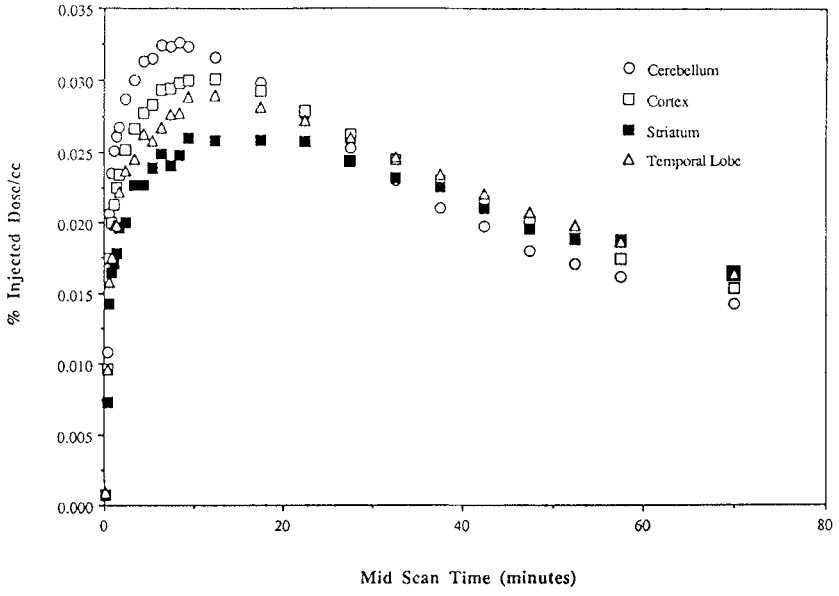

Fig. 3. [^{11}C]Cocaine Uptake in Human Brain (Ref. 3)

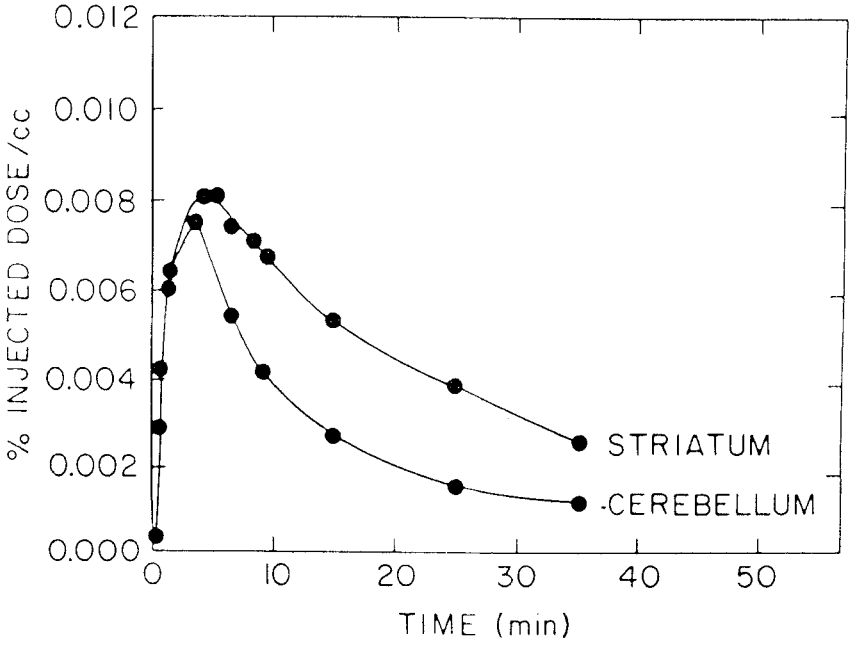

Solid Phase Hydrolysis of Acetyl Protecting Groups in the FDG Synthesis.

MULHOLLAND, G.K.* and JEWETT, D.M.#; Indiana University Department of Radiology*, Indianapolis IN 46202 ands University of Michigan Division of Nuclear Medicine#, Ann Arbor, MI. 48109.

Solid phase reagents offer numerous benefits in the synthesis of radiochemicals. This paper presents a simple new method for cleaving ester groups from [^{18}F]FDG-Ac$_4$ labeling reaction mixtures using commercially available sulfonic acid exchange resins.

METHOD Dowex 50 X-2, 100-200 mesh, H^+ form, was washed first with methanol, then water, then 3.6 M H_2SO_4, and finally water until the filtrate was neutral. One gram of the moist resin was placed in a magnetically stirred hydrolysis vial and a reaction solution containing the intermediate tetraacetyl-[^{18}F]FDG, tetraacetyl-2-triflyl-mannose (10 mg), K-222 (10 mg), and K_2CO_3 (20 μmol) in 1 mL of CH_3CN was added along with 2 x 2 mL of Et_2O. Organic solvents were driven off by heating the vial under a nitrogen stream, 1mL of water was added to the hydrolysis resin and then the vial was sealed and heated at 120-130°. The reaction was followed by TLC; hydrolysis was complete in 25-30 min. Filtration of the resin and rinsing with 3 x 2 mL of water recovered 98% of the radioactivity in aqueous solution. It was identical to FDG by both TLC and HPLC[1], except for a small amount of inorganic [^{18}F]fluoride. The clear, nearly colorless solution had a pH 4-5.5.

RESULTS AND DISCUSSION Three Dowex 50 X-2 bead size ranges were examined: 50-100, 100-200, and 200-400 mesh. All three catalyzed hydrolysis at similar rates in stirred vials. The medium size range was chosen because it was easy to handle and filter. The use of swellable cation exchange resins with low crosslinking appears important to the success of this approach; highly crosslinked macroporous resins, with high surface area, ie. Dowex MP-50, failed to catalyze acetyl cleavage at significant rates, even though these materials had higher acid site densities than the Dowex 50 X-2 resins; 1.5 vs 0.6 meq/mL of wet resin. Nafion resin (-100 mesh) also failed to hydrolyze acetyl groups under the conditions described above.

Use of a solid phase acid hydrolysis carries a number of advantages. Corrosion of apparatus due to leaking or spilled 1-1.5 N HCl is eliminated. The product solution is practically neutral in pH after filtration from the resin, so the acid neutralization column, with its attendant cost and transfer losses, is avoided. Resin hydrolysis appears to be gentle; less caramelization occurs than with HCl. The resins can be reused for a second hydrolysis. No chloride ion is present in the resin so the possibility of forming the contaminant 2-Cl-deoxyglucose during hydrolysis[1] is eliminated. Finally, since sulfonic acid resins very avidly bind kryptofix as well as many activated metal species formed in water targets, the resin hydrolysis provides an additional measure of safety in preventing these contaminants from reaching the final product.

CONCLUSION Incorporation of a solid phase hydrolysis step leads to simplification and improvement of FDG production.

This work was partly supported by DOE DEFG-02-87ER60561.

1. Alexoff DL, Casati R, Fowler JS, Wolf AP, Shea C, Schlyer D, Shiue C-Y. Appl Radiat. Isot. 43:1313-1322 (1992)

Nitric Oxide Synthase (NOS): Approaches to the Design and Synthesis of Inhibitors of this Enzyme Suitable for Radiolabeling and Measurement of *in vivo* biodistribution.

McCARTHY, T.J.; WELCH, M.J.; and ZHANG J.; Mallinckrodt Institute of Radiology, Washington University School of Medicine, St. Louis, MO 63110.

Research into the biological significance of endogenous nitric oxide has been intense in recent years[1]. This small, highly reactive molecule has been identified[2] to be the endothelium derived relaxing factor, an activator of macrophages, and suggested to be a neuronal messenger. This molecule is biosynthesized from L-arginine by either the constitutive or inducible isoforms of the enzyme nitic oxide synthase. At present, their are five classes of compounds known to inhibit this enzyme[3]. Among these are N^{ω}-substituted arginines (1), N-substitued guanidines (2) and flavoprotein binders such as diphenyleneiodonium bisulfate (3). We are attempting to synthesize derivatives of these molecules that will retain inhibitory activity and yet be suitable for labeling with fluorine-18, subsequently giving access to a method of probing this enzyme *in vivo* using positron emission tomography (PET) and single photon emission tomography (SPET).

Initially we were interested in the report that substituted guanidines[4], for example, N,N-dimethylguanidine, were selective inhibitors of the inducible isoform of NOS. We proposed that by synthesizing the corresponding fluoroalkyl derivatives of this simple substrate, that we could target these molecules as novel inhibitors for evaluation. We prepared a number of derivatives, including the N,N-diethyl and N-methyl,N-benzylguanidnes by nucleophilic displacement of methane thiol from the readily prepared isothiouronium salt (4). Unfortuantely were unable to approach the potency observed for the N,N-dimethyl or N-amino-substituted derivatives. At present we are using a similar synthetic strategy to target N^{ω}-substituted arginines, in the hope that these derivatives will better tolerate these structural changes and demonstrate good inhibitory activity.

We have had more success with the flavoprotein inhibitor class of compounds[5]. Initial experiments indicated[6] that diphenylene[I-125]iodonium bisulfate could probe nitric oxide synthase levels *in vivo*. The structural simplicity of this molecule does not allow for the simple introduction of fluorine-18. We synthesized an analog (5) of this compound which proved to be less potent than the parent molecule, but still showed promising inhibitory activity with an IC_{50} of 5μM. Attempts have been made to synthesize the corresponding fluorinated derivatives (6), however due to the intrinsic instability of the required intermediate tosylate (7) we have been unable to prepare this compound. At present we are attempting to synthesize tosylate (8) as the corresponding diphenyl derivative has been prepared and is known to be more stable[7]. This will therefore allow us to prepare a fluorine-18 radiolabeled flavoprotein binder for evaluation as an inhibitor of nitric oxide synthase.

The authors acknowledge N.I.H. (PO1-HL-13851) for funding this research, and the Department of Molecular Pharmacology, Monsanto Corporate Research, St. Louis for kindly testing our compounds for NOS inhibitory activity.

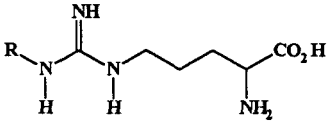

(1)

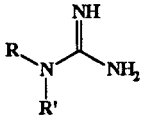

(2)

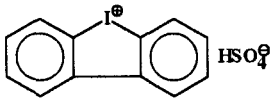

(3)

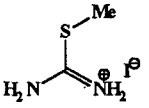

(4)

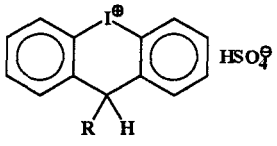

(5) R=H
(6) R=F

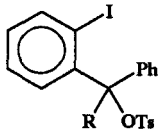

(7) R=H
(8) R=CF_3

References

(1) The Biology of Nitric Oxide; Portland Press: London (1992)
(2) Marletta, M. A.; Tayeh, M. A.; Hevel, J. M., BioFactors, 2, 219 (1990)
(3) Nathan, C. F., FASEB, 6, 3051 (1992)
(4) Misko, T. P.; Moore, W. M.; Kasten, T. P.; Nickols, G. A.; Corbett, J. A.; Tilton, R. G.; McDaniel, M. L.; Williamson, J. R.; Currie, M. G., Eur. J. Pharmacol., 233, 119 (1993)
(5) Stuehr, D. J.; Fasehun, O. A.; Kwon, N. S.; Gross, S. S.; Gonzalez, J. A.; Levi, R.; Nathan, C. F., FASEB, 5, 98 (1991)
(6) McCarthy, T. J.; Welch, M. J., J. Nucl. Med., 34, 89P (1993)
(7) Netscher, T.; Prinzbach, H., Synthesis, 683 (1987)

The Pharmacokinetics of [^{11}C] Fluoxetine in a Monkey Brain.

SHIUE C.-Y., Shiue G.G., Cornish† K.G., O'Rourke† M.F., and Sunderland J.J. Center for Metabolic Imaging, Creighton University, Omaha, Nebraska 68108. †University of Nebraska Medical Center, Omaha, Nebraska 68198.

Fluoxetine, (±)-N-methyl-3-phenyl-3-[(α,α,α-trifluoro-p-tolyl)-oxy] propylamine, is an antidepressant with potential applications in the treatment of other psychiatric disorders (1, 2). The mechanisms of action of antidepressants have been attributed to their abilities to increase neurotransmitter levels in presynaptic neurons by either inhibiting their uptakes or enzymatic degradations. The mechanism of action of fluoxetine has been proposed as a selective inhibition of serotonin reuptake in presynaptic neurons. In order to study the brain uptake and pharmacokinetics of [^{11}C] fluoxetine (2) in the brain, we have synthesized [^{11}C] fluoxetine and studied its distribution in mice and regional distribution in a monkey brain.

Carbon-11 labeled fluoxetine (2) has been synthesized previously (3, 4). We have synthesized compound 2 by methylation of desmethyl fluoxetine (1) with [^{11}C] H_3I in tributyl phosphate at 120°C for 7 minutes followed by purification with HPLC (C_{18} column, 10 x 250 mm, CH_3CN: 0.1M HCO_2NH_4, 80:20, 6 ml/min) in approximately 20% yield in a synthesis time of 40 minutes from EOB (Scheme 1). Following tail vein injection, the uptake of 2 in mouse brain was high and the retention of the radioactivity remained constant throughout the study (approximately 3-4% at 5 and 60 minutes post-injection) (Table 1). Similarly, following I.V. administration of 2, the uptakes of radioactivity in different monkey brain regions (cerebellum, cortex and temporal lobe) were similar and the retention of the radioactivity in these regions remained constant throughout the study (Fig. 1). The appearance of metabolites in the monkey plasma following injection of 2 was relatively rapid. Analysis of arterial plasma by HPLC showed that only approximately 20% of radioactivity in the plasma remained as compound 2 at 30 minutes post-injection (Table 2). These results suggested that the uptake and the retention of 2 in both the mouse brain and the monkey brain were probably non-specific and that blood flow or other transport mechanisms may play a role in its uptake.

1. Murphy D.L., Mueller E.A., Garrick N.A., and Aulakh C.S. J Clin Psychiatry, 47, (suppl 4), 9 (1986).
2. Fuller R.W., Wong D.T., and Robertson D.W. Med Res Rev, 11, 17 (1991).
3. Kilbourn M.R., Hara M.S., Mulholland G.K., Jewett D.M., and Kulh D.E. J Label Compd and Radiopharm, 26, 412 (1989).
4. Scheffel U., Dannals R.F., Suehiro M., Wilson A.A., Ravert H.T., Stathis M., Wagner H.N. Jr., and Ricaurte G.A. J Nucl Med, 31, 883 (1990).

TABLE 1: TISSUE DISTRIBUTION OF [^{11}C] FLUOXETINE IN MICE*
% Dose/Gram (Mean±SD)

	Time After Injection		
Organ	**5 Minutes**	**30 Minutes**	**60 Minutes**
Blood	0.50±0.02	0.56±0.07	0.67±0.04
Brain	3.91±1.26	3.88±0.72	3.96±0.76
Heart	9.54±2.37	2.81±0.52	2.86±1.31
Lungs	28.52±3.96	22.66±1.57	22.97±1.50
Liver	4.88±0.83	5.74±0.84	6.21±1.40
Spleen	3.90±0.25	6.18±0.88	5.86±0.88
Kidneys	9.19±0.09	5.80±0.61	4.42±1.29
Small Intestine	3.73±0.38	4.13±1.04	3.63±0.61

*n = 3

TABLE 2: ANALYSIS OF ^{11}C RADIOACTIVITY IN MONKEY PLASMA SAMPLES*

Minutes After Injection	Percent of Total Radioactivity Extracted	Percent of ^{11}C in MeOH as Unchanged Compound as Determined by HPLC	Percent of Unchanged Compound in Plasma
1	83	86	71
10	84	61	51
30	85	26	22
60	82	27	22

*Plasma samples were extracted with 2 ml of MeOH.

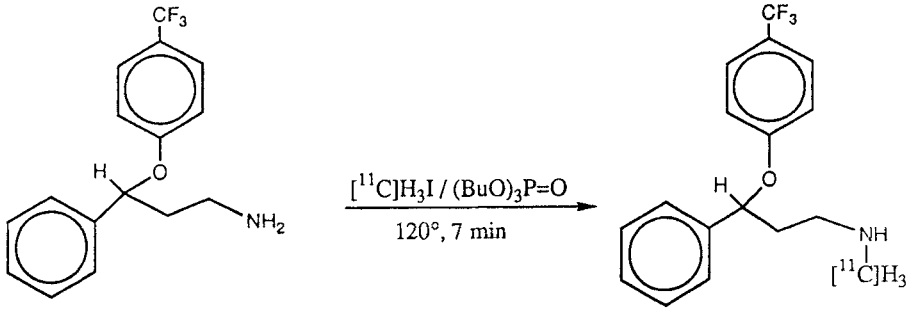

Scheme 1. Synthesis of [^{11}C] Fluoxetine

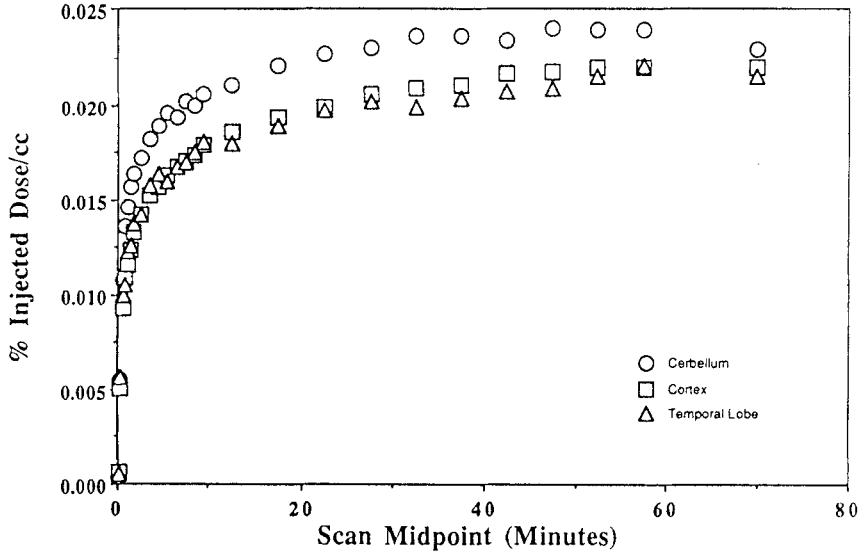

Fig. 1. Time Course for [^{11}C] Fluoxetine Distribution to a Monkey Brain

Metabolite Analysis of the Antitumour Agent, [*N*-^{11}*C-methyl*]NSC 601316

OSMAN, S.; LUTHRA*, S.K.; VAJA, V.; BROWN, G.D.; HARTE, R.J.A.; TILSLEY, D.W.O.; HUME, S.; PRICE, P.M.; JONES, T.; DENNY[1], W.A.; BAGULEY[1], B.C. and BRADY, F. MRC Cyclotron Unit* and Royal Postgraduate Medical School, Hammersmith Hospital, Ducane Road, London W12 OHS, [1]Cancer Research Laboratory, University of Auckland, School of Medicine, Auckland New Zealand.

We have labelled the anti-tumour agent NSC 601316[1,2] in the *N*-methyl position with carbon-11 (I) and have completed a series of human PET studies prior to Phase I clinical trial. The assessment of [^{11}C]NSC 601316 and labelled metabolites in plasma and tissue are required to develop the methodology of PET data analysis. Human metabolism of NSC 601316 has not previously been established.

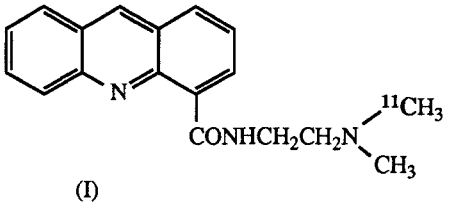

(I)

Rapid methods were used for analysing labelled metabolites in serial plasma samples and extracted tissue samples. Analyses of samples were either by solid phase extraction or protein precipitation followed by HPLC[3]. A reverse phase HPLC column ("μ" Bondapak C_{18}, 30 x 0.78 cm i.d.) was used and eluted with a mixture of acetonitrile:water [32:68 v/v] containing triethylammonium phosphate, pH 3.5 (10 mM) and heptane sulphonic acid (5 mM). A typical HPLC trace of [^{11}C]NSC 601316 at tracer dose (typically 10 μg of carrier) in human plasma at 15 min post-injection is shown in Figure 1. Several radiolabelled metabolites were observed. At least four of the labelled metabolites eluted before the [^{11}C]NSC 601316 peak and two eluted after. The human plasma profile of [^{11}C]NSC 601316 and its labelled metabolites over the period of 45 min is shown in Figure 2. The level of unchanged [11C]NSC 601316 was 72% at 5 min and decreased to 20% at 45 min post-injection. At tracer dose [^{11}C]NSC 601316 is highly protein bound (> 98%).

Human PET studies at tracer dose have characterised ^{11}C-tracer uptake and retention in the myocardium, liver, lung, kidney, LV blood and muscle (Figure 3). The PET signal observed in these tissues could be from [^{11}C]NSC 601316, labelled metabolites or combination of [^{11}C]NSC 601316 and labelled metabolites. To assist in the interpretation of the PET data, rat studies were carried out to determine the relative levels of [^{11}C]NSC 601316 and its labelled metabolites in tissues and urine (Figure 4). In rat brain and lung > 80% of the activity was [^{11}C]NSC 601316, whereas in the liver and urine < 20% of the activity was [^{11}C]NSC 601316 at 15 min post-injection. Further studies to assist PET data interpretation are in progress.

Work is also in progress to identify the metabolites by comparison with synthetic reference samples of putative metabolites using HPLC and mass spectrometry. We have established that demethylated species are not present to any significant extent (< 5%) in plasma over one hour.
This work was supported by Cancer Research Campaign Grant ST2 193/0101.

References

1. Schneider E., Darkin S.J., Lawson P.A., Ching L-M., Ralph R.K. and Baguley B.C. - Eur. J. Cancer Clin. Oncol. 24: 1783(1988).
2. Finlay G.J. and Baguley B.C. - Eur. J. Cancer Clin. Oncol. - 25: 271(1989).
3. Luthra S.K., Osman S., Turton D.R., Vaja V., Dowsett K. and Brady F. - J. Label. Compd. Radiophar. 32, 518(1993).

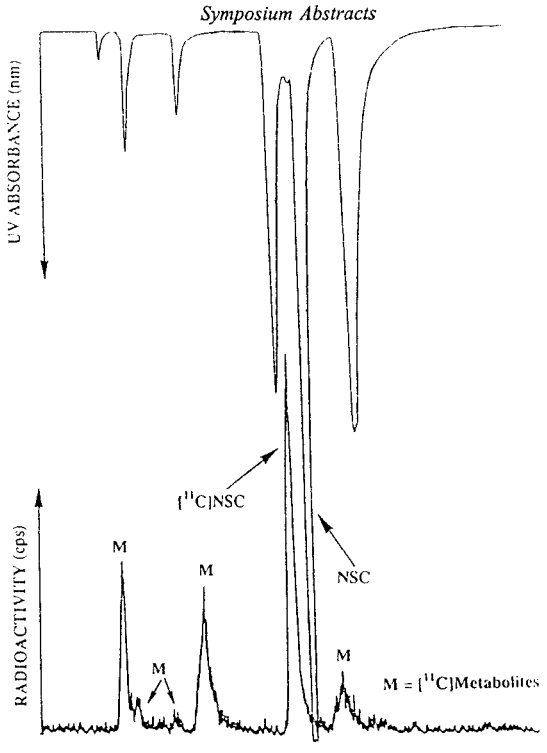

Figure 1. Typical HPLC trace of [^{11}C]NSC 601316 and its labelled metabolites in human plasma (15 min post-injection).

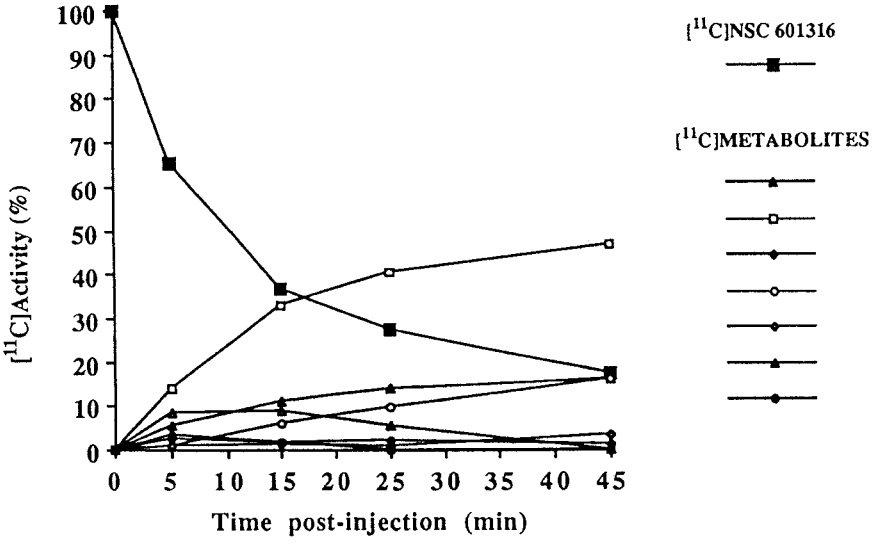

Figure 2. The level of unchanged [^{11}C]NSC 601316 and its labelled metabolites in human plasma.

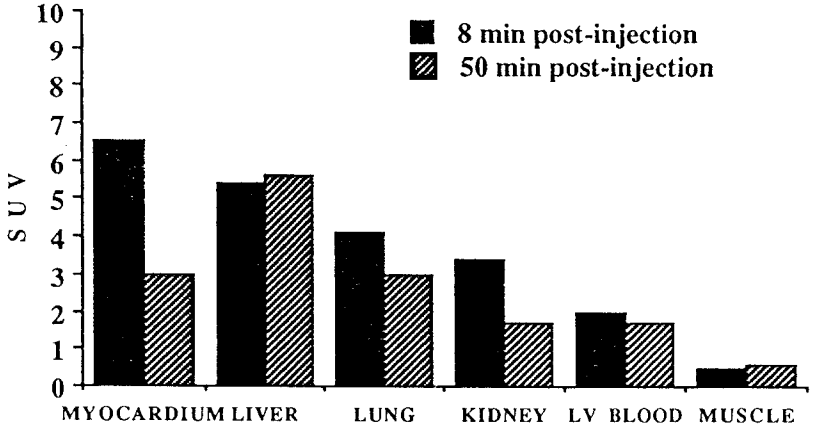

Figure 3. The Uptake of [^{11}C]NSC 601316 and its Metabolites in Human Tissue.

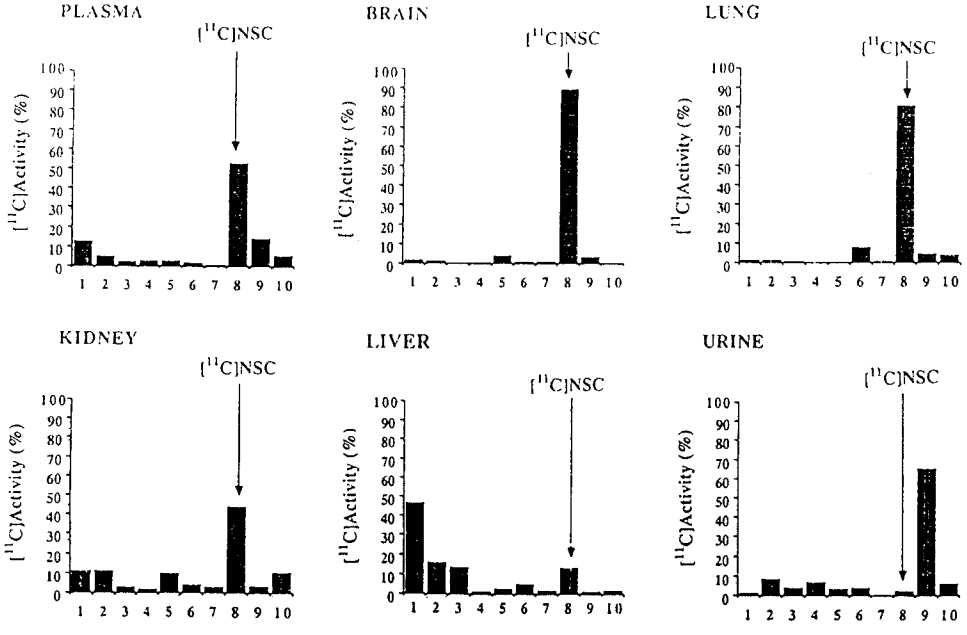

Figure 4. HPLC Profile of [^{11}C]NSC 601316 and its Metabolites in Rat Tissue.

METABOLISM IN HUMAN PLASMA DETERMINED BY HPLC FOR FIVE ^{11}C-LABELLED BENZAZEPINES - RADIOLIGANDS FOR PET EXAMINATION OF THE DOPAMINE D-1 RECEPTOR.

C.-G. Swahn, C. Halldin, L. Farde, P. Karlsson and G. Sedvall. Department of Psychiatry and Psychology, Karolinska Institute, Stockholm, Sweden.

A suitable receptor ligand labelled with a short-lived radionuclide has to meet several qualifications. To study receptors in brain it is important that radioactive metabolites do not pass the blood-brain barrier and bind to the receptors. Several benzazepines have been prepared for the examination of the dopamine D-1 receptor by PET (1-3). In this study we have determined the metabolism in human plasma by HPLC after i.v. administration of ^{11}C-labelled SCH 23390, SCH 39166 and its inactive stereoisomer SCH 39165, NNC 687 and NNC 756.

A recently developed plasma handling procedure and HPLC method (4-6) was used for optimal separation between radioligand and its metabolites. There were minor modifications of the gradient system. The total time for the plasma handling procedure was less than 4.5 minutes with a radioactive recovery >95%. A sample for chromatography was prepared from plasma and centrifuged after the addition of acetonitrile and standards. The total supernatant was injected into the HPLC column. The computer aided HPLC system consisted of two Kontron 420 pumps, a Kontron 491 solvent mixer, a Rheodyne 1761 injector with a 1 ml loop, a Waters μ-Bondapak C-18 column (7.8 x 300 mm, 10μm), a Kontron 432 UV detector operated at 275 nm and a Beckman 170 radioisotope detector. The data were stored and processed by a Kontron 450 computer system. The column was eluted with a gradient of a mobile phase consisted of acetonitrile and 0.01 M phosphoric acid with a total run length for all compounds less than 7.5 minutes. The recovery of radioactivity from the column was >98%.

The compounds were metabolised to a different degree (Figure 1). SCH 23390 and NNC 756 were extensively metabolised. Only 10% of plasma radioactivity represented unchanged ligand at 60 minutes after injection. NNC 687, a nitro analogue of NNC 756, and SCH 39166 were metabolised to a lesser extent (50% and 30% unchanged after 60 minutes). SCH 39165, the inactive stereoisomer of SCH 39166, was metabolised to a lower degree than its active enantiomer (60% unchanged after 60 minutes). A biexponential function is commonly used to describe plasma metabolism. Such a function was fitted to the mean data of [^{11}C]SCH 23390 and gave a good fit with a correlation coefficient of 0.99 (Figure 2). The study shows that structurally closely related radioligands may have very different rates of metabolism. A thourough determination of metabolism is thus required for any new radioligand.

1. Halldin C., Stone-Elander S., Farde L., Ehrin E., Fasth K.-J., Långström B. and Sedvall G. - Appl. Radiat. Isot. 37: 1039 (1986).
2. Halldin C., Farde L., Barnett and Sedvall G. - Appl. Radiat. Isot. 42: 451 (1991).
3. Halldin C., Hansen K., Foged C., Grønvald F.C. and Farde L. - J. Nucl. Med. 32: 934 (1991).
4. Halldin C., Swahn C.-G., Farde L., Litton J.-E. and Sedvall G. - Eur. J. Nucl. Med. 18: 526 (1991).
5. Halldin C., Någren K., Swahn C.-G., Långström B. and Nybäck H. - Nucl. Med. Biol. 19: 871 (1992).
6. Swahn C.-G., Halldin C., Farde L. and Sedvall G. - Hum. Psychopharmacol. (submitted).

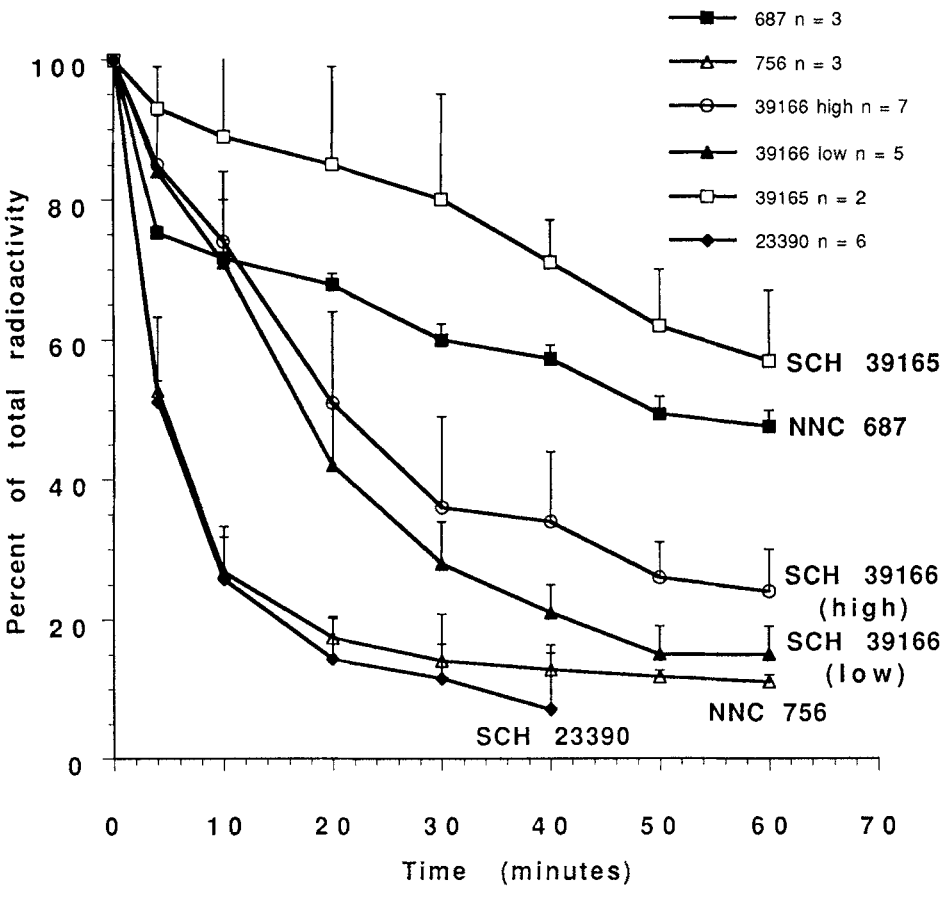

Figure 1.

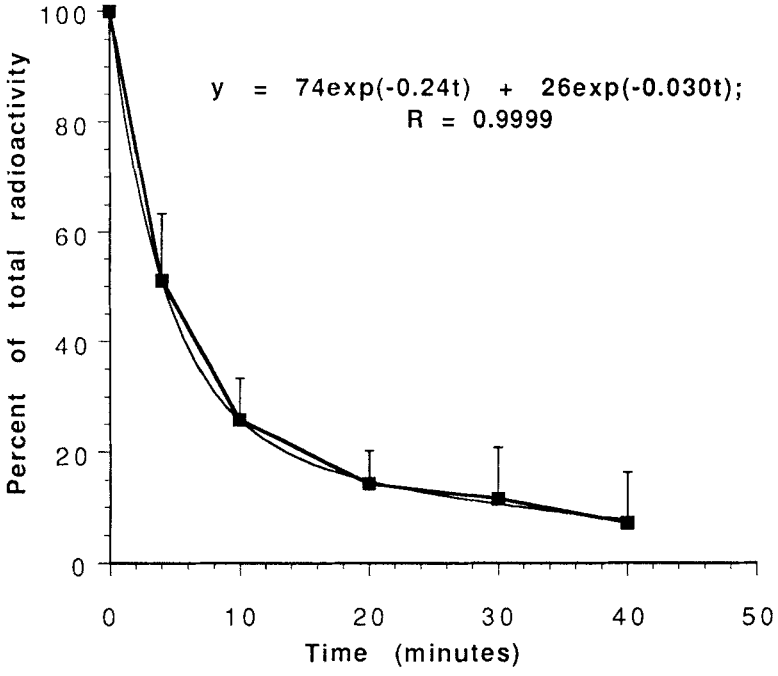
y = 74exp(-0.24t) + 26exp(-0.030t);
R = 0.9999
Percent of total radioactivity
100
80
60
40
20
0
0
10
20
30
40
50
Time (minutes)

Figure 2.

The Effect of Peripheral Catechol-*O*-methyl transferase inhibitor OR-611 (Entacapone) on the metabolism of 6-[^{18}F]Fluoro-L-Dopa

OSMAN, S.; LUTHRA*, S.K.; VAJA, V.; BRADY, F.; BURNS, D. and SAWLE, G.
MRC Cyclotron Unit*, Hammersmith Hospital, Ducane Road, London W12 OHS.

6-[^{18}F]Fluoro-L-Dopa (6-[^{18}F]FDOPA) is now an established tracer for assessing the dopaminergic nigrostriatal neuronal system with PET[1,2]. However, a major problem with the use of this tracer is the extensive peripheral metabolism[3,4]. 6-[^{18}F]DOPA is rapidly decarboxylated to 6-[^{18}F]fluorodopamine (6-[^{18}F]FDA) by aromatic amino acid decarboxylase (AAAD) and *O*-methylated to 3-O-methyl-6-[^{18}F]fluorodopa (6-[^{18}F]3-O-Me-Dopa) by catechol-O-methyl transferase (COMT) before penetrating the brain (Fig. 1). Both pathways reduce the level of 6-[^{18}F]FDOPA available in plasma and additionally 6-[^{18}F]3-O-Me-Dopa increases the non-specific signal in the brain which makes the quantification of 6-[^{18}F]FDOPA uptake difficult. Carbidopa is routinely used to inhibit the action of AAAD but the action of COMT is not usually blocked. Recently, selective COMT inhibitors have become available[5,6]. To assess the effect of a new COMT inhibitor, entacapone (OR-611), we have measured the levels of 6-[^{18}F]FDOPA in plasma in subjects receiving carbidopa alone and when receiving carbidopa and OR-611.

Two normal volunteers (NV) and four patients with Parkinsons disease (PD) were each studied twice. For the first PET study, the subjects were pre-treated with 150 mg of carbidopa before injection of 6-[^{18}F]DOPA. In the second study, the subjects were given carbidopa with OR-611 (800 mg). Serial arterial blood samples were withdrawn at 5, 10, 20, 30, 45, 60 and 90 min after injection of 6-[^{18}F]DOPA. The level of unchanged 6-[^{18}F]-DOPA and its metabolites in plasma were measured using two different methods, alumina extraction[7] and HPLC analysis[8].

Alumina Extraction Protocol: Cell-free plasma (CFP) was prepared by centrifugation (2000 g for 2 min) of arterial blood samples. An aliquot of CFP (500 µL) was dispensed into a tube containing equal volume of 0.5 M Tris-HCl, pH 9.0; 10mM EDTA and 0.1% sodium metabisulfate. After mixing, alumina (100 mg) was added to the tube and the sample vortexed for few seconds, rotated for 5 min and centrifuged. The supernatant was removed and the alumina pellet washed with water, vortexed and centrifuged. The resultant supernatant was pooled with the previous sample. The [^{18}F] activity in CFP, supernatant from alumina and alumina pellet were counted using a gamma-counter. Duplicate samples were analysed for each time point. The level of unchanged [^{18}F]-6-DOPA was calculated from the amount of ^{18}F-activity bound to alumina pellets after washing. This method was validated by analysing the supernatant and PCA extract of the alumina pellet (extraction essentially quantitative) by HPLC as described below. The supernatant contained 6-[^{18}F]3-O-Me-Dopa only, whereas the PCA extract contained only 6-[^{18}F]DOPA.

HPLC Analysis: CFP (500 µL) was mixed with an equal volume of ice cold PCA (0.5 M containing EDTA 4mM) and sodium metabisulfite (0.05 %) for 5 min and centrifuged. The supernatant was removed and the pH adjusted to 3.5. The solution was filtered and injected onto an HPLC column (Nucleosil 5 C_{18}, 5 µm, 25 cm x 10 mm i.d.) eluted at a flow rate of 3.0 mLmin^{-1} with a mixture of NaH_2PO_4 (0.1M), octane sulphonic acid acid (1.9 mM), EDTA (0.1 mM) adjusted to pH 3.5 and MeOH [90:10]. The HPLC eluent was monitored for UV absorbance (280 nm) and radioactivity. Both detectors were linked to a PC based integrator which allows the HPLC data to be recorded, corrected for decay and integrated. The level of unchanged [^{18}F]-6-DOPA and its metabolites at a given time point was obtained from the integrated radioactivity trace. The HPLC analysis of serial plasma samples showed mainly [^{18}F]DOPA and 3-O-methyl-6-[^{18}F]DOPA. The levels of other radiolabelled metabolites was < 10%. The results obtained with alumina extraction and HPLC analysis were in good agreement (Fig. 2).

The levels of unchanged 6-[^{18}F]DOPA in arterial plasma in NV and PD patients before and after administration of OR-611 are shown in Figs. 4a and 4b. In NV and PD patients when carbidopa was administered alone, the levels of 6-[^{18}F]DOPA in plasma were ca. 20% at 90 min. When OR-611 was administered in combination with carbidopa, the plasma levels of 6-[^{18}F]DOPA in both groups was considerably enhanced (ca. 60% at 90 min). It was also observed that in PD patients the levels of 6-[^{18}F]DOPA were slightly higher than NV in both cases when carbidopa alone (Fig. 4c) and carbidopa plus OR-611(Fig. 4d) was administered.

The use of the peripherally active COMT inhibitor OR-611 in combination with carbidopa has been shown to improve the level of 6-[^{18}F]-DOPA in arterial plasma by ca. 2.5 fold. Full kinetic analysis of the PET data also showed increased availability of 6-[^{18}F]DOPA to the brain.

References

1. Leenders K.L., Salmon E.P., Turton D., Tyrrell P., Perani D., Brooks D.J., Sagar H., Jones T., Marsden C.D. and Frackowiak R.S.J. - Arch. Neurol. 47: 1290(1990).
2. Luxen A., Guillaume M., Malega W.P., Pike V.W., Solin O. and Wagner R. - Nucl. Med. Biol. 19: 149(1992).
3. Cumming P., Boyes B.E., Martin W.R.W., Adam M., Grierson J., Ruth T. and McGeer E.G. - J. Neurochem. 48: 601(1987).
4. Firnau G., Sood S., Chirakal R., Nahmias C. and garnett E.S. - J. Neurochem. 48: 1077(1987).
5. Laihinen A., Rinne J.O., Rinne U.K., Haaparanta M., Ruotsalainen U., Bergman J. and Solin O. - Neurology 42: 199(1992).
6. Backstrom R., Honkanen E., Pippuri A., Pystynen J., Heinola K., Nissinen E., Linden I.-B., Mannisto P., Kaakkola S. and Pohto P. - J. Med. Chem. 32: 841 (1989).
7. Boyes B.E., Cumming P., Martin W.R.W. and McGeer E.G. - Life Sci. 39: 2243(1986).
8. Melega W.P., Luxen A., Perlmutter M.M., Nissenson C.H.K., Phelps M.E. and Barrio J.R.- Biochem. Pharmacol. 39: 1853(1990).

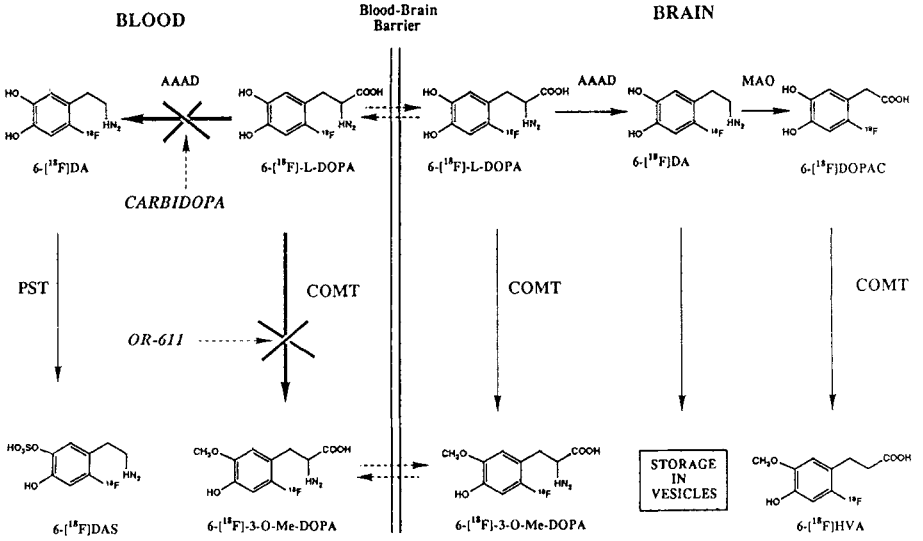

Fig. 1. Principal metabolic pathways of 6-fluoro-dopa in blood and striatal tissue.

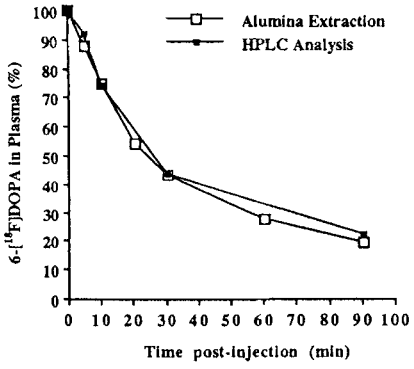

Fig. 2. [^{18}F]DOPA in plasma determined by (a) alumina extraction (b) HPLC analysis.

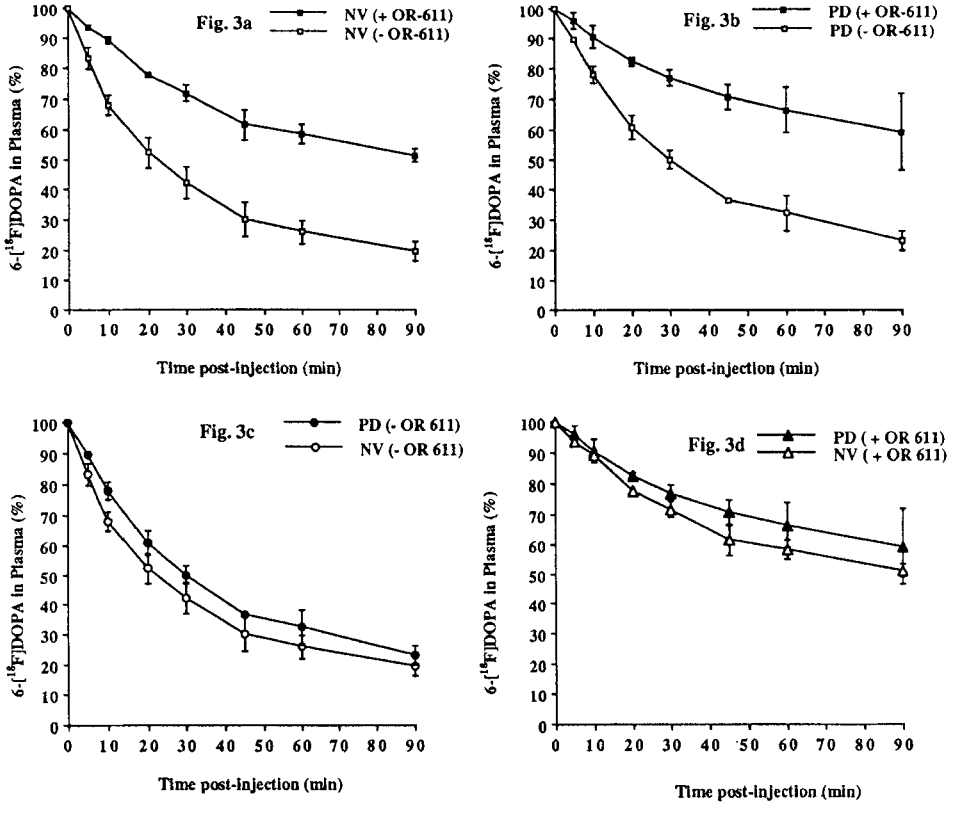

Figs. 3a-3b The level of unchanged 6-[^{18}F]DOPA in arterial plasma of normal volunteers (NV) and Parkinsonian patients (PD). All subjects had carbidopa; without COMT inhibitor (- OR-611), with COMT inhibitor (+ OR-611).

[^{86}Y]Citrate and [^{86}Y]EDTMP: Preparation, Chemical Characterization and in-vivo Quantitation of their Pharmacological Data with PET.

RÖSCH, F.; NEUMAIER, B.; STÖCKLIN, G.; QAIM, S.M., HERZOG, H.; MÜLLER-GÄRTNER, H.-W.
Institute für Nuklearchemie und Medizin, Forschungszentrum Jülich GmbH, D-52425 Jülich, Germany

^{90}Y ($T_{1/2}$ = 64 h, β^- = 100 %, E_{β^-} = 0.98 MeV) is widely used in Europe as a therapeutic nuclide in targeted tumor endotherapy in the form of chemical complexes, microspheres or monoclonal antibodies. It is conveniently available in no-carrier-added concentration from a ^{90}Sr/^{90}Y-generator. However, the in-vivo behaviour of ^{90}Y-therapeuticals can hardly be imaged. The introduction of the positron emitting isotope ^{86}Y ($T_{1/2}$ = 14.74 h, β^+ = 33 %, $E_{\beta^+,max}$ = 1.2 MeV) offers an ideal approach to quantitate regional biokinetics of the corresponding compounds by positron emission tomography (PET) [1,2].

One of the therapeutical applications of ^{90}Y-compounds, worthwhile to investigate by this method, is the palliative therapy of disseminated bone metastases with [^{90}Y]citrate. Using [^{86}Y] citrate, in-vivo data of this pharmaceutical such as metastases to healthy bone accumulation ratio, uptake kinetics for different organs, in-vivo dosimetry etc. can be obtained preparatory to the clinical application of [^{90}Y]citrate. Since [^{153}Sm]EDTMP, another bone seeking agent currently under clinical evaluation, is reported to offer a good therapeutical potential, it is also interesting to study the effect of citrate / EDTMP ligand substitution in ^{90}Y complexes on the in-vivo behaviour.

For the production of ^{86}Y two nuclear reactions, namely ^{86}Sr(p,n) and ^{nat}Rb(^{3}He,2n), were considered and the excitation functions measured, Table 1.

able 1: Comparison of the two ^{86}Y production routes

Parameter	^{86}Sr(p,n)-route	^{nat}Rb(^{3}He,xn)-route
Target isotope	^{86}Sr, highly enriched	natural rubidium
Target compound	$^{86}SrCO_3$	$^{nat}Rb_2CO_3$
Particle range investigated	19 → 6 MeV	36 → 5 MeV
σ_{max} for $^{86m+g}$Y	1200±100 mb (13 MeV)	250±20 mb (19 MeV)
Optimum production range	14 → 10 MeV p	24 → 12 MeV ^{3}He
Theroretical thick target yields	**10.8 mCi / μAh** (400 MBq / μAh)	5.2 mCi / μAh (190MBq / μAh)
Isotopic impurities at EOB (^{85,85m}Y, ^{87,87m}Y, ^{88}Y)	**< 4 %**	≈ 300 %
Radiochemical separation	Precipitation, ion exchange	Precipitation, ion xchange
Recovery of target material	Necessary; 90 % yield	**Not necessary**
Routine ^{86}Y production yields	**30 mCi,** irrading 300 mg $^{86}SrCO_3$ (226 mg/cm^2) for 4 h at 4 μA	---

Maximum cross section values of 1200 ± 100 mb at $E_p \approx 13$ MeV for the former reaction and 250 ± 20 mb at $E_{^3He} \approx 19$ MeV for the later process were measured. Considering production yields and levels of radionuclidic impurities, the optimum production ranges were $E_p = 14 \rightarrow 10$ MeV and $E_{^3He} = 24 \rightarrow 12$ MeV, resulting in theoretical thick target yields per µAh of 10.8 mCi (400 MBq) for $^{86}Sr(p,n)$ and 5.2 mCi (190 MBq) for $^{nat}Rb(^3He,xn)$. The sum of relevant radionuclidic impurities ($^{85m,g}Y$, $^{87m,g}Y$, ^{88}Y) amounts to < 4 % for the (p,n)-reaction on highly-enriched ^{86}Sr and to about 300 % for the $^{nat}Rb(^3He,xn)$-process [1]. In conclusion, the $^{86}Sr(p,n)$-route using highly enriched $^{86}SrCO_3$ as target material was found to be more suitable and is now routinely used for production purposes.

The [^{86}Y]citrate and [^{86}Y]EDTMP complexes were synthesized by adding one drop of $^{86}Y(III)$ stock solution (10^{-4} N HCl) to ligand solutions of the following composition: for citrate: 3 ml of 7.5 mg/ml sodium citrate, pH 7.4, overall sodium citrate amount 0.087 mol, overall ionic strength 0.17 M; for EDTMP: 2 ml aqueous solution of 22.8 or 36.5 mg/ml EDTMP, adjusted with NaOH to pH 7.5, and 1 ml saline to obtain isotonicity. The mixed solutions were stirred for 5 min at room temperature, sterile filtered and radiochemically analysed. Standard methods used were paper electrophoresis (0.075 M TRIS acetate, pH 6.0), and paper chromatography (on MN 261 using pyridine / ethanol / water (1 : 2 : 4) mixtures, pH 7.4). Radiochemical yields were found to be > 80 and 95 % for citrate and EDTMP. After purification, the radiochemical purity amounted to > 98 %.

First clinical studies were performed to measure the in-vivo pharmacokinetics of [^{86}Y]citrate and [^{86}Y]EDTMP in patients with multiple bone metastases and to assess the radiation doses. All patients investigated were male, aged 45-75 years, with prostatic cancer. 4 patients were administered intraveneously with [^{86}Y]citrate and 2 with [^{86}Y]EDTMP (100-300 MBq ^{86}Y). PET measurements (Scanditronix PC4096-15WB) were performed dynamically between 0 and 4 hours after injetion over the liver section. Whole-body distribution was measured between 4 h and 3 d after injection. Uptake data were determined by regions of interest placed in normal bone tissue, bony metastases, and liver. Images of coronal and sagittal whole-body sections were obtained by reformating the transversal PET images.

Kinetic analysis indicated an exponential accumulation in the metastases reaching a plateau 5 hours after injection. The early uptake kinetics for [^{86}]Ycitrate are shown in Fig. 1. Continuous measurements for up to 3 days gave no evidence for remarkable decrease of the ^{86}Y activity concentration in the metastases. All the ^{86}Y cleared from the blood unexcreted is accumulated in the skeleton and the bone metastases. Ratios of ^{86}Y activity concentration in metastases to that in normal bone ranged from 9 : 1 to 15 : 1 for the two ligands.
These observations are similar for both the ligands. The only important exception is the liver, where ^{86}Y accumulation was significant in the case of citrate. In contrast, EDTMP did not accumulate in this organ.

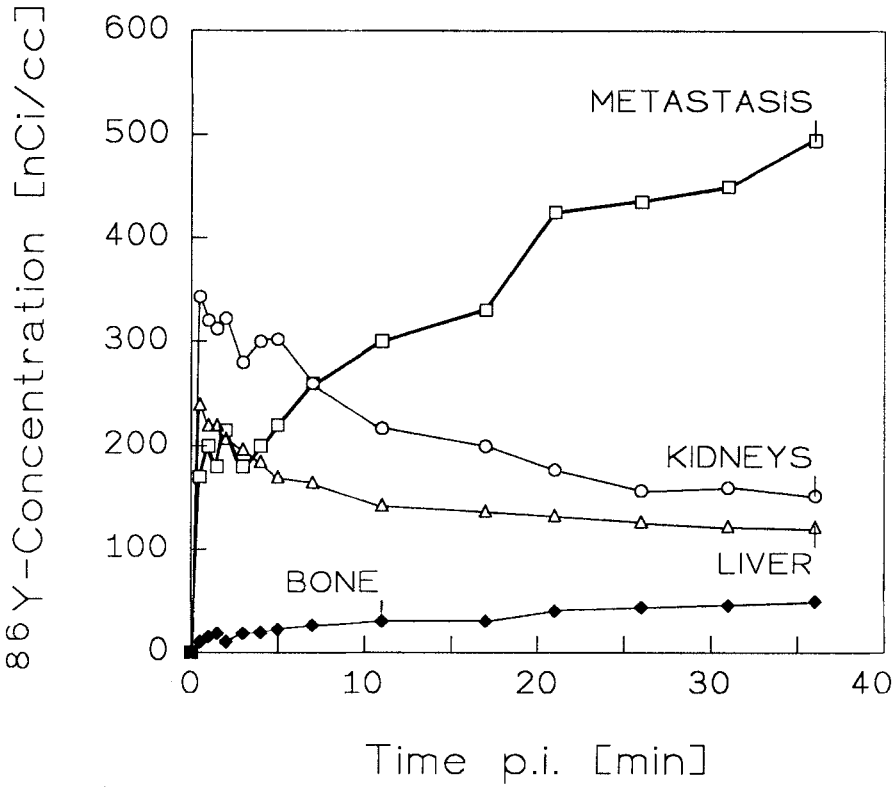

Fig. 1 Uptake kinetics of [^{86}Y]citrate immediately after injection

Using the uptake kinetics of [^{86}Y]citrate and [^{86}Y]EDTMP and the MIRD pamphlets 5 and 11, the radiation doses per 1 MBq of the injected ^{90}Y-compound were calculated. Values obtained for [^{90}Y]citrate and [^{90}Y]EDTMP were 28.5 ± 6.8 and 18.1 ± 2.9 mGy / MBq for the metastases, 2.6 ± 0.4 and 1.7 ± 0.3 mGy / MBq for the red marrow and 1.8 ± 0.3 and zero mGy / MBq for the liver, respectively. These results need to be verified in a greater number of patients.

In conclusion, the investigation demonstrates that the quantitation of human pharmacokinetics and radiation doses for a particular pharmaceutical as well as the quantitative evaluation of chemically different compounds of the therapeutically used beta-emitting ^{90}Y become possible by PET measurements using the positron-emitting isotope ^{86}Y.

[1] F Rösch, S M Qaim, G Stöcklin: Radiochimica Acta, in press

[2] F Rösch, S M Qaim, G Stöcklin: Appl.Radiat.Isot. **44**, 677 (1993)

Tc-99m Labeled Somatostatin Analogue, RC-160: ^{1}H-NMR and Computer Modeling Conformational Analysis

Varnum, J.M.[1], Mayo,K.H.[1], Schally,A.V.[2], Thakur,M.L.[3]
[1]Departments of Pharmacology and Biochemistry & Molecular Biology Jefferson Cancer Institute, and [3]Department of Radiation Oncology and Nulcear Medicine, Thomas Jefferson University, Philadelphia, PA 19107, and [2]Endocrine, Polypeptide and Cancer Institute, VA Medical Center, New Orleans, Louisiana, 70146.

Somatostatin, a neuropeptide discovered nearly 20 years ago, is known to be an antiproliferation agent (1-3). A large number of tumors have been found to have a high density of Somatostatin receptors (4). Since the half-life clearance of Somatostatin is less than about 3 minutes, a large number of analogues with longer clearance times have been synthesized. One of these analogues, RC-160, having the amino acid sequence D-Phe-Cys-Tyr-D-Trp-Lys-Val-Cys-Trp-NH_2 (S-S bond cyclized via cysteine oxidation), was prepared by Dr. Schally and was obtained from Biopharm, Switzerland (5). RC-160 has been shown to have an inhibitory effect on the growth of prostate, breast, and pancreatic tumors (5).

Sandostatin, another analogue of Somatostatin, has been labeled with In-111 or I-123 and used as a tumor imaging agent with highly encouraging results (6). We have labeled Sandostatin with Tc-99m, a shorter lived, inexpensive and commonly available radionuclide. This analogue has been used successfully to localize experimental tumors (7).

Using similar chemistry, we have labeled RC-160 with rhenium. Briefly, 0.005 M RC-160 was incubated with Na-ascorbate at 22°C for 1 hour, and 0.015 M ReO_4^- containing 500 Ci of freshly eluted Tc-99m as a tracer and reduced with stannous citrate was added. The reaction was allowed to react at 70°C for 1 hour. Upon cooling, a white precipitate was obtained that contained approximately 165 Ci Tc-99m. The precipitate was washed three times with ice cold water and dried in vacuuo. The goal of this investigation was to obtain a solution conformation of RC-160 with and without rhenium, by using high resolution ^{1}H-NMR spectroscopy.

Freezed-dried RC-160 samples were dissolved in $^1H_2O/^2H_2O$ (9:1). RC-160 concentration was in the range of 5 mM. pH was adjusted by adding µL quantities of NaO^2H or ^2HCl to the peptide sample. For most experiments, the temperature was controlled at 278 K. All NMR spectra were acquired on a Bruker AMX-600 NMR spectrometer. For two-dimensional ^{1}H-NMR spectroscopy, standard experiments were used (8). For sequence specific proton resonance assignments, homonuclear magnetization transfer (HOHAHA) spectra, used to identify many amino acid spin systems completely, were obtained by spin-locking with a MLEV-17 sequence (9) with a mixing time of 64 ms, and nuclear Overhauser effect spectroscopy (NOESY) (10, 11) experiments were performed to sequentially connect spin systems. All spectra were acquired in the phase sensitive mode (12). The water resonance was suppressed by direct irradiation (1 s) at the water frequency during the relaxation delay between scans as well as during the mixing time in NOESY experiments.

The majority of the two-dimensional-NMR spectra were collected as 512 or 1024 t_1 experiments, each with 1k or 2k complex data points over a spectral width of 5kHz in both dimensions with the carrier placed on the water resonance. 64 or 96 scans were generally time averaged per t_1 experiment. The data were processed directly on the

Bruker AMX-600 X-32 or offline on Sun SPARC-II computers with Bruker UXNMRP or FELIX programs. Data sets were multiplied in both dimensions by 0 to 60 degree shifted sine-bell or lorentzian to gaussian transformation function and generally zero-filled to 1k in the t_1 dimension prior to Fourier transformation.

NOESY spectra analysis then provided the necessary information for obtaining inter-proton distance constraints used in computer modeling studies. A clear network of NOEs indicates a tight type-II -turn centered at residues Trp-4 and Lys-5 and an anti-parallel β-sheet structure running through the remainder of the short cyclic peptide.

Based primarily on NOE distance constraints and $^3J_{\alpha N}$ coupling constants derived for RC-160, a computer modeled structure for the cyclic-peptide was generated as shown in Figure 1. The time dependence of NOEs was used to check for possible spin diffusion. Below about a 0.5 s mixing time in the NOESY experiment, little discernable spin diffusion could be detected. NOEs were ranked relatively as strong (2.2 - 3 Å), medium (2.8 - 3.5 Å), and weak (3.3 - 5 Å). An additional 1 Å degree of freedom was allowed for each non-backbone atom (or pseudoatom) involved in any given distance constraint. Restrained energy minimization and dynamics simulations were performed by using the Biosym Insight-II software package. Electrostatic potentials for charged groups were varied from full charge to about 50% full charge. Following restrained energy minimization and dynamics simulations, RMSD values among structures generated varied at most by 0.5 $Å^2$; most RMSD values were less than 0.5 $Å^2$. No inputed distance violations were found. Structures generated in this way were found to be consistent with the NMR data.

The NMR-derived structures of RC-160 with and without the rhenium, were essentially identical. Small variances in NOE magnitudes indicate distance changes at most on the order of 0.1 Å. The structure shown is that without the rhenium atom which can not be observed directly by ^{1}H-NMR techniques. Based on proton chemical shift changes, however, it appears that the rhenium atom is coordinated at the C-and N-termini of the peptide, on that side of the anti-parallel β -sheet where both cystine methylene groups are oriented.

References

1. Guillemin, R. (1978) Science 202, 390-402.
2. Lamberts, S. W. J., Koper, J. W., and Reubi, J. C. (1987) Eur.J. Clin.Inv.17, 281-287.
3. Lamberts, S. W. J. (1988) Endocr. Rev. 9, 417-436.
4. Lamberts, S. W. J., Krenning, E. P., Klijn, J. G. M. et al . (1990) Baillieres Clin. Endocrinology and Metab. 4, 29-50.
5. Srkalovic, G., Cai, R., and Schally, A. V. (1990) J. Clin. Endocr. and Metab. 70, 661-669.
6. Kvols, L. K., Brown, M. L., O'Connor, M. K., et al. (1993) Radiology 187, 129-133.
7. Thakur, M. L., Eshback, J., Wilder, S., et al. (1992) J. Labelled Comp. 365-367.
8. Wüthrich, K. (1986) NMR of Proteins and Nucleic Acids, Wiley- Interscience, New York.
9. Bax, A., & Davis, D. G. (1985) J. Magn. Reson. 65, 355-360.
10. Jeener, J., Meier, B. H., Bachman, P., and Ernst, R. R. (1979), J. Chem.Phys. 71, 4546-4553.
11. Wider, G., Macura, S., Anil-Kumar, Ernst, R. R., & Wuthrich, K. (1984) J. Magn. Reson. 56, 207-234.
12. States, D. J., Haberkorn, R. A., and Ruben, D. J. (1982), J. Magn. Reson. 48, 286-293.

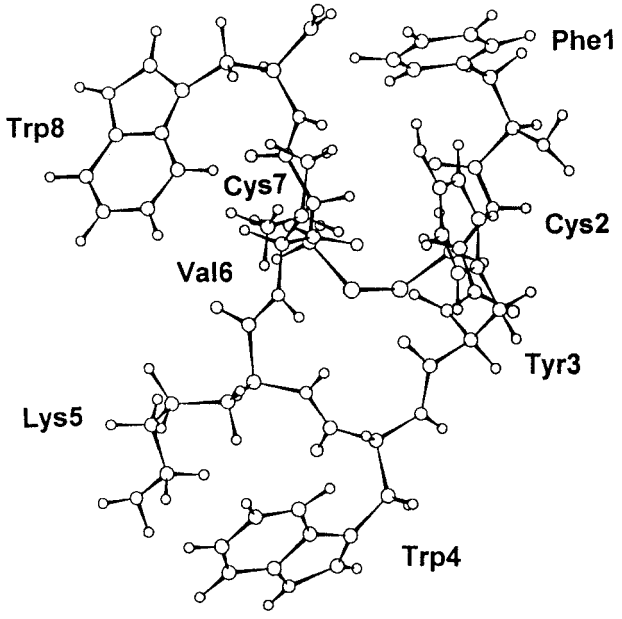

Figure 1. Average conformation of RC-160 as determined by restrained molecular dynamics and energy minimization.

Robotic synthesis of F-18 and C-11 radiopharmaceuticals at Massachusetts General Hospital.

LIVNI, E.; BABICH, J.W.; and FISCHMAN, A.J. Division of Nuclear Medicine, Department of Radiology, Massachusetts General Hospital. Boston MA 02114.

Automated synthesis of positron labeled radiopharmaceuticals reduces the radiation exposure to the chemist, provides a high degree of reproducibility and allows the chemist to use time more efficiently. Two systems are available for automated synthesis : 1)computer controlled chemistry modules (black boxes) and 2) computer controlled robotics.

At the MGH PET laboratory three hot cells are used for routine production of PET radiopharmaceuticals. Two of the cells are equipped with Anatech RB-86 robots. The robots are mounted along a rail positioned on the rear wall of the hot cell and work in a box like volume. Each robot has five degrees of freedom (wall, lift, turn, rotation, and grip) and three interchangable hands, 1 and 5 ml syringe hands and fingers hand. The software for controlling the robot is written in the Anatech Robot Controller (ARC) language for an IBM-PC or compatible computer. To supplement the robot, work stations are available which are controlled by computer through a sequencer interface. The work stations are operated through pneumatic or electro mechanical drivers. The work stations include the following: evaporation unit, solid phase extraction station, electronic dispenser, capping station, sterile filtration unit, and vortex.

The robot was provided with programs for the production of [F-18]FDG (1) and [C-11]CH3I. By using the available work stations and modifying or combining both programs a flexible enviroment exists which can be adapted to a variety of synthetic needs. We now routinely synthesize F-18 labeled fluconazole (2) and fleroxacin (3) for human use (Table 1). Carbon-11 labeled compounds produced by robotic synthesis (40-45 minutes) include CFT, Dapoxetine, and 3-O-D-methyl glucose (Schemes 1-3, Tables 2, 3).

From our experience at MGH we conclude that the robot and work stations can form the basis for reliable automated production of F-18 and C-11 radiopharmaceuticals for human use.

1. Hamacher K. Coenen H.H. and Stocklin G.-J. Nucl. Med. 27: 235(1986)
2. Livni E. Fischman A.J. Ray S. Sinclair I. Elmaleh D.R. Alpert N.M. Weiss S. Correia J.A. Webb D. Dahl R. Robeson W. Margouleff D. Liss R. Strauss W.H. and Rubin R.H.-Nucl. Med. Biol. 19: 191(1992)
3. Livni E. Babich J. Alpert N.M. Liu Y. Thom E. Cleeland R. Prosser B. Correia J.A. Strauss W.H. Rubin R.h. and Fischman A.J.-Nucl. Med. Biol. 20: 81(1993)

Scheme 1. Synthesis of [C-11]CFT

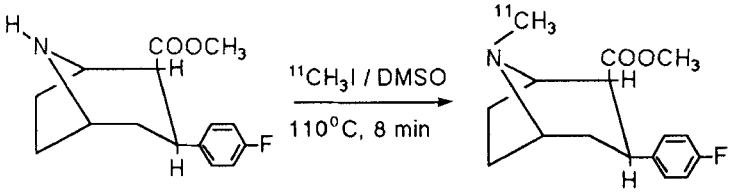

Scheme 2. Synthesis of [C-11]Dapoxetine

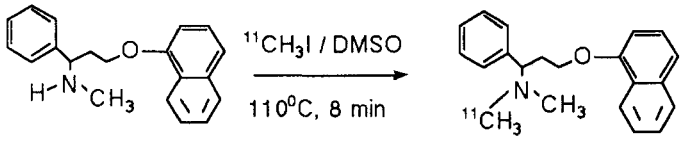

Scheme 3. Synthesis of 3-[11-C]-methyl-D-glucose (MG)

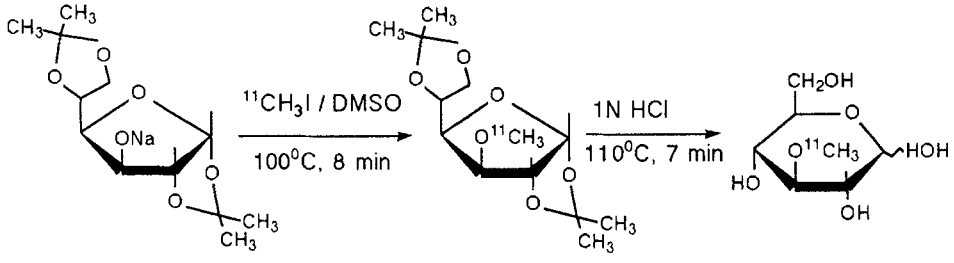

Table 1
Yield and radiochemical purity (RCP) of F-18 radiopharmaceuticals

Compound	% Yield (S.D)	RCP (%) (S.D)
FDG	19.5 (1.7)	96.5 (0.4)
Fleroxacin	8.1 (2.2)	95.0 (1.9)
Fluconazole	0.8 (0.2)	95.8 (2.5)

Table 2
Yield (EOS), RCP and specific activity (SA) of C-11 labeled compounds

Compound	% Yield (S.D)	RCP (%) (S.D)	SA (mci/umole)
CFT	7.7 (2.6)	99.0 (0.8)	538 (113)
Dapoxetine	8.0 (2.8)	99.5 (0.2)	445 (132)
MG	3.1 (1.0)	98.0 (1.6)	› 30

Table 3
Conditions for HPLC purification of C-11 compounds

Compound	Column	Solvent #	Flow (ml/min)	Elution time (min)
CFT	Beckman ODS 15cm*1cm, 5u	A:B, 60:40	6	4.5
Dapoxetine	Waters C-18 10cm*0.8cm	A:B, 75:25	6	5
MG	RSIL NH_2 25cm*1cm, 10u	C:D, 80:20	8	4.5

#A-Methanol, B-Phosphate buffer pH 7.2, C-Acetonitrile, D-Water

Automated Synthetic System of C-11 Labeled Ethylketene

Ryou Fujii, Yoshio Imahori*, Tadasu Sugawara**, Tatso Ido***, Takehiko Yagyu, Noburo Higashi, Satoshi Ueda*, Hisamitsu Nakahashi and Takahiro Kanatsuna
Nishijin Hospital, Kyoto, Japan; Department of Neurosurgery, Kyoto Prefectural University of Medicine, Kyoto, Japan; The Japan Steel Works LTD., Tokyo, Japan**, Cyclotron and Radioisotope Center, Tohoku University, Sendai, Japan****.

C-11 labeling agent $^{11}CH_3I$, which labeles a precursor with N-methylation, is widely used in radiopharmaceutical chemistry. However there is no good C-11 labeling agent for the acylation. In general organic reaction we use carbonate unhydrides for acylation or DCC for condensation reaction. Those method are not useable for C-11 labeling because of taking long time for the reaction. Ketene has a high reactivity and acylate hydroxyl-residue or amino-residue. We reported the C-11 labeled ethylketene synthesis method(1-2). The C-11 ethylketene is a strong C-11 labeling by acylation potently. This C-11 labeling method is useful for labeling bioactive compounds such as C-11 labeled diacylglycerols or phorbor esters. From those above C-11 ethylketene will be more used from now on and the radiation exposure on chemists will have to be reduced. Thus we developed the automated synthesis system of C-11 labeled ethylketene. This system has not only the open/close action valves but also the movement mechanism on glass vesseles, reagents vials and microsyringes. By using this synthetic system, C-11 ethylketene was obtained with high yield and good reproducebility. And the radiation exposure on chemists was reducted on the synthesis of C-11 ethylketene.

The C-11 ethyl ketene automated synthesis system is showen in Figure 1. This system is consist of the three units.
1) Control unit This system is automatically controlled using parsonal computer (PC9801 VM1, NEC, Japan). In this synthesis system the three heaters are installated, and these heaters are controled using sub-controller (E5AX, Omron, Japan) because of the simplification of program and of protection of the heaters from a rise of temperature which is occurred with emergency of the controller.
2) Main unit The unit is constituted with two parts. One is the part of the process from trapping of C-11 dioxide to produce C-11 butyric acid lithium salt. The other part consist of the process from producing of C-11 butyric acid vapor to producing C-11 ethylketene. The former is consisted two turn table, which one is for set of the microsyringes and the other is for set of reagents vials. The reaction vessel is settled in the center and the liquid nitrogen bath is settled under the reaction vessel. The turn tables are moved by a stepping motor for accurate movement to the fixed position. All microsyrindges and liquid nitrogen bath are moved by an air cyrinder in order to speedy movements. The later is consisted of the C-11 butyric acid vapor producing unit and pyrolysis. The dummy vessel is settled on the C-11 butyric acid producing unit to avoid the influence of moisture until C-11 butyric acid lithium salt is produced. The reaction vessel and dummy vessel are moved up/down and turn left/turn right by a DC motor and a rotary actuator, respectivery. The fixer of adapter for connection of vessels is made from Tefron because of accurate couppling and prevention of damage of vessels. The column containing pentaoxidase is setttled to the gas line for reduction of moisture.
3) HCl gas flow regulation unit Flow rate and concentration of HCl are controled by this unit. This unit is consisted of two mass flow controlers, which one is used as HCl gas-control and the other is used as helium gas flow control. Both gasses are mixed with in the apparatus.

Systemic synthesis procedure is shown in Figure 2. C-11 ethylketene synsesis method was previously reported in our articles(1-2). Beforehand, the propyl lithium, as a precursor of C-11 ethylketene, was produced by the reaction of lithium (5mg) and propyl bromide (3mmol) in dried diethylether (10ml). Four vials,which contain with PrLi, CH_2Cl_2, H_2O and wasting vial, microsyringes, two vessels and liquid nitrogen are settled manually. The automatic synthesis procedure is started up after the preparation. These implements are set up into initial poitions and the pyrolysis is heated at 530°C. After dryness of reaction vessel by sweeping with dry herium gas into the reaction vessel and heating with hot air(150°C) from out side, the reaction vessel is cooled by liquid nitrogen. Then C-11 dioxide can be trapped. Propyl lithium in ether solution is added into the reaction vessel after the three times of washing process of microsyringe which reagent is sucked up from the vial and is exhausted to waste vial. Water (100µl) is equally added for decomposition of surplus propyl lithium. Water in the products is evaporated under the heated condition by hot air blow at 150°C. Then dichloromethane (100µl) is added and evaporated again to obtain the complete

dryness C-11 butyric acid lithium salt. After then the dummy vessel are removed from C-11 butyric acid vapor producing unit, the reaction vessel is moved into it. The diluted dry HCl gas is blew into the reaction vesel and produced C-11 butyric acid vapor is carriered into the pyrolysis with helium gas. Thus C-11 ethylketene is obtained by decomposition of C-11 butyric acid.

The yield and specific activity of C-11 ethylketene is greatly influenced with two factors, one is a carbon dioxide and the other is a moisture in air. Propyl lithium is reacted to carbon dioxide and non labeled butyric acid is produced so, as a result, the specific activity of C-11 ethyketene is lowered. Moisture influences to the yield of C-11 ethylketene greatly. From those above, we contrived how to reduce those influences. For certain addition of a smoll amount of reagents to reaction vessel the microsyringes are used. Because it is difficult to transfer the 50μl of pure propyl lithium by using tefron tube. At the pyroritic decomposition process the yield of C-11 ethylketene is greatly influenced with the moisture. Accordingly the countermeasure to those above, the parts of C-11 butyric acid lithium salt and the parts of producing C-11 butyric acid vapor are departed for reduction of moisture-influence. Those parts are connected by movment of the reaction vessel. The fixer of adapter for connection of the reaction vessel is made from Teflon and complete connection is performed. And this automated sythesis system have a good reproducibility. By means of the deveropment of C-11 automated synthesis system, various C-11 labeled bioactive compounds can be obtained easily with high yield and high specific activity (2). As a most important effect the radiation exposure to chemists can be reduced on the synthesis of C-11 labeled ethylketene. C-11 ethylketene has a potent reactivity to amino-residue or hydroxyl-residue. In our study this agent is very useful as a C-11 labeling precursor for rigands of second messenger imaging and elucidation of signal transduction system (3-6) such as diacylglycerols (3-5), phorbol esters (1,6) and forskolins. This C-11 labeled ethylketene automated synthesis system can be synthesize the various bioactive compounds and useful to development of C-11 labeling compunds as a powerfull tool.

1. Y. Imahori, R. Fujii, T. Ido et al., J. lab. Comp. Radiopharm., 27, 1025-1034(1989)
2. R. Fujii, Y. Imahori, T. Ido et al., J. lab. Comp. Radiopharm., 29, 497-505(1991)
3. Y.Imahori, R.Fujii, S. Ueda et al., J.Nucl. Med., 32, 1622-1626(1991)
4. Y.Imahori, R.Fujii, S. Ueda et al., J.Nucl. Med., 33, 413-422(1992)
5. Y.Imahori, R.Fujii, S. Ueda, J.Nucl. Med., 33, 465-466(1992)
6. Y. Ohmori, Y. Imahori, S. Ueda et al. , J.Nucl. Med., 34, 431-439(1993)

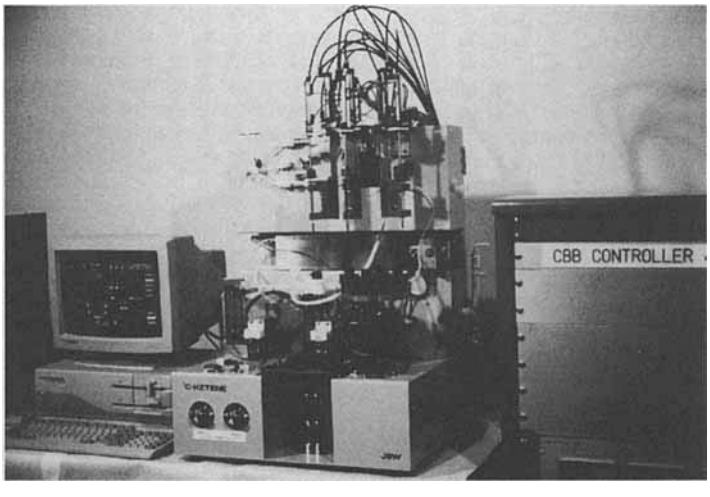

Figure 1 Photographic View of C-11 Ethylketene Automated Synthetic system

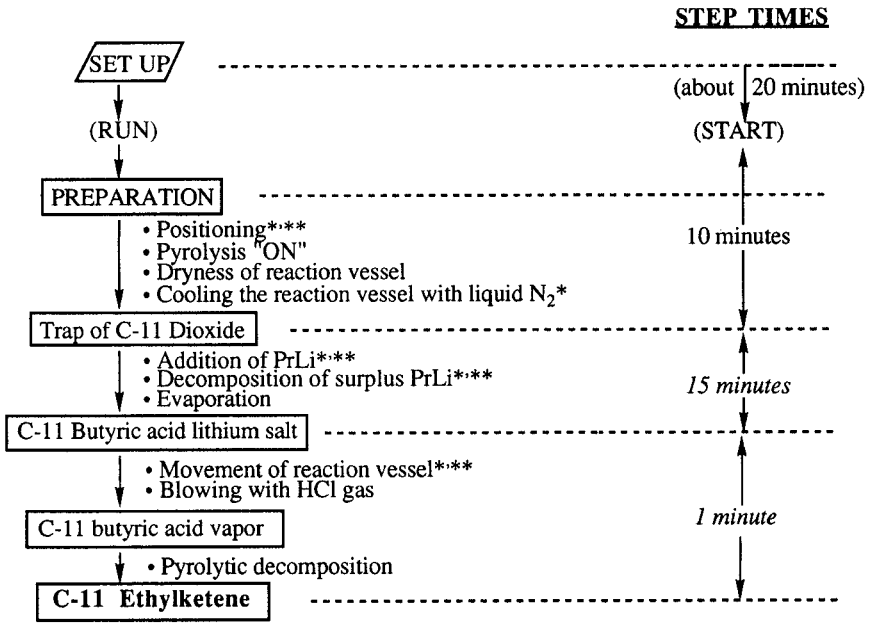

Figure 2 Systemic synthesis procedure and time schedule

Movement direction *: Up and Down
**: Turn Right and Left

Table 1 Specifications of C-11 Alkylketene Automated Synthetic System

Dimension (mm) [W X D X H]	520 X 450 X 810
Weight (kg)	10
Power Consumpton	AC 100V 3.5kW
Radiochemical Yield (%)*	55 ~ 60
Specific Activity (GBq/μmol)*	148 ~ 185

*: C-11 labeled diacylglycerol was adopted for analysis of radiochemical yield and specific activity.

Carbon-11 Labelling of the Antitumour Agent, [*N*-^{11}C-*methyl*]NSC 601316 for Pre-Clinical Evaluation in Man by PET.

BROWN, G.D.; TURTON, D.R.; LUTHRA, S.K.; OSMAN, S.; WATERS, S.L.; HARTE, R.J.A.; TILSLEY, D.W.O.; PRICE, P.M.; JONES, T.; DENNY[1], W. A. and BRADY*, F.
MRC Cyclotron Unit* and Royal Postgraduate Medical School, Hammersmith Hospital, Ducane Road, London W12 OHS, [1]Cancer Research Laboratory, University of Auckland, School of Medicine, Auckland New Zealand.

N-[2-(dimethylamino)ethyl]acridine-4-carboxamide (DACA or NSC 601316) is a topoisomerase II inhibitor, showing promising activity against multi-drug resistant tumours in animal models[1,2]. To assist the evaluation of NSC 601316 we have labelled it with carbon-11 in the *N*-methyl position (II) and have determined its pharmacokinetics in normal and tumour tissues in man by PET prior to Phase I clinical trial. PET studies will also be carried out in parallel with Phase I trial in collaboration with the Cancer Research Campaign (U.K.).

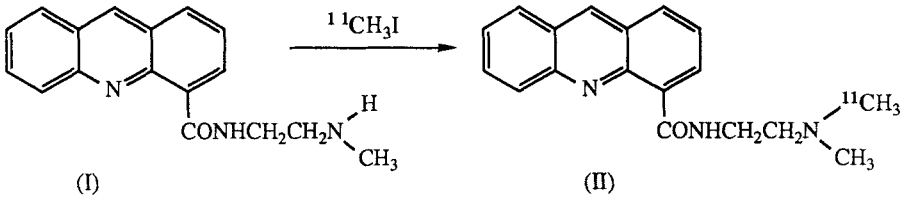

(I) (II)

[^{11}C]Iodomethane was prepared from [^{11}C]carbon dioxide using a remotely controlled apparatus operated by a Toshiba EX-40+ programmable controller. The [^{11}C]iodomethane produced was then distilled into a vial containing a solution of *N*-desmethyl precursor (I) (1.0 mg) in dry acetone (400 µL). The reaction mixture was heated at 90 °C for 5 min. Acetone was removed and the residue dissolved in chloroform (1 mL) and injected onto an HPLC column ("µ" Porasil, 30 x 0.78 cm i.d.). The column was eluted at a flow rate of 3.0 mLmin^{-1} using a mixture of chloroform:ethanol [80:20]. [*N*-^{11}C-*methyl*]NSC 601316 (II) eluted at 8 to 9 min. The HPLC solvent was removed and the product formulated for injection as the hydrochloride in isotonic saline. The radiochemical yield was ca. 65% from [^{11}C]iodomethane.

The formulated [*N*-^{11}C-*methyl*]NSC 601316 was analysed by HPLC using a Phenomenex Bondclone column (250 x 3.9 mm i.d.) eluted at 1.5 mLmin^{-1} with a mixture of ammonium formate (0.1 M) and methanol [50:50, v/v]. Radiochemical and chemical purities were greater than 99%. The specific activity of [*N*-^{11}C-*methyl*]NSC 601316 was in the range of 0.9-1.5 Ci/µmol at EOS, corresponding to 10 µg (34 nmol) of stable NSC 601316 in the formulated sample.

A sample of [*N*-^{11}C-*methyl*]NSC 601316, as formulated for injection, was analysed during and after radioactive decay by mass spectrometry (CI +ve mode). The spectra obtained were identical to those of reference NSC 601316 (*m/z* = 294 [M+H]+). For validation of the radiosynthesis a preparation was carried out using ^{13}C-enriched (90 atom %) iodomethane. The product in $CDCl_3$ was examined by proton-decoupled ^{13}C-NMR spectrometry (62.9 MHz) with multiplicity determined by DEPT. A single peak was observed having the same chemical shift (δ = 44) as reference NSC 601316. Mass spectrometry on the product (CI +ve mode) gave a peak at *m/z* = 295 [M+H]$^+$.

This work was supported by Cancer Research Campaign Grant ST2 193/0101

References

1. Schneider E., Darkin S.J., Lawson P.A., Ching L-M., Ralph R.K. and Baguley B.C. - Eur. J. Cancer Clin. Oncol. 24: 1783(1988).
2. Finlay G.J. and Baguley B.C. - Eur. J. Cancer Clin. Oncol. 25: 271(1989).

^{18}F-Lomefloxacin: Human *In Vivo* Pharmacokinetic Studies Using Fluorine-18 Labelled Drugs.

T. J. Tewson, D. Yang*, G. Wong*, D. Macy,* O. J. DeJesus!, R. J. Nickles!, S. B. Perleman!, M. Taylor!, P. Frank#.

The University of Texas Health Science Center at Houston, Houston, Texas 77030. *The M. D. Anderson Cancer Center, Houston,Texas. !The University of Wisconsin Medical School, Madison, Wisconsin. #Searle, 5200 Old Orchard Road, Skokie Il, 60077

Lomefloxacin (Maxaquin) is a new fluorinated quinoline antibiotic whose mode of action is as a gyrase inhibitor. The compound has the structure shown. We wished to perform whole body pharmacokinetic studies with this compound in humans using fluorine-18 as the tracer and positron tomography as the measuring system. This raises two rather unusual requirements in preparing the radio pharmaceutical. First we needed the normal human dose of 455 mg, and second the compound had to be administered orally.

We have prepared the fluorine-18 derivative by fluorine exchange with fluorine-18 fluoride and 5 mgs of the free base in DMSO at 160 °C for 60 minutes. The DMSO solution is then added to a refluxing solution of 550 mgs of Lomefloxacin in 30 ml of 2N HCl/15% Ethanol. This solution is then cooled in ice and the product filtered, washed with 2N HCl and dried. Analysis, by HPLC, shows no detectable chemical or radioactive impurities present in the product including fluorine-18 fluoride. Typically 25-30 mCi and 420-450 mgs of material are obtained. This material is then mixed with additional Lomefloxacin hydrochloride such that 7 mCi's of activity are present in 455 mgs (the normal adult dose of the compound). In some cases the activity was administered in a gel capsule, in others as an aqueous slurry.

Initial PET studies where performed in the pig, in order to determine the residence time of the compound in the stomach and gastro-intestinal system for dosimetry calculations. The animal was anesthetized and a gastric tube inserted in to the stomach from the mouth. The gel capsule containing the radioactive drug was then placed in the tube and washed down with water. PET data was collected in four minute blocks and the capsule in the stomach was clearly visible in the first four minute collection but had disappeared in the second. Thus the residence time of the capsule before dissolving is 4 minutes or less. Transport of the drug from the stomach to the small intestine was 80% complete in 30 minutes and adsorption from the small intestine was sufficiently rapid such that there was little accumulation. With conservative estimates of the geometry of the human stomach and the known distribution in rats this data showed that the critical organ in terms of exposure was the stomach and that 6 mCi's could be administered and still stay within the regulatory guidelines.

We have performed three human studies to date, in which the drug was swallowed and then whole body rectilinear scans and tomographic images where performed in the PET.

Initially the rectilinear scans where collected every twenty minutes with the data collection time increasing as the fluorine-18 decayed and data collection continuing for seven and a half hours. Tomographic images of the lungs, liver and prostate where obtained seventy minutes after administration of the drug. In addition blood and urine samples where taken. With the use of appropriate attenuation correction the rectilinear scan data can provide quantitative information on the distribution of the compound in each body section but not on individual organs. However with the addition of the tomographic data giving a single data point on the individual organs an estimate of the time activity curve for that organ can be made.

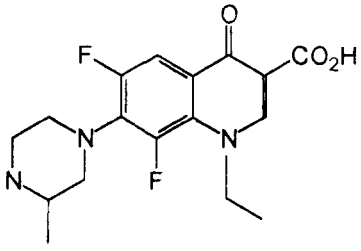

Activity Concentration of F-18 in Urine Samples After Ingestion of Radiolabeled Lomefloxacin

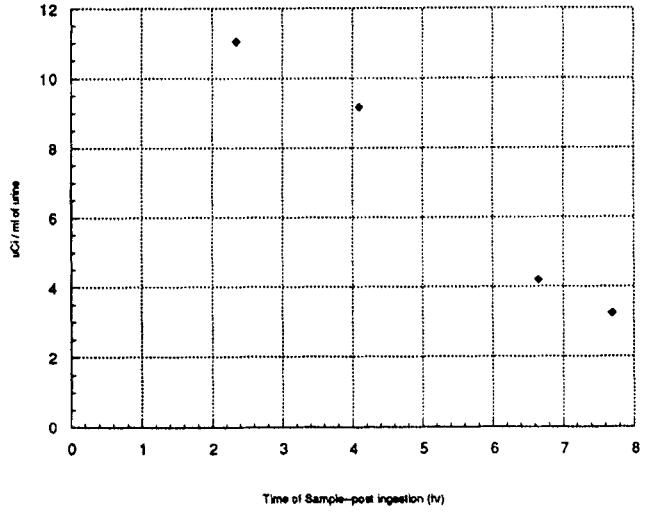

Activity of F-18 in Whole Blood Samples After Ingestion of Radioloabeled Lomefloxacin

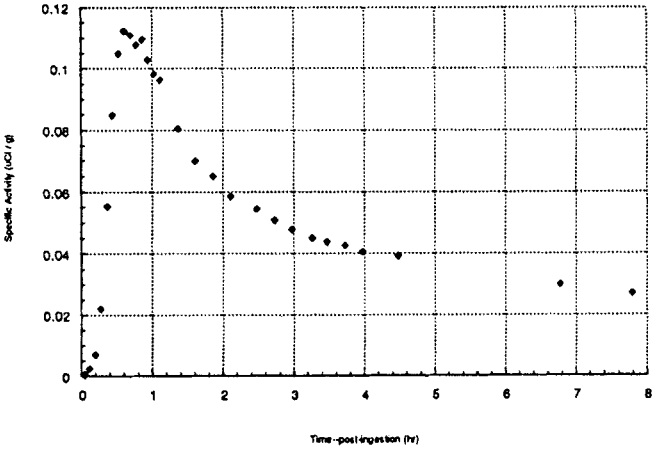

^{18}F-Nucleophilic Heteroaromatic Substitution: Some Data on the Reactivity and Selectivity of the ^{18}F-Fluorination Reaction.

G.ANGELINI, A.MARGONELLI, C.SPARAPANI, O.URSINI; Istituto di Chimica Nucleare-CNR-Area della Ricerca di Roma-C.P.10-00016 Monterotondo Stazione (Roma)-Italy

P.SALVADORI, S.DI SACCO, A.RIVA, L.FUSARI; Laboratorio Ciclotrone- Istituto Fisiologia Clinica-CNR-Via Savi 7-Pisa-Italy

The increase in the use of PET (Positron Emission Tomography) technique is depending on the development of methods suitable for the radio-synthesis of pharmaceuticals labeled with positron emitters. Among them, the Fluorine-18 is a positron emitter with excellent characteristics for tomographic imaging.

The longest half-life of 18-F and its chemical reactivity have attracted great attention and a very large radiochemistry has grown around it.

The nucleophilic aromatic substitution with NCA(18F) fluoride ion was studied more than ten years ago (1) and actually can classify this reaction as a widespread method for the synthesis of high specific activity fluorine-18 radiotracers.

Recently, we have began to study the 18-F nucleophilic fluorination of heteroaromatic rings.

Such aromatic structures, containing one or more heteroatoms (i.e. nitrogen) are quite frequent in biological molecules potentially useful for PET studies. The reduced π-electron density owing to the with-drawing action of the heteroatom and the functional groups present on the ring, can facilitate the nucleophilic attack of the fluoride ion. In spite of these peculiarities, few examples of nucleophilic heteroaromatic fluorination are reported in literature (2). More recently several specific nucleophilic fluorination ($18\text{-}F^-/K^+$/Kryptofix 222/DMSO/ 155°C) of particularly substituted pyridazines, have been reported (3).

We have reported in this work a preliminary study on reactivity and positional selectivity of 18-F-fluoride on several substituted pyridine and diazine (Scheme I) in CH_3CN at 80°C. The (18-F) fluoro heteroaromatic compounds were isolated by liquid-liquid extraction and analyzed by radio-HPLC and compared to authentic "cold" samples prepared by specific syntheses.

Considering the electronic density of the 18-F fluoride ion ("naked" in the presence of the criptand agent) it is clear that a carbon atom, which is in an ortho/para position with respect to one or more aza groups, has a very low level of local electronic density (or high electron positive nature) and easily draws the 18-F anion by its high negative charge density. This is higly enhanced by the presence of de-activating (electron with-drawing) groups in appropriate position.

As a general comment, the soft conditions used in this study (useful for labelled syntheses of more complex biological molecules) does not permit to note the absolute reactivity of a single monosubstituted piridine (i.e. 2-Chloro) whose yield results very low.

However, considering this results as a starting point several considerations can be made in function of the structural and substituent modifications of the substrates:

a) An increase of the yield is observed when N-oxide-pyridine is used and, when present, the fluorine atom is a better leaving group than chlorine.

b) The presence of a second electron with-drawing group in the ring generally produces a net increase of the yield and the nucleophilic substitution is preferred when the second group is ortho/para with respect to the leaving group.

c) When we have two meta groups only when the aza group is between them we have a large increase of yield.

d) The presence of a second aza group does not modify the reactivity if the same substituents are present in the rings, but if the former is present in an activating position for the nucleophilic substitution the reactivity is increased at least of one order of magnitude;

e) Comparing the substitution yields of 2,4-dichloropyrimidine and 2,6-dichloro-3-nitro-pyridine, it can be observed that the presence of the nitro group, has the same inductive effect of the aza group.

REFERENCE:

(1)- Cacace F., Speranza M., Wolf A.P. and Fowler J.S. - J.Label.Compds.Radiopharm. 18:1721 (1981);

Angelini G., Speranza M., Wolf A.P. and Shiue C-Y. - J.Fluorine Chem. 27: 177 (1985);

Shiue C-Y., Watanabe M., Wolf A.P., Fowler J.S. and Salvadori P.- J.Label. Compds.Radiopharm. 21: 533 (1984).

(2)- Clark J.H. and Macquarrie D.J.- Tetrahedron Letts. 28: 111(1987).

(3)- Mourad A. and Kilbourn M.R.- Eighth Int.Symposium Radioph.Chem.Princeton : 137 (1990).

SCHEME I

Heteroaromatic rings $\xrightarrow[CH_3CN,\ 80°C,\ 30']{18F^-/K^+/K222}$ Fluorinated Products

Pyridines

L	R	Yield(%)
2-Cl	H	2
2-Cl,N-Oxide	H	5
2-F	H	15
3-Cl	H	6
3-F	H	9
2-Cl	3-NO2	24
2-Cl	5-NO2	7
2-Cl	6-Cl	46 a)
2-Cl	3-Cl	24 b)
2-Cl	5-Cl	22 b)
3-Cl	5-Cl	3 a)
2-Cl	3-NO2, 6-Cl	54 c)
6-Cl	3-NO2, 2-Cl	19 c)

Dichlorodiazines

3,6 Dichloro-pyridazine	4.5 a)
2,4 Dichloro-pyrimidine	74 d)
2,6 Dichloro-pyrazine	44 a)

a) single positional yield; b) monoproduct; c) total yield:73%; d) the value schedule is the total yield. Radio-HPLC analysis (as indicate below, flow 0.8ml/min): 2-(18F):60% and 4-(18F):40%.
Radio HPLC analysis: isocratic condiction (H_2O :82, CH_3CN:18) flow: 1.0ml/min, column: LC-ABZ Supelco, radioactive detector: Beckman 170, UV detection:254 nm.

5-[^{18}F]Flurouracil - The Problem of Metabolites in Tissue

LUTHRA*, S.K.; OSMAN, S.; HUME, S.; TILSLEY, D.W.O.; VAJA, V.; BROWN, G.; HARTE, R.J.A.; JONES, T.; PRICE, P.M. and BRADY, F. Medical Research Council*, Cyclotron Unit and Royal Postgraduate Medical School, Hammersmith Hospital, Ducane Road, London W12 OHS.

5-Flurouracil (5-FU) is an important anti-cancer agent in extensive clinical use. However, 80% of tumours fail to respond. Currently, biochemical modulators are being used to improve the efficacy of 5-FU[1]. We are investigating the effect of these modulators in man with PET using 5-[^{18}F]FU. However, 5-FU is rapidly catabolised *in vivo* to α-fluoro-β-alanine (FBAL)[2,3] and "contamination" of the PET signal by this metabolite currently restrains data interpretation[4]. Approaches to metabolite correction of human tissue PET data are limited. This is a basic methodological problem that must be overcome if PET is to make a contribution. In the case of 5-FU, one approach would be to label FBAL with fluorine-18 and follow its kinetics in man. We are in the process of developing this synthesis. As a preliminary we have (i) followed the kinetics of 5-[^{18}F]FU in the rat with PET, corrected the data at selected time-points for [^{18}F]FBAL by analysing tissue samples by HPLC, (ii) recovered [^{18}F]FBAL from rat urine, reinjected it into another rat and followed its kinetics using PET. Both of these approaches allow correction of the 5-[^{18}F]FU tissue data for [^{18}F]FBAL in the rat.

(i) 5-[^{18}F]FU at tracer dose[5] was injected via tail-vein into Sprague-Dawley rats and serial blood, tissue and urine samples were taken. Blood and tissue samples were processed before analysis and urine samples were directly injected onto the HPLC column. Proteins were removed by methanol precipitation of cell free plasma. Tissue samples were homogenised and the activity extracted using methanol. Methanol extracts were rotary evaporated and the residue taken up in HPLC solvent. Solutions were injected onto a Nucleosil 5-C_{18} column (5 μm, 25 cm x 10 mm i.d.) eluted with ammonium formate (0.1M) at a flow rate of 3.0 mLmin^{-1}. The HPLC eluent was monitored for UV absorbance and radioactivity. Both detectors were linked to a PC based integrator and the 5-[^{18}F]FU and [^{18}F]FBAL content obtained from the integrated radioactivity traces. From preliminary studies, the percent of 5-[^{18}F]FU and [^{18}F]FBAL in rat plasma, liver, kidney and urine over an hour is shown in Table 1.
(ii) Using the above system [^{18}F]FBAL was isolated from rat urine, formulated and reinjected into another rat. A PET study was carried out and the time activity profile of [^{18}F]FBAL in the liver, kidney and heart is shown in Fig. 1.

We have carried out PET studies using 5-[^{18}F]FU in man at tracer (< 10 mg/m^2) and therapeutic (400 mg/m^2) doses of 5-FU. Serial blood samples were taken and analysed as above. Typical HPLC traces of plasma samples are shown in Fig 2. At a tracer dose rapid metabolism of 5-[^{18}F]FU was observed (Fig 3). The level of unchanged 5-[^{18}F]FU at a tracer dose was 12 ± 5% and at therapeutic dose 77 ± 5% at 10 min post-injection, illustrating the saturation of 5-FU catabolism.
Two approaches to correcting 5-[^{18}F]FU rat tissue PET data for 5-[^{18}F]FBAL are presented. The kinetics of [^{18}F]FBAL have been characterised in the rat. A compartmental model is being developed. It is anticipated that this model will be applicable in studies of normal and tumour tissue in man.

1. Yarbro J.W., Bornstein R.S. and Mastrangelo M.J. (Eds.), Seminars in Oncology, Recent Developments in Biomodulation: Second International Workshop on Gastrointestinal Cancer, 19: Suppl 3 (1992).
2. Strauss L.G. and Conti P.S. - J. Nucl. Med. 32: 623(1991).
3. Zhang R., Soong S.-J., Liu T., Barnes S. and Diasio R.B. - Drug Metab. Disp. 20: 113(1992).
4. Heggie G.D., Sommadossi J.-P., Cross D.S., Huster W.J. and Diasio R.B. - Cancer Res. 47: 2203(1987).
5. Brown G.D., Khan H.R., Steel C.J. *et al.* - J. Label. Compd. 32: 521(1993).

Table 1. 5-[^{18}F]FU and [^{18}F]FBAL in rat following injection of 5-[^{18}F]FU at tracer dose.

TIME	PLASMA		LIVER	KIDNEY		URINE	
(min)	5-[^{18}F]FU (%)	[^{18}F]FBAL (%)	[^{18}F]FBAL (%)	5-[^{18}F]FU (%)	[^{18}F]FBAL (%)	5-[^{18}F]FU (%)	[^{18}F]FBAL (%)
2.5	58	42	-	37	63	-	-
5	44	56	100	3	97	81	19
15	17	83	100	-	-	-	-
30	6	84	100	-	-	-	-
60	0	100	100	1	99	20	80

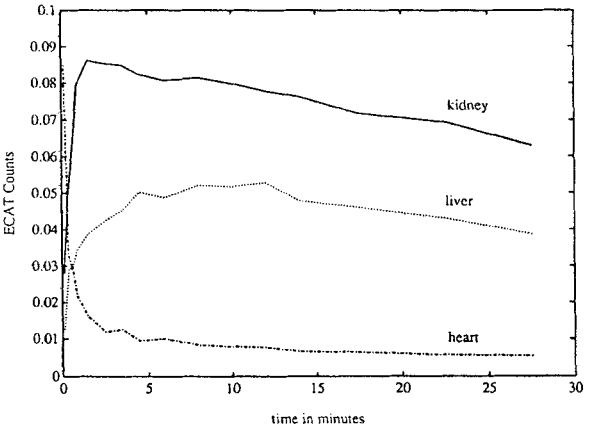

Figure 1. Time activity profile of [^{18}F]FBAL in rat from PET study.

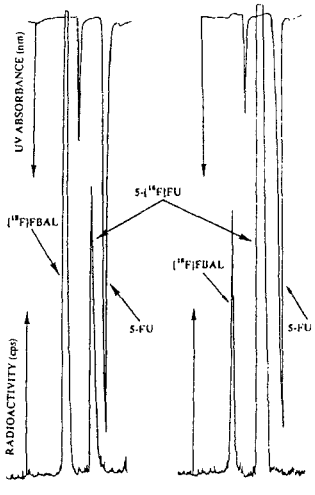

5-[^{18}F]FU at a tracer dose

5-[^{18}F]FU co-injected with 5-FU at therapeutic dose

Figure 2

Typical HPLC traces of 5-[^{18}F]FU and its metabolites in human plasma at 5 min.

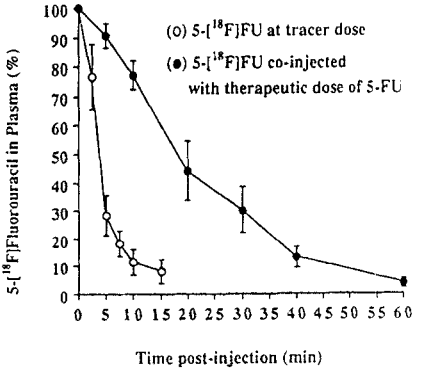

Figure 3

The level of unchanged 5-[^{18}F]FU in human plasma with time.

Chemistry of Radionuclide, Ligand and Radiopharmaceutical as an Aid to Achieve Radionuclide-Lesion Affinity during Radionuclidic Detection and Therapy of Cancer

SHUKLA, S.K.[a,b]; CIPRIANI, C.[a]; ARGIRO', G.[a]; SCHOMÄCKER, K.[c]; LIMOURIS, G.S.[d]; OSSICINI, L.[b]; CRISTALLI, M.[b]; ATZEI, G.[a]; BOEMI, S.[a] a) Servizio di medicina Nucleare, Ospedale S. Eugenio, Roma; b) Istituto di Cromatografia, C.N.R., Roma, Italy; c) Klinik u. Poliklin., Universitätskliniken, Köln, Germany; d) Nuclear Medicine Sec., Areteion University Hospital, Athens, Greece.

In conclusion of his article (1): Horizons in radionuclide therapy: 1985 Update, Beierwaltes wrote: "Many cancer therapists agree that surgery, teletherapy, and chemotherapy are crude and nowhere near as effective as we want them to be, and what is really needed is an innovative, effective, and less harmful form of cancer therapy - radionuclide therapy has begun to demostrate that potential". Even after 5 years following that statement, there is unfortunately no radiopharmaceutical which in vivo behaves only as lesion-seeking (2,3). During more than 3 past decades the main object of our research has been: I. to study the cause of this nonspecificity of the radionuclide, administered as simple compound or as labelled targetting agent, commercially available, and II. to find conditions under which the radionuclide could be made lesion-affine. This has permitted us to do early diagnosis and effective therapy of some types of cancer. The radionuclide-tumour affinity has been realized by: I. choosing chemically suitable radionuclide, II. choosing suitable ligand, and III. keeping the patient on suitable diet which favours the integrity and uptake of the radionuclide from the radiopharmaceutical injected.

I. Chemically suitable radionuclide for cancer diagnosis and therapy

So far radionuclide physical properties (short half-life, monochromatic gamma-emission of energy 150 KeV, nonradioactive daughter), easy availability, and low cost have been main conditions for the choice of a radionuclide for radionuclidic diagnosis, while beta- and alpha-emitting radionuclides are being tried to treat cancer. Seventh group element radionuclides, I-131, I-123, and Tc-99m have so far been most popular radionuclides in nuclear medicine procedures. According to a recent estimate, ^{99}Mo-^{99m}Tc-generator produces Tc-99m radiopharmaceuticals, compounded with simple ligands or targetting agents (antibodies, liposomes, peptides, or receptors) constitute 90% of all nuclear practices performed. Chemical considerations, however, make these high oxidation state, 7+, unsuitable for the synthesis of stable radiopharmaceutical. Tc-99m radiopharmaceuticals in oxidation state 7+, 5+, and 4+, etc., get easily hydrolysed in aqueous solution, usually used for the preparation and administration of radionuclide, and high liver, spleen, and bone marrow activity is observed which renders the diagnosis very difficult.

Although III group element radionuclides, Ga-67, In-111, Tl-201, Y-90, and Sm-153, have found application in radionuclidic diagnosis and therapy of cancer, their total-body distribution in cancer patients injected with commercially available radiopharmaceuticals is equally tumour-nonspecific showing high concentration again in the liver, spleen and bone marrow. We found the central element of the Periodic Table, gallium, biochemically

very interesting due to its high charge density, 4.84. Its radionuclide, Ga-67, has been used in tumour diagnosis since 1969, and the cold gallium has been used in chemotherapy of cancer. It has a very interesting therapeutic counterpart, Y-90, a pure beta emitter of 2.27 MeV with half-life of 64 h. For our radionuclidic diagnosis and therapy research work we selected, therefore, the radionuclide couple Ga-67 -- Y-90. The stable oxidation state, 3+, of these radionuclides with high charge density permits the preparation of cationic, neutral and anionic species of the radionuclides in pure form by varying the nature and concentration of the ligand. Their higher and left homologues, on the other hand, make cationic complexes easily while lower and right ones favour the formation of covalent or anionic complexes preferentially.

We prepared chromatographically and electrophoretically pure species of Ga-67 in aqueous solution using different ligands and used them as probes for studying the biochemical nature of cancer. By studying the radionuclide tumour-uptake in different types of cancer-bearing subjects injected with cationic or anionic Ga-67, we could classify tumours into two groups:

I. Cationic Ga-67-Affine Tumours: Lung cancer, thyroid cancer, neuroblastoma, Hodgkin's disease, Morris hepatoma-3924A, skeletal metastases from prostate or breast cancer, ...
II. Anoinic Ga-67-Affine Tumours: Breast cancer, prostate cancer, melanoma, hepatoma, osteosarcoma, Ewing's sarcoma, fibrosarcoma, liposarcoma, ...

Although the preparation of both anoinic and cationic radionuclide complexes in pure form in aqueous solution has been difficult with radionuclides of higher and lower oxidation state, their total-body uptake confirmed the affinity of tumours with other radionuclide species as well. Thus the new tumour classification according to their affinity for radionuclide species in aqueous solution is:

I. Cationic Metal Complex-Affine Tumours, and II. Anoinic Metal Complex-Affine Tumours. We confirmed this affinity by studying the radionuclide as well as the metal ionic complex species of In-111, In-114m, Tl-201, Tc-99m, Sm-153, and Y-90.

II. Ligands for the Formation of Pure Tumour-Affine Radiopharmaceuticals. Chromatographic and electrophoretic study of the nature and stability in aqueous solution of the radionuclides in neutral chloride, nitrilotriacetate (NTA), EDTA, and DTPA showed that citrate ion is a very suitable ligand for the formation of cationic, neutral and anionic species of metal radionuclides, because unlike the ligands of lower complexing capacity, e.g., Cl^-, Br^-, etc., the radionuclide species are not hydrolysed, and the radionuclide from citrate-radionuclide complexes is easily bound to tumour components, while it is very slow with stronger complexes formed with ligands, e.g., NTA, EDTA, or DTPA, where major portion of the soluble radionuclide complex is also eliminated through the kidney.

We made citratocomplexes of Ga-67 and Y-90 and studied their chemical properties chromatographically and electrophoretically. The tumour-affinity was examined by total-body radionuclide distribution. The total uptake of both cationic and anionic

radionuclide species is complete within 4 h postinjection of the tumour-affine radiopharmaceutical. The radionuclide binds strongly in the tumour and is homogeneously distributed. It remains bound to the tumour permitting the follow-up studies during nearly ten days. At pH 7, no side effect of the therapy with Y-90 is observed.

The labelling of antihepatoma antibody, hepama-1, studied by us yielded chromatographically and electrophoretically pure product. We made pure radionuclide species react with chemically suitable form of the antibody. Total-body distribution of both Ga-67-, and Y-90-hepama-1 showed high tumour specificity of the radiopharmaceutical in nude mice with human hepatocellular carcinoma transplants. The studies with Ga-67- and Y-90-hepama-1 for radioimmunoscintigraphy and radioimmunotherapy in patients are in progress.

III. Choice of Dietary Factors for Getting High Radionuclide-Tumour Specificity in Vivo. The nature of radionuclide species in extracts of some foods and usual drinks was studied chromatographically and electrophoretically. We also studied the effect of foods and drinks on the radionuclide distribution in cancer-bearing subjects injected with tumour-affine radiopharmaceuticals.

Ingestion of solid food, coffee and caffein containing drinks had adverse effects of the tumour-affinity of radiopharmaceuticals in vivo. Food intake increased the intestinal concentration of the radionuclide. The patients were therefore advised to be on fast before the radiopharmaceutical administration and to avoid solid food at least 3 hours after the injection.

Coffee and caffein containing drinks (tea, coca-cola, pepsi, etc.) reacted with the radionuclide of the radiopharmaceutical and formed insoluble radionuclide species which made the radionuclide concentrate in the liver spleen and bone marrow. The intake of such drinks was therefore discouraged before and after the administration of the radiopharmaceutical and especially during the whole period of radionuclidic therapy with Y-90 radiopharmaceuticals.

Acidic drinks favoured the uptake of the cationic metal radionuclide radiopharmaceuticals in the tumour. In such patients sweet fruit juice had adverse effect on the diagnostic or therapy results.

Sweet orange, mandarine or clementine juice favoured the stability of anoinic metal radionuclide complex radiopharmaceuticals and also of the Ga-67 or Y-90-labelled antibodies. The intake of such drinks some hours before the injection of such radiopharmaceuticals to cancer-bearing subjects was therefore advised. The patients were asked to drink such fruit juices often during the examination of the disease and during the therapy.

References

1. Beierwaltes, W.H. - J. Nucl. Med. 26: 421 (1985).
2. Tilou S.M. - J. Nucl. Med. 31(12): 15A (1990).
3. Malmud L.S. - J. Nucl. Med. 33(3): 31N (1992).

Novel Approach for Tumor Detection by Focusing on Hepatic Metallothionein Level.

TAKEDA, A.; TAMANO, H.; SATO, T.; and OKADA S. Department of Radiobiochemistry, School of Pharmaceutical Sciences, University of Shizuoka, Shizuoka.

As a new approach for the detection of early-stage malignant disease by radio-imaging, we have focused on the variations in the hepatic level of metallothionein (MT), a trace metal-binding protein involved in the maintenance of homeostasis of essential trace metals such as zinc (Zn) and copper (Cu)[1-2]. Actually, it has been reported that in tumor-bearing subjects the Zn level in liver, which itself showed no carcinomatous invasion, was significantly higher than that in controls[3-4].

Recently we found a tumor growth-dependent elevation of hepatic levels of MT and Zn in mice and rats bearing experimental solid tumors (Ehrlich, L-1210, AH7974F, etc.) in the inguinal region[5]. Furthermore, hepatic MT levels were found to be significantly and continuously elevated from the early stage of pancreatic adenocarcinoma in hamsters and of hepatoma in rats, induced by the treatment with N-nitrosobis(2-oxopropyl)amine (BOP) and 3'-methyl-dimethylaminoazobenzene (3'-Me-DAB), respectively. In the hepatoma-induced rats, this elevation preceded that of serum γ-glutamyl transpeptidase (γ-GTP) activity. The elevation of hepatic MT level occurred similarly in mice received experimental lung metastasis. On the other hand, both in mice having inflammation caused by the s.c. injection of turpentine or carrageenan and in rats having pancreatitis caused by the administration of deoxycholate, the hepatic MT levels elevated only transiently. These results suggest that radiological measurement of hepatic MT level is useful for the detection of early-stage malignancy.

The induction of hepatic MT in tumor-bearing mice was compared with that in inflammation-induced mice. When mice were s.c. transplanted with Ehrlich tumor cells or s.c. injected with turpentine after being fed a Zn-deficient diet (2 mg Zn/kg) for 1 week, the hepatic MT levels did not increase in the tumor-bearing mice but increased in the turpentine-injected mice. Further, when the mice 2 days after transplantation of the tumor cells were fed on the Zn-deficient diet, the hepatic MT level lowered with the time after the replacement of diet during the tumor growth. This suggests that the induction of MT in the tumor-bearing mice required an increase of Zn in liver prior to MT synthesis, while in the inflammation-induced mice this was not the case.

Next, dexamethasone, an inducer of MT synthesis, was used to further reveal the difference between the hepatic MT inductions by tumor and inflammation. Dexamethasone stimulated MT synthesis in liver of the tumor-bearing mice, but inhibited that of the inflammation-induced mice. These results suggest that the mode of

induction of hepatic MT in the case of tumor is different from that in the case of inflammation and that the measurement of the variation of hepatic MT level may enable a discriminative detection of tumor and inflammation.

In order to detect tumor by means of the radio-imaging of hepatic MT level, a trial to measure the level was performed using ^{65}Zn. When $^{65}ZnCl_2$ was i.v. injected into the mice and rats s.c. transplanted with Ehrlich tumor cells and ascites hepatoma 7974F (AH7974F), respectively, ^{65}Zn distribution in the livers 1 h after injection increased with the growth of tumors. Sephadex G-75 elution profile of the cytosol fraction of liver showed that the elevation of ^{65}Zn level was due to that of the MT level. At 2 days after tumor transplantation in mice, ^{65}Zn-image demonstrated elevation of hepatic MT level, while currently utilized ^{67}Ga-citrate was not sufficient to image the tumor at such early period of growth. Further, in livers of the tumor-bearing and inflammation-induced mice which were also treated with dexamethasone, ^{65}Zn-image closely reflected the variation of MT level, indicating that ^{65}Zn-imaging of MT level may be useful for discrimination between tumor and inflammation. These results suggest that the radio-imaging of hepatic MT level by use of a short-life gamma or positron emitting isotope, e.g., ^{69m}Zn or ^{62}Zn, would be useful to detect malignancy at the early stage.

References

1. Cousins R.J.- Physiol.Rev. 65: 238 (1985).
2. Bremner I. and Beattie J.H.- Annu.Rev.Nutr. 10: 63 (1990).
3. Wright E.B. and Dormandy T.L.- Nature 237: 166 (1972).
4. Griffith K., Wright E.B., and Dormandy T. L. - Nature 241: 60 (1973).
5. Takeda A., Sato T., Tamano H. and Okada S.- Biochem. Biophys.Res.Commun. 189: 645 (1992).

Stability of Antisense Radiopharmaceuticals: Effect of Beta-energy on the Degradation of Phosphodiester vs. Phosphorothicate Derivative of DTPA-conjugated Deoxyoligonucleotides.

M.K. DEWANJEE, A.K. GHAFOURIPOUR, A.T. SAMY, A.N. SERAFINI, G.N. SFAKIANAKIS. Division of Nuclear Medicine, Department of Radiology, University of Miami, Miami, FL 33136

Due to high tumor-specificity and membrane permeability, the antisense radiopharmaceuticals provide an efficient avenue for delivering ß-emitting radionuclides to the tumor cells for effective therapy by inducing DNA degradation. Antisense radiopharmaceuticals (ASRP) were labeled with I-125 and Sm-153 radionuclides (1-4). The c-myc oncogene is amplified in several types of cancer (leukemia, colon/rectum, breast, prostate and lung); the c-myc mRNA was used as a model cytoplasmic receptor-like target for noninvasive imaging of oncogene activation. Effect of storage temperature on the stability of ASRP was studied at -4°C and 25°C. In spite of oncogene activation and amplification, the number of oncogene mRNAs in cancer cells is much lower than the corresponding membrane-associated tumor antigens, suggesting the need for development of ASRP at high specific activity. This goal was achieved for I-125 and Sm-153 radionuclides. The radiolabeling (1-4) was carried out by conjugation of oligonucleotide with paramethoxyphenyl-isothiocyanate (PMPITC) for radioiodination and conjugation with DTPA-isothiocyanates for chelation with metallic radiounuclides (In-111, Tc-99m, Ga-67, Sm-153).

The kinetics of degradation of Sm-153 labeled antisense (AS), sense (SN, control) and oxo and thio derivatives by P388 cells was evaluated. The 15-mer oligonucleotide sequence for the initiation-codon domain was synthesized, aminolinked [sense (SN) and antisense (AS) phosphodiester (O) and monothioester (S)] and coupled to isothiocyanate of DTPA and aliquots (10μg) were lyophilized. Sm-153 (100-500 μCi) was chelated to probes; aliquots of 1-2 μCi (0.1 μg) was added to P388 cells ($10X^6$ cells/ml in log [L, exponentially growing] and plateau [P] phase growth in nutritionally deprived media) and incubated at 37°C for 10, 20, 40 and 60 minutes, washed and cell-uptake CU(%) was determined.

The antisense deoxyoligonucleotides are degraded by endo- and exonucleases; the degradation rate is higher at higher temperature. Conjugation of deoxyoligonucleotides with polyaminopolycarboxylates generates steric hindrance for the nucleases. The phosphorothioate derivatives are more nuclease-resistant than phosphodiester. This advantage is partially lost when the deoxyoligonucleotides are conjugated with ß-emitting radionuclides. The technique of radiolabeling with Sm-153 is shown in Figure 1. The kinetics of hybridization of I-125 and Sm-153 antisense probes with P338 cells and purified mRNA is shown in Figure 2. The hybridization efficiency is almost one-third of that obtained with In-111 labeled antisense probe in the same leukemic cells; the I-125 probe had the least hybridization. This lower value may result from lower specific activity, higher probe degradation rate and loss of cellular radioactivity due to enhanced cell-lysis.

References

1. Dewanjee M.K. and Preiss I.L. - Decay of samarium isotopes ^{141}Sm, ^{141}Sm, ^{142}Sm and $^{143(m+g)}$Sm. J Inorg Nucl Chem 34: 1105-1 117(1972)

2. Dewanjee M.K. and Kahn P.C. - Myocardial mapping techniques and the evaluation of In-113m labeled polymethylenephosphonate for myocardial imaging. Radiology 117: 723-

726(1975)
3. Dewanjee M.K., Ghafouripour A.K., Werner R.K., Serafini A.N., Sfakianakis G.N. - Development of sensitive radioiodinated anti-sense oligonucleotide probes by conjugation technique. Bioconj Chem 2: 195-200(1992)
4. Dewanjee M.K. - Radiolabeled antisense oligonucleotides: diagnosis and therapy. Diagnostic Oncology (1993)

Supports by NHLBI (HL47201, Shannon Award), NIH-NS22603-08, Baxter Healthcare Corporation, Department of Energy grant DE-FG05-88ER60728 and Florida High Technology and Industry Council are gratefully acknowledged.

Figure 1. General scheme of radiolabeling of antisense deoxyoligonucleotide probes with DTPA-derivatives for labeling with Sm-153 radionuclide.

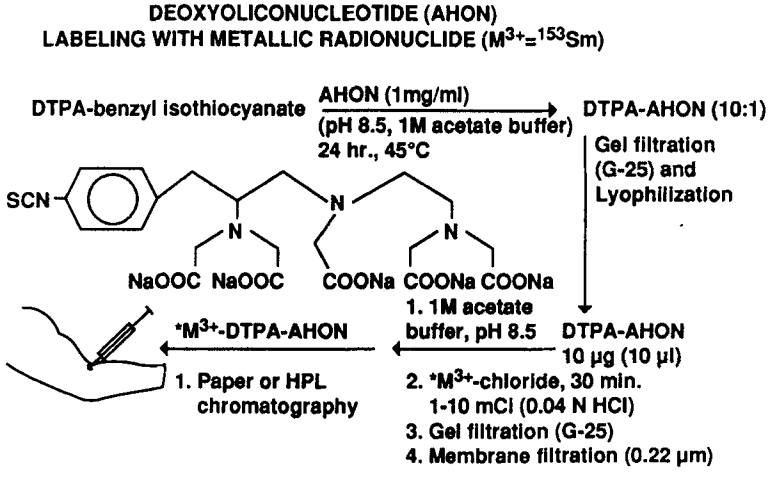

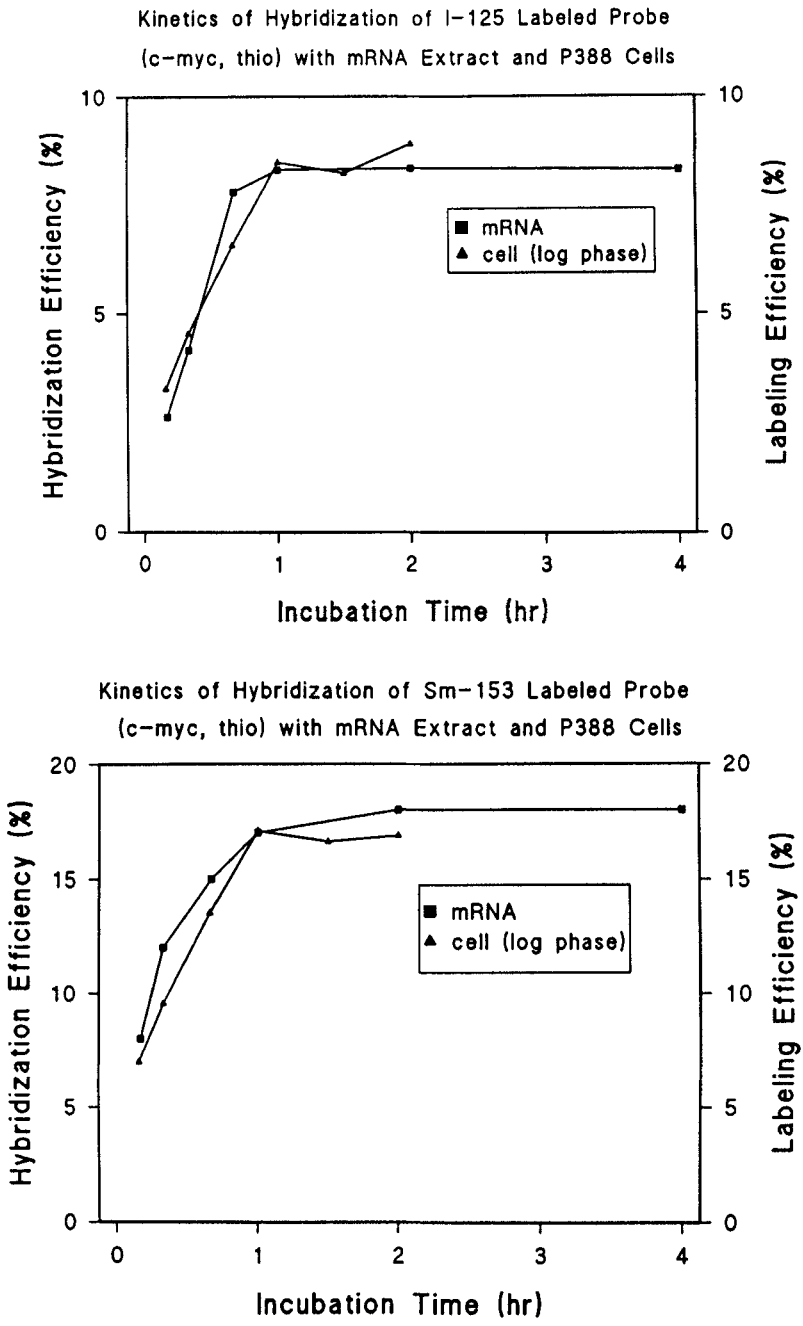

Figure 2. Kinetics of intracellular hybridization of c-myc oncogene mRNA with I-125 and Sm-153 labeled antisense deoxyoligonucleotide (SMASDON) probes in leukemic cells (P388).

SOMATOSTATIN RECEPTORS ON TWO HUMAN CANCER CELL LINES: CLINICAL IMPLICATION IN NUCLEAR MEDICINE.

AMARTEY, J.K*., PARHAR R.S., and AL-SEDAIRY S.T. King Faisal Specialist Hospital & Research Centre, MBC-3, Box 3354 Riyadh 11211, Kingdom of Saudi Arabia.

Bioactive peptides have played a major role in the detection and management of certain tumors. One of these peptides is somatostatin and the analogs (1-3).

Recently the synthesis and partial characterization of ^{99m}Tc-labeled somatostatin and analogs was described (4). We now report additional *in vitro* characterization of the complex. An efficient radioiodination method has also been developed for labeling these peptides for comparative studies. Binding assays and cell growth inhibition studies were performed on two human cancer cell lines, small cell lung cancer (HTB-119) and breast cancer (HTB-121) cell lines *in vitro*.

The radioiodination was carried out by a modified chloramine-T method, which gave a better and cleaner product than the other methods attempted. In brief, the peptide and chloramine-T were dissolved in 0.05M phosphate buffer, pH 7.5. The required amount of ^{125}I-NaI was added to the peptide followed by chloramine-T, in a total reaction volume of 50 ul. The reactants were incubated for 60 seconds. The reaction mixture was then analyzed by HPLC on Econosil C-18, 10u, 250 x 4.6mm column. The eluent used was 50:50 v/v of acetonitrile:0.05M ammonium acetate containing 2mM tetrabutylammonium hydroxide, pH 7.0 and at a flow rate of 1.5 ml/min. One minute fractions were collected. The isolated product was lyophilized and stored at -20^{o}C. The radiochemical purity was greater than 99% on ITLC-SA in acetone, and an estimated specific activity >1850 GBq/mmol (50 Ci/mmol). The technetium complex was synthesized according to the method previously described (4).

The results of the binding data is shown in table 1. The radioiodinated somatostatin analog revealed two types of receptors; a high affinity but low capacity and low affinity but higher capacity sites on the small cell lung cancer cells (HTB-119). However, the ^{99m}Tc-SS-14 complex showed only one set of relatively high affinity site. The human breast cancer (HTB-121) cells showed a single high affinity binding site. The values obtained were similar to those obtained with radioiodinated material from a commercial source. The biodistribution of the Tc-complex in normal rats was reported previously (4). Dose dependent cell growth inhibition (as was measured by ^{3}H-thymidine uptake) was observed in both cell-lines. The inhibition data for HTB-119 is shown in figure 1.

These results suggest that radiolabeled somatostatin and analogs may be of potential clinical application for the detection, planning and monitoring of (SS-receptor positive tumor) cancer treatment and further studies are in progress.

References.

1. Bakker W.H., Krenning E.P., Breeman W.A. et al. J. Nucl. Med. 31: 1501 (1990)
2. Bakker W.H., Albert R., Breeman W.A., et al. J. Nucl. Med. 32: 1084 (1991)
3. Schally A.V. Cancer Res. 48: 6977 (1988)
4. Amartey J.K. Nucl. Med. Biol. (1993) In press

Figure 1. The inhibition of HTB-119 cells by SRIF in vitro

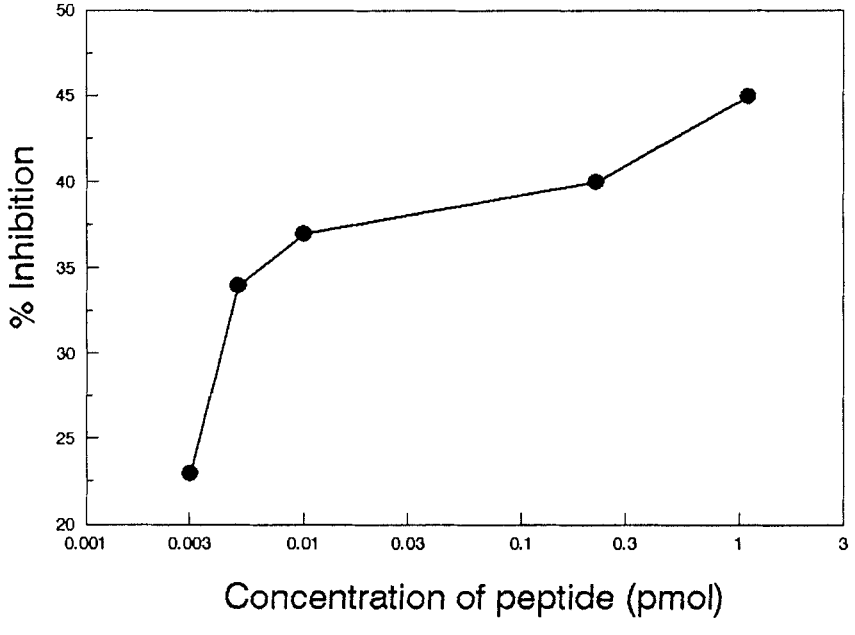

Table 1. The results of the Scatchard analysis of the binding data on the cell lines using the two radioligands.

	Kd. (pM)	Bmax. (pM)
HTB-119 Cell-line		
I-125-tyr(1)-SS-14	33.5	3.5
	3060	16.4
Tc-99m-2IT-SS-14	1873	85.0
HTB-121 Cell-line		
I-125-tyr(1)-SS-14	2340	77.8
Tc-99m-2IT-SS-14	ND	ND

RADIOLABELED LIPOSOMES FOR TUMOR IMAGING

OGIHARA-UMEDA, I.; SASAKI*, T.; and NISHIGORI, H.
*Faculty of Pharmaceutical Sciences, Teikyo University, Suarashi 1901-1, Sagamiko, Tsukui, Kanagawa 199-01, JAPAN; *Division of PET Center, Tokyo Metropolitan Institute of Gerontology, Sakae-cho, Itabashi, Tokyo 173, JAPAN*

Liposomes, or artificial lipid vesicles, are one of the most promising drug carriers because of their biodegradability, ease of preparation, and non toxicity. Their distribution and pharmacokinetics can be modified by changing their size, charge, lipid composition and so on (*1*). These properties also make liposomes attractive as radiopharmaceuticals. Some attempts have been made to apply liposomes as tumor imaging agents by encapsulating gamma-emitters in them (*2-8*), and some clinical trials have been already done (*9, 10*). However, systematic studies on the relation between the tumor imaging capacity of liposomes and their distribution and pharmacokinetics have been scarcely made until now. In this paper, we searched optimal liposomes for tumor imaging and studied what factors were essential to them.

Materials and methods

Preparation of radiolabeled liposomes. Lipids used in this work were as follows: L-α-phosphatidylcholine from frozen egg yolk (PC), L-α-dimiristoylphosphatidylcholine(DMPC), L-α-dipalmitoylphosphatidylcholine(DPPC), L-α-distearoylphosphatidylcholine(DSPC), L-α-diarachidoylphosphatidylcholine(DAPC), sphigomyelin from bovine brain (SM), and cholesterol (CH). Multilamellar liposomes (MLV) and small unilamellar liposomes (SUV) were prepared as previously described (*3,5*). For the experiments on the effects of particle size, liposomes were prepared from DSPC and CH (molar ratio, 2:1). On the effect of the phospholipid component, they were prepared from various phospholipids and CH (2:1). To study on effects of CH content, DSPC was used as the liposomal base. Each liposome preparation was encapsulated ^{67}Ga-nitrilotriacetic acid (NTA) complex by the loading method (*3, 5*).

Tumor models. Ehrlich solid tumor or Sarcoma 180 (2×10^6 cells/mouse) was subcutaneously transplanted to the left hind leg of male ddY mice, 6-7 week-old. Lewis lung carcinoma (3LL) or B16 melanoma (1×10^6 cells) was transplanted to male C57Bl/6 mice, and MH134 hepatoma (5×10^5 cells) or MM46 carcinoma (1×10^6 cells) was transplanted to male C3H/He mice, respectively. When the tumor weighed between 0.1 and 0.5 g, mice were used for the following experiments.

In vivo and in vitro studies. Tissue distribution of ^{67}Ga radioactivity after the intravenous injection of liposomes was determined as described earlier (*3*). Blood clearance of liposomes was evaluated using high performance liquid chromatography (HPLC) with a gel permeation column (*6*). Liposome stability in vitro was assayed as previously described (*5*).

Results

Radionuclide delivery to the tumor by various liposomes. Figure 1 shows the ^{67}Ga accumulation in the tumor of mice bearing Ehrlich solid tumor 24 h after the intravenous injection of various liposomes encapsulating ^{67}Ga-NTA, that were different in the particle size, phospholipid components, or cholesterol contents. All of these three factors had a great influence upon ^{67}Ga tumor uptake. It was found liposomes that were fairly small (0.08μm in diameter), CH-rich (molar ratio of DSPC:CH; 1:0.5 or 1:1) and composed of so-called rigid phospholipids (DSPC, DAPC and SM), that had high temperature phase transition acylmoieties, could deliver a large amount of radionuclides to the tumor (10-13% of administered dose(AD)/g). Under the same conditions, tumor uptake of ^{67}Ga-citrate, which is clinically used as a tumor-imaging agent, was 4.3%AD/g.

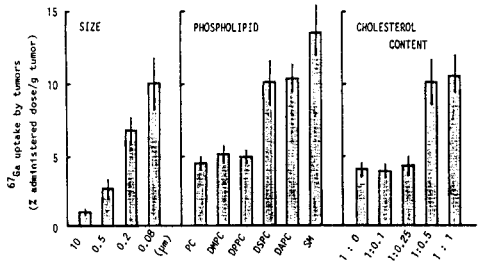

FIGURE 1 Tumor uptake of ^{67}Ga in mice bearing Ehrlich solid tumor at 24 h after the administration of various liposomes encapsulating ^{67}Ga-NTA.

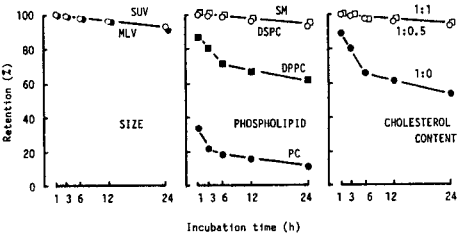

FIGURE 3 Stability of various liposomes in serum at 37°C *in vitro*.

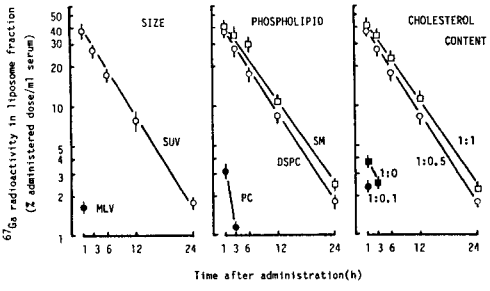

FIGURE 2 Blood clearance of various liposomes in mice bearing Ehrlich solid tumor.

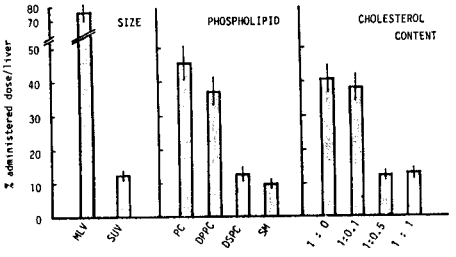

FIGURE 4 Liver uptake of ^{67}Ga in mice bearing Ehrlich solid tumor at 1 h after the administration of various liposomes encapsulating ^{67}Ga-NTA.

Blood clearance of liposomes. Figure 2 shows the blood clearance of various liposomes in Ehrlich tumor-bearing mice. The amount of intact liposomes existing in serum was determined with the HPLC analysis by monitoring ^{67}Ga radioactivity in liposome fraction. It became apparent that the small, rigid, CH-rich liposomes remained in the blood circulation for a much longer time than the other ones.

Liposome stability in serum in vitro. The stability of liposomes was estimated by the retention of ^{67}Ga in liposomes incubated at 37°C with fresh mouse serum. As shown in Fig. 3, rigid and CH-rich liposomes were fairly stable during 24 h incubation in serum. However, liposomal size had no effect on the liposome stability.

Liposome uptake by the reticuloendotherial system (RES). Figure 4 shows ^{67}Ga accumulation in the whole liver of tumor-bearing mice 1 h after the i. v. injection of liposomes encapsulating ^{67}Ga-NTA. It was clear that the liver uptake of small, rigid, CH-rich liposomes was much lower than the other liposomes. In the spleen uptake, similar results were obtained (data not shown).

Tumor uptake and tumor-to-blood ratio of ^{67}Ga delivered by liposomes in various tumor models. Liposomes composed of DSPC and CH (molar ratio; 2:1) and encapsulated ^{67}Ga-NTA, were administered to various tumor-bearing mice. Tumor uptake and tumor-to-blood ratio (T/B) 24 h after the administration were shown in Fig. 4. The result with ^{67}Ga-citrate is also shown. In every tumor model, high tumor uptake and excellent T/B were obtained. Those values were 1.5-4 times higher than those with ^{67}Ga-citrate in the same tumor model.

Discussion

In this paper, we showed that the tumor accumulation of radionuclides delivered by liposomes was varied by the particle size, phospholipid component and CH content of liposomes, and if appropriate conditions were chosen, large tumor accumulation was obtained, that would be enough for tumor imaging. The appropriate conditions are namely being fairly small in particle size, composed of rigid phospholipids, and CH-rich. We have confirmed that the tumor uptake of liposomes themselves was high when they had such physical properties (data not shown). In the pharmacokinetic and distribution studies, it was revealed that liposomes that could deliver a large amount of ^{67}Ga to the tumor exhibited prolonged blood circulation (Fig. 2), and they were fairly stable in serum (Fig. 3). Their uptake by the RES was much lower than the other liposomes (Fig. 4). These observations indicated that the physical properties of liposomes described above made them fairly stable in serum and reduced the uptake of liposomes by the RES, and consequently retained a large amount of liposomes in the circulation for a long time. Liposomes that have long half lives in the circulation are expected to have a greater opportunity to come into contact with the tumor and to be taken up by it, resulting in greater ^{67}Ga accumulation in the tumor. Radiolabeled liposomes that have long half-lives in the circulation gave the high tumor uptake and T/B values in various tumor models (Fig. 5), suggesting they would be an excellent tumor imaging agent. The results shown here suggest that the stability in serum and reduction of RES uptake were important factors for enhancing radionuclides delivery to the tumor further by liposomes. However, in the tumor imaging, the extended blood retention would be an obstacle, as the blood level is the background for the image (*11*), therefore we would have to give attention to also the balance of the tumor uptake and blood level.

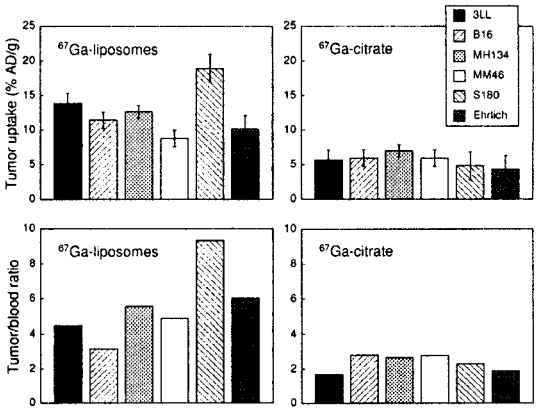

FIGURE 5 Tumor uptake and tumor-to-blood ratio of ^{67}Ga in mice bearing various tumors at 24 h after the administration of liposomes encapsulating ^{67}Ga-NTA or ^{67}Ga-citrate.

References

1. Machy P. and Leserman L. -Liposomes in cell biology and pharmacology, John Libbey & Co., Ltd, London, 1987
2. Proffitt R. T., Williams L. E., Presant C. A. et. al. -J Nucl Med 24: 45-51(1983)
3. Ogihara I., Kojima S. and Jay M. -Eur J Nucl Med 11: 405-411(1986)
4. Ogihara I., Kojima S. and Jay M. -J Nucl Med 27: 1300-1307(1986)
5. Ogihara-Umeda I. and Kojima S. -J Nucl Med 29: 516-528(1988)
6. Ogihara-Umeda I. and Kojima S. -Eur J Nucl Med 15: 612-617(1989)
7. Ogihara-Umeda I., Sasaki T. and Nishigori H. -Nucl Med Biol 19: 753-757(1992)
8. Caride, V. J. -Nucl Med Biol 17: 35-39 (1990)
9. Presant C. A., Proffitt R. T., Turner A. F., et. al. -Cancer 62: 905-911(1988)
10. Presant C. A., Blayney D., Proffitt R. T. et. al. -Lancet 335: 1307-1309(1990)
11. Ogihara-Umeda I., Sasaki T. and Nishigori H. -Eur J Nucl Med 20: 170-172 (1993)

Synthesis and Biological Evaluation of ^{77}As-Labelled Diarsonic Acids as Potential Bone Agents.

KNIGHT CASTRO, H.H.; PANEK*, K.; MOET*, F.; BAAS, J.; TEUBEN, J.H.; VAALBURG, W. Groningen Centre for Catalysis and Synthesis, State University of Groningen, Nijenborgh 4, 9747 AG Groningen, The Netherlands. *Mallinckrodt Medical B.V., P.O. Box 3, 1755 ZG Petten, The Netherlands.

The possibility of utilizing arsenic as a substitute of phosphorus in radiopharmaceuticals was first considered by Hosain et al.(1) who found that when methylenediphosphonic acid (MDP), arsonomethyl phosphonic acid (AMP) and methylenediarsonic acid (MDA, 1) (Fig 1) were labeled with ^{99m}Tc, the presence of phosphorus was not a requirement for bone uptake. Two years later, results of preliminary studies describing the first incorporation of radioactive arsenic into this kind of compounds were published (2).

Short living Technetium-99m, though usable in combination with phosphonates for diagnostic purposes, is unsuitable as therapeutic tool. On the other hand, the diversity of arsenic radionuclides makes it in principle possible to synthesize compounds which, depending on the choice of the arsenic isotope, can be used for diagnosis or therapy of bone tumors. This work describes the first utilization of Arsenic-77 for direct synthesis of analogues of bone seeking compounds with potential as therapeutic agents.

The presently most efficient synthetic route for aliphatic arsonic acids is the Meyer reaction (3), which is also usable for the preparation of MDA when a 10 N NaOH solution of sodium arsenite is made to react with dibromomethane at 80°C. In general, better yields and shorter reaction times can be achieved when dihalo alcohols are used. Following this principle, sodium arsenite was treated with 1,3-dibromo-2-propanol and with 2,3-dibromopropanol separately to give the corresponding diarsonic acids 3 and 4 (Fig 2) in excellent yields within 4 hours. Ethylenediarsonic acid (EDA, 2), (Fig 2) can be prepared in a one-step reaction by decarboxylation of propionic acid in the presence of $KAsO_2$ (4).

Corroboration of the structure of ^{77}As-analogues was based on comparison of the R_F values obtained for the As-75/As-77 compounds by means of radio-chromatographic scanning in two different solvent systems for TLC as well as their retention times in HPLC.

Tissue distribution studies of the compounds were performed on Wistar rats one and three hours after tail injection of the tracer solution. Blood samples were taken by heart puncture and the organs of interest (liver, kidney, muscle and femurs) were removed and weighed to determine the uptake of radioactivity. Results of these experiments are given in Table I. All four diarsonic acids tested showed significant bone uptake, comparable, in the cases of MDA and EDA, with their phosphorus analogues labeled with Technetium-99.

This work was partly supported by the Foundation for Medical Technology of the Ministry of Economic Affairs of The Netherlands.

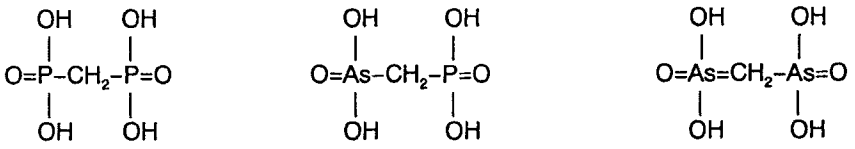

Fig. 1. Structural formula of methylenediphosphonic acid (MDP), arsonomethylphosphonic acid (AMP) and methylenediarsonic acid (MDA,**1**)

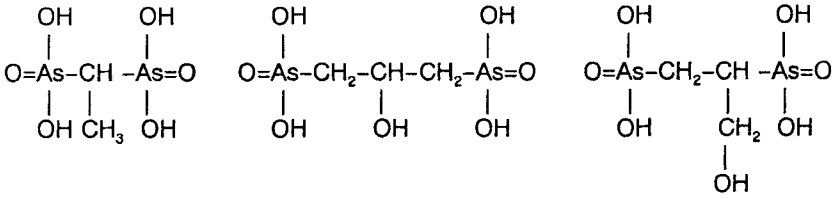

Fig. 2. Structural formula of ethylenediarsonic acid (**2**), 2-hydroxy-1,3-propylenediarsonic acid (**3**) and 1-hydroxy-2,3-propylenediarsonic acid (**4**)

% injected dosis/gr of organ

Code	Time/hr	Blood	Liver	Kidney	Muscle	Femur
1	1	0.16 ± 0.01	0.05 ± 0.02	3.65 ± 0.51	0.06 ± 0.03	1.53 ± 0.06
	3	0.20 ± 0.01	0.33 ± 0.06	3.70 ± 0.67	0.24 ± 0.08	1.71 ± 0.03
2	1	0.10 ± 0.02	0.06 ± 0.03	0.83 ± 0.06	0.04 ± 0.01	1.54 ± 0.06
	3	0.09 ± 0.01	0.06 ± 0.03	0.35 ± 0.02	0.06 ± 0.01	0.76 ± 0.06
3	1	0.10 ± 0.01	0.03 ± 0.01	1.30 ± 0.00	0.20 ± 0.06	0.67 ± 0.04
	3	0.06 ± 0.00	0.02 ± 0.01	0.65 ± 0.17	0.15 ± 0.00	0.34 ± 0.07
4	1	0.20 ± 0.02	0.00	1.61 ± 0.02	0.00	0.76 ± 0.03
	3	0.14 ± 0.02	0.00	0.55 ± 0.05	0.00	0.27 ± 0.03

Table I. Tissue distribution of ^{77}As-diarsonic acids in rats at 1 and 3 h. after I.V. injection

REFERENCES

1. P. Hosain, R.P. Spencer, F. Hosain, P.K. Sripada, *Int. J. Nucl. Med. Biol.* 7, 51 (1979)
2. P. Hosain, P.K. Sripada, R.P. Spencer and F. Hosain, *Int. J. Nucl. Med. Biol.* 8, 209 (1981)
3. G. Meyer, *Ber.* 16, 1439 (1883)
4. V.K. Sommer and M. Becke-Goehring, *Z. Anorg. Allg. Chem.* 370, 31 (1969)

PRODUCTION AND PROPERTIES OF FINE AEROSOLS LABELLED WITH VARIOUS RADIONUCLIDES

T. Nozaki, T. Jizaimaru, T. Hara*, and T. Suzuki*

School of Hygienic Sciences, Kitasato University, Kitasato, Sagamihara, 228 Japan; * National Nakano Chest Hospital, 3 Egota, Nakano-ku, Tokyo 165, Japan

Ultra-fine aerosols of ^{99m}Tc-containing carbon are used for lung diagnosis. The aerosols are produced by an apparatus called TECHNEGAS;[1] ^{99m}Tc and a minute amount of carbon are sublimed from a graphite boat into ambient argon to give the aerosols. We thought that aerosols labelled with various radionuclides and provided with various physicochemical properties was able to be produced by the same principle, and often by the same apparatus. The aerosol particles of ^{99m}Tc are insoluble in water, but those readily soluble are expected to be effective for the study on plumonary uptake of aerosol substances into the blood and to thus be more suitable for diagnosing interstitial pneumonia than radioactive mists of larger sizes from neblizers. Using TECHNEGAS apparatus, we have prepared aerosols labelled with ^{18}F, ^{42}K, ^{64}Cu, ^{68}Ga, and ^{99m}Tc, and studied on the yield and the behaviour of the radionuclides in the collection on air-filters, dissolution in water and acids, and, after being introduced in water, adsorption and elution in ion exchange columns. The effect of additives on the yield and behaviour was also studied. Tc-99m was eluted both by salin and pure water to examine the effect of NaCl.

F-18 was produced by proton bombardment of $H_2{}^{18}O$, and made a carrier-free solution containing K_2CO_3 (200 μg in 0.3 ml). Sometimes the K_2CO_3 was removed by a cation exchange column. K-42 and ^{68}Ga were milked from ^{42}Ar-^{42}K and ^{68}Ge-^{68}Ga generators by pure water and 1 N hydrochloric acid, respectively, evaporated just to dryness, and then dissolved in pure water (100 to 200 μl). Cu-64 was produced by reactor irradiation, with radionuclidic concentration by the nuclear recoil, in Japan Atomic Energy Research Institut and offered in a dilute acetic acid solution. From 50 to 100 μl of each solution, after activity measurement, was added to a graphite boat of TECHNEGAS apparatus, which was then operated to give, within 20 min, the aerosol in 0.8 l argon by its completely automated sequence. The aerosol was then swept out with nitrogen (2 to 3 l/min flow rate) through a usual filter paper sheet and air-filter sheets, often placed in series, and the radioactivity on each sheet was measured to give the labelling yield. A part of the aerosol flow was led into a particle counter for monitoring the concentration and size of the particles.

Each filter was then immersed in water or 1 N hydrochloric acid for 2 min and pressed between paper sheets, and the remaining radioactivity was measured. The water or acid containing the radioactivity (2 ml) was added to columns (0.8 mm inner diameter) of cation and anion exchange resins (Dowex 50W-X8, H-form, 100-200 mesh; and Dowex 1X8, OH-form, 100-200 mesh; both 1 ml apparent volume). The column was first washed with water (5 ml) and then eluted with water, 0.5 N HCl, 0.5 N NaCl, ethanol, or acetone for the measurement of elution curve.

The main results are shown in Table 1. Aerosols made from salin-eluted ^{99m}Tc showed maximum size-distribution at about 200 nm diameter, which is constantly observed for usual NaCl sublimate. For water-eluted ^{99m}Tc and for the other no-carrier- and no-salt-added radionuclides, the maximun in size-distribution was found slightly under 100 nm, where the reliability of the particle counter decreases with the decrease of particle size. More than 90 % of the activity was always caught by the air-filters, but the break-through fraction was larger for water-eluted ^{99m}Tc than salin-eluted ^{99m}Tc. The usual filter paper sheet caught 30 to 60 % for all the radionuclides. In Table 1, no great variation is seen in the labelling yield. The main cause of the activity loss is clearly the deposition of the aerosol particles on the inside wall of the TECHNEGASS apparatus. For ^{18}F, the addition of NaF, KF or NaCl (1 wt% of the solution) deteriorated the yield slightly, so did the removal of the K_2CO_3 from the original solution by cation exchange. The two different elutions of ^{99m}Tc gave the same yield of the aerosol. In Table 1, the radionuclides are seen to be divided into two groups in water leaching efficiency. The different efficiencies can be regarded as natural from the properties of the elements. So is the efficiecy in the acid leaching. F-18 leached into water behaved equally as F^- ion of an ordinary concentration in both cation and anion exchange columns. K-40 was shown to exist as cation, but ^{68}Ga leached out into water exhibited the behaviour partially of cation, anion and also particulates. No enough data as yet has been obtained for the behaviour of ^{64}Cu. Tc-99m leached into water was shown to exist as particulates; it behaved equally in both cation and anion exchange columns and for all aqueous and organic eluents, being once trapped in the column and then washed out very slowly and steadily.

We have just begun the volunteer test in the use of the ^{18}F aerosol for diagnosing interstitial pneumonia. By PET, we can obtain more quantitative reasults in shorter time intervals than by SPECT and shall thus be able to undertake more reliable kinetical treatment on blood uptake of inhaled aerosol substances. It is probable that various uses of TECHNEGAS-produced radioactive aerosols will be found. The apparatus, however, is so highly automated that no modification is possible in the operation conditions, such as the heating temperature and time sequence. We intend to take contact with the producer of the apparatus to make possible the modification in research use.

Table 1. Labelling Yield and Properties of Aerosols.

Nuclide	Yield	Washed Out Fraction (%)		Anion Exchange Column		
		Cold Water	Aq. HCl	Adsorption	Water Elut.	HCl Elut.
F-18	20 - 25	> 99	> 99	Quantit.	Neglig.	Complete
K-40	30 - 35	> 99	> 99	None		
Cu-64	30	< 10	60 - 70			
Ga-68	30 - 35	< 15	> 95	Partial	Neglig.	Mostly
Tc-99m	30 - 45	< 15	< 15	High	Very Slow	Very Slow

(1) Burch, W., Sullivan, P., McLaren, C. Nucl. Med. Comm., 7, 865 (1986).

N, N'-Ethylene-di-L-Cysteine: A Potential Ligand for Gallium and Indium Radiopharmaceuticals

C.J. Anderson[1], C.S. John[2], R.K. Keast[2], H.V. Lee[1] and M.J. Welch[1]. [1]Mallinckrodt Institute of Radiology, Washington University School of Medicine, St. Louis, MO, and [2]Radiopharmaceutical Chemistry Section, The George Washington University Medical Center, Washington, D.C.

The ligands BAT-TECH and BAT-TE, which contain two nitrogens and two sulfurs (N_2S_2) for metal binding, have been evaluated as radiopharmaceuticals for myocardial imaging.[1,2] The *in vivo* stability of BAT-TECH has recently been questioned,[3] therefore one of the primary objectives of this research was to investigate an alternative N_2S_2 chelate containing two carboxylates which may enhance the stability of the Ga^{3+} and In^{3+} complexes. L,L-ethylenedicysteine (EC) (Figure 1) when labeled with ^{99m}Tc at high pH forms a very stable chelate that has been shown to be rapidly excreted through the kidneys with low retention in the kidneys and liver.[4] In the present study the chemistry and rat biodistribution of both ^{111}In- and ^{67}Ga-labeled EC will be discussed, as well as *in vivo* plasma stability of ^{67}Ga-EC.

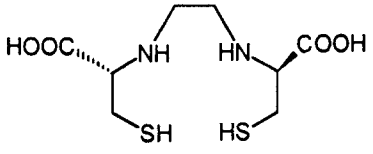

FIGURE 1: EC

N,N'-ethylene-di-L-cysteine was synthesized as reported in the literature.[5] The dihydrochloride salt of EC (1-2 mg) was dissolved in 1:1 ethanol:water, and a solution of ^{67}Ga- or ^{111} In-acetate was added to the ligand solution. The pH of the mixture was adjusted to between 4 and 5, and the solution was incubated at room temperature for 5 minutes. Quality control was performed by radio-thin layer chromatography (radio-TLC) using paper chromatography (Whatman No. 1) in 3:1 ethanol:0.4 M NaOAc pH 5. In this system the ^{67}Ga- and ^{111}In-labeled EC had an R_f of 0.4, while the radiolabeled acetate remained at the origin. The radiochemical purity of both ^{67}Ga- and ^{111}In-EC was > 95%. Electrophoresis on ^{67}Ga-EC in 0.1 M HEPES, pH 7.35 showed the complex to have a negative charge, suggesting that the carboxylates participate in the complexation.

Biodistribution studies were performed in Sprague-Dawley rats (150-200 g) after injection of either ^{111}In- or ^{67}Ga-EC (Tables 1 and 2). The ^{67}Ga tracer clears slowly from the blood from 20.7 %ID/organ at 2 minutes to 1.73 %ID/organ after 60 minutes. The excretion of the complex takes place through the hepatobiliary and renal systems. ^{111}In-EC shows a similar biodistribution pattern.

Although the heart and brain uptake for the ^{67}Ga- and ^{111}In-EC were less than optimal, the *in vivo* stability of these complexes warrents further study of this class of compounds for the development of PET radiopharmaceuticals.

Acknowledgement: This work was supported by the National Institutes of Health grant CA 4292925.

REFERENCES

1. Kung H.F., Liu B. L., Mankoff D., Kung M.P., Billings J.J., Francesconi L. and Alavi A. - J. Nucl. Med. 31: 1635 (1990).
2. Liu B.L., Kung H.F., Jin Y.T., Zhu L. and Meng M. - J. Nucl. Med. 30: 367 (1989).
3. Mathis C.A., Kung H.F., Budinger T.F., Wong P.J., Coxson P.G. and Brennan K.M. - J. Nucl. Med. 32: 974(1991) (abstract).
4. Verbruggen A., Nosco D.L., Van Nerom C.G., et al. - J. Nucl. Med. 33:551(1992).
5. Blondeau P., Berse C. and Gracel D. - Canadian J. Chem. 45:49(1967).

Table 1
^{67}Ga-EC Biodistribution in Sprague Dawley Rats (n=4)

%ID/g

Organ	2 minutes	5 minutes	15 minutes	30 minutes	60 minutes
Blood	2.02 ± 0.02	1.39 ± 0.26	0.70 ± 0.05	0.44 ± 0.05	0.17 ± 0.03
Lung	1.50 ± 0.05	1.01 ± 0.20	0.52 ± 0.05	0.35 ± 0.05	0.15 ± 0.04
Liver	0.67 ± 0.10	0.79 ± 0.09	0.81 ± 0.11	0.78 ± 0.08	0.57 ± 0.13
Spleen	0.42 ± 0.01	0.32 ± 0.09	0.18 ± 0.02	0.12 ± 0.01	0.06 ± 0.01
Kidney	9.41 ± 0.94	6.45 ± 1.13	3.64 ± 0.46	2.39 ± 0.29	0.91 ± 0.15
Muscle	0.51 ± 0.11	0.43 ± 0.08	0.23 ± 0.02	0.20 ± 05	0.07 ± 0.01
Heart	0.93 ± 0.06	0.55 ± 0.15	0.28 ± 0.03	0.19 ± 0.03	0.08 ± 0.03
Brain	0.09 ± 0.01	0.07 ± 0.01	0.05 ± 0.01	0.03 ± 0.01	0.01 ± 0.00

Table 2
^{111}In-EC Biodistribution in Sprague Dawley Rats (n=4)

%ID/g

Organ	2 minutes	5 minutes	15 minutes	30 minutes	60 minutes
Blood	1.97 ± 0.46	1.30 ± 0.10	0.65 ± 0.07	0.28 ± 0.05	0.09 ± 0.01
Lung	1.33 ± 0.27	0.99 ± 0.17	0.53 ± 0.06	0.22 ± 0.04	0.09 ± 0.01
Liver	1.25 ± 0.13	1.35 ± 0.17	0.82 ± 0.14	0.42 ± 0.02	0.13 ± 0.02
Spleen	0.40 ± 0.10	0.30 ± 0.02	0.17 ± 0.01	0.09 ± 0.02	0.03 ± 0.00
Kidney	9.76 ± 2.88	7.14 ± 1.38	3.64 ± 0.40	1.82 ± 0.18	0.62 ± 0.08
Muscle	0.43 ± 0.10	0.54 ± 0.22	0.25 ± 0.06	0.11 ± 0.03	0.03 ± 0.01
Heart	0.78 ± 0.22	0.59 ± 0.09	0.26 ± 0.04	0.12 ± 0.02	0.04 ± 0.01
Brain	0.12 ± 0.04	0.07 ± 0.01	0.04 ± 0.01	0.02 ± 0.00	0.01 ± 0.00

In vivo plasma stability on ^{67}Ga-EC was determined in rats at times out to 2 hours post-injection by radio-TLC. The complex appeared to be > 90% intact by 2 hours, and showed minimal transchelation to transferrin.

Meta-[^{211}At]astatobenzylguanidine: Further validation of _in vitro_ and _in vivo_ uptake mechanisms.

VAIDYANATHAN, G., STRICKLAND, D.K., AFFLECK, D.A., WELSH, P. and ZALUTSKY, M.R. Department of Radiology, Duke University Medical Center, Durham, N.C. 27710.

Radioiodinated *meta*-iodobenzylguanidine (MIBG) has been widely used for the detection and treatment of neuroendocrine tumors such as neuroblastoma. MIBG, being an analog of the neurotransmitter norepinephrine, is taken by innervated tissues such as the heart and adrenal medulla by an active Uptake-1 mechanism and the human neuroblastoma SK-N-SH cell line also takes up MIBG via Uptake-1. This process has been shown to be saturable and energy-dependent. In addition, MIBG uptake can be blocked by tricylic antidepressants such as desimipramine (DMI) and by competitive inhibition with norepinephrine. Since uptake is energy-dependent, it also is blocked by the ATP-ase inhibitor ouabain, by oxygen depletion by sodium dithionite, and by low temperature incubation.

Due to the therapeutic advantages of α-particles, Mairs et al. (1) have suggested that *meta*-[^{211}At]astatobenzylguanidine (MABG) could be more effective in the treatment of neuroblastoma, provided that At for I substitution did not compromise the specificity and mechanism of its uptake in these tumors. We have developed an efficient synthesis of MABG and investigated its tissue distribution in normal mice (2). A drawback of MABG is the high myocardial uptake which may limit its potential as a therapeutic agent. The current study was undertaken to investigate whether: 1) the uptake process of MABG is the same as that of MIBG; 2) MABG is retained to the same degree and by the same mechanism as MIBG by SK-N-SH cells; and 3) it is feasible to reduce myocardial uptake using tetrabenazine without interfering with tumor uptake.

The results of blocking experiments using SK-N-SH cells and MABG are summarized in Figure 1. Norepinephrine at 1 μM, 10 μM and 1 mM decreased uptake of MABG to 84%, 13% and 4% respectively, of control levels. With desimipramine, uptake of MABG was 11%, 12% and 21%, respectively, of controls at 0.1, 0.5 and 1 μM concentrations of DMI. In mice, 10 mg/kg desimipramine also reduced myocardial uptake to 85% and 67% of controls at 5 min and 60 min post-injection. As seen with MIBG, MABG uptake by SK-N-SH cells was found to be energy-dependent; 1 mM ouabain reduced uptake to 8% of the control. Addition of sodium dithionite (1.5 mM) reduced the uptake to 18% of the control. The uptake was also reduced to 12% when the incubation was performed at 4°C. Taken together, these data support the belief that MABG is taken up by means of the same active Uptake-1 mechanism as MIBG.

Tetrabenazine, a granular uptake inhibitor, did not block the uptake of MABG in SK-N-SH cells at 1, 10 or 100 μM concentrations; however, at 500 μM uptake was reduced to 65% of the control. In normal mice, myocardial uptake of MABG at 1 hr was reduced to 68% of the control following pretreatment with 40 mg/kg tetrabenazine. These results suggest that it might be possible to use tetrabenazine to reduce myocardial uptake with minimal effect on tumor uptake.

The cellular retention characteristics of MABG was compared to that of MIBG. Only about

40% of the initially bound MABG activity was cell-associated at 4 hr compared to 80% for n.c.a. [^{131}I]MIBG. By 24 hr, only 10% of the bound MABG activity was retained. This apparent lower retention of MABG may be due to impaired cell function or death due to the extreme cytotoxicity of MABG (D_0 = 0.023 pCi/cell (3)). Further studies using lower doses of MABG are in progress to address this issue. Reserpine, another granular uptake inhibitor, and the calcium channel blockers nifedipine and verapamil (4) had no significant effect on the cellular retention of both tracers.

In summary, the results of this study indicate that the specificity of uptake of MABG is similar to that of MIBG and suggest that further investigations of MABG in human tumor xenograft mouse models are warranted.

REFERENCES

1) Mairs, R.J., Angerson, W.J., Babich, J.W. and Murray, T. (1991) In*: Advances in Neuroblastoma Research* 3 (A.E. Evans, G.J. D'angio, A.G. Knudon, Jr., and R.C. Seeger, Eds) pp 495-501, Wiley-Liss, Inc., New York (*Progress in Clinical and Biological Research, Vol* 366).

2) Vaidyanathan, G. and Zalutsky, M.R. *Bioconjugate Chem.* 1992; 3:499-503.

3) Vaidyanathan, G., Harrison, C., Welsh, P., Affleck., D. and Zalutsky, M.R. *J. Nucl. Med.* 1993; 34:218P.

4) Mairs, R.J., Gaze, M.N. and Barret, A. *Br. J. Cancer* 1991; 64:293-295.

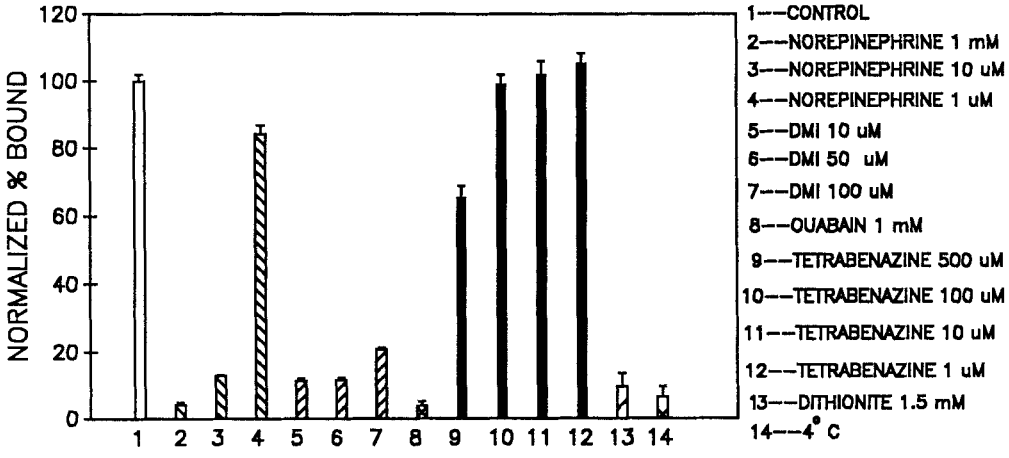

Figure 1. MABG Binding to SK–N–SH Cells

$^{99}Tc^{m}$-Fluoroalbumins ($^{99}Tc^{m}$-FA's): Internal Standards for Semi-quantitative *in vivo* ^{19}F Magnetic Resonance Spectroscopy.

Schmidt, R.P. and Wiebe, L.I. □Faculty of Pharmacy and Pharmaceutical Sciences, U. Alberta, and Dept. of Nuclear Medicine, Cross Cancer Institute, Edmonton, Canada.

Magnetic Resonance Spectroscopy (MRS) is a powerful technique for the study of molecular structure. Application of MRS to the study of xenobiotic biotransformations *in vivo*, *in situ*, specifically to establish the chemical structure of metabolites, is now a routine procedure in many laboratories. Advantages of *in vivo* MRS include its non-invasiveness; disadvantages include its low sensitivity and frequently, noisy backgrounds. A relative standard is required if quantitative measurements are to be made. ^{19}F-MRS has the advantage over ^{1}H-MRS in *in vivo* studies in that the background is virtually free of any fluorine resonances. ^{19}F-MRS has been used with great success in resolving metabolic pathways for fluorinated xenobiotics that are used in relatively large doses in clinical or experimental settings.[1] Although qualitative *in situ* detection of metabolites in various regions/tissues of the body represents a substantial improvement over metabolite determination in excreta, blood or excised tissue, the quantification of these metabolites is often equally important. This is particularly true in cases where metabolites may give rise to regioselective toxicity, regioselective pharmacology or to 'metabolic pool' effects; the latter phenomenon is particularly important when dealing with therapeutic nucleosides or nucleobases such as 5-fluoro-2'-deoxyuridine or 5-fluorouracil (5-FU), respectively.[2]

The liver is a major drug metabolizing organ. Therefore, the development of an internal standard to support quantitative MRS measurement of metabolites has high priority. Our approach to the design of an internal standard for *in vivo, in situ* ^{19}F-MRS is based on a well-known radiopharmaceutical, $^{99}Tc^{m}$-albumin. This agent, after appropriate formulation, is taken up to varying degrees, uptake being dependent on particle size of the denatured macromolecule. We have postulated that a $^{99}Tc^{m}$ labelled, fluorinated albumin (FA) derivative could be used as a semi-quantitative internal standard by applying scintigraphic imaging (SPECT) techniques to determine the $^{99}Tc^{m}$ load and, by cross calculation, the F content.

F_6-FA: Human serum albumin (HSA; certified free of HIV and hepatitis B virus) was fluorinated by the addition of bis(trifluoromethyl)benzoic acid. The F_6-containing benzoic acid was sequentially converted to its acyl chloride and acyl azide. The acyl azide in DMF was added dropwise to a cooled (0 °C) solution of HSA in buffer (pH 9.1), and the resulting mixture was stirred at 5 °C for 24 h. Low molecular weight components of the reaction mixture were then removed by dialysis against distilled water (72 h), across a SPECTR/POR molecularporous membrane #1 (cut-off 6-8k daltons). The purified FA was recovered from solution by lyophilization, and was stored protected from light, at -20 °C. The fluorine content of FA's prepared under various reaction conditions was determined by neutron activation analysis using the U Alberta SLOWPOKE nuclear reactor. The ^{19}F MRS of F_6-FA is shown in Fig 1. The fluorine load per molecule of HSA was found to be between 2.8% and 12.2% $^{w}/_{w}$, depending on reaction conditions.

F_5-FA was prepared in a similar manner, starting with pentafluorobenzoic acid; this compound exhibits fluorine resonances at chemical shifts different from that of F_6-FA, but detection by MRS is less sensitive on a molar basis than F_6-FA because the fluorine atoms on the aromatic ring are not equivalent and therefore several smaller signals are detected (Fig. 1). The MRS of F_5-FA (2.5% F $^{w}/_{w}$) is shown in Fig. 1 for comparative purposes.

$^{99}Tc^{m}$-F_6-FA was prepared by dissolving F_6-FA in sterile water for injection, followed by the addition of Poloxamer 188; this mixture was allowed to stand for 1 h at 5 °C, after which it was added to a freshly-prepared, buffered (pH 5.7) solution of stannous chloride. The final solution was prepared by the addition of freshly-eluted $^{99}Tc^{m}$ pertechnetate, dilution with water and adjustment to pH 7.

I*n vivo* studies in mice and rats showed that hepatic uptake could be accurately estimated by simple region-of-interest measurements in these small animal models. Determination of F in liver by NAA confirmed the fidelity in the $^{99}Tc^{m}$ radiolabel. *In vivo, in situ* ^{19}F MRS using a surface coil placed over the liver (Fig. 2) demonstrated the utility of $^{99}Tc^{m}$-FA's as an internal, semi-quantitative standards for the quantification of F-containing xenobiotics in the liver.

---

1 Tandon, M., Kumar, P., Wiebe, L.I. and Wiebe, G. Detection of New Metabolites of Trifluridine (F_3TdR) using ^{19}F NMR Spectroscopy. *Biochem. Pharmac.* 44: 2223-2228 (1993).

2 McSheehy, P.M.J. and Griffiths, J.R. ^{19}F MRS Studies of Fluoroprymidine Chemotherapy: A Review. *NMR Biomed.* 2:133-41 (1989).

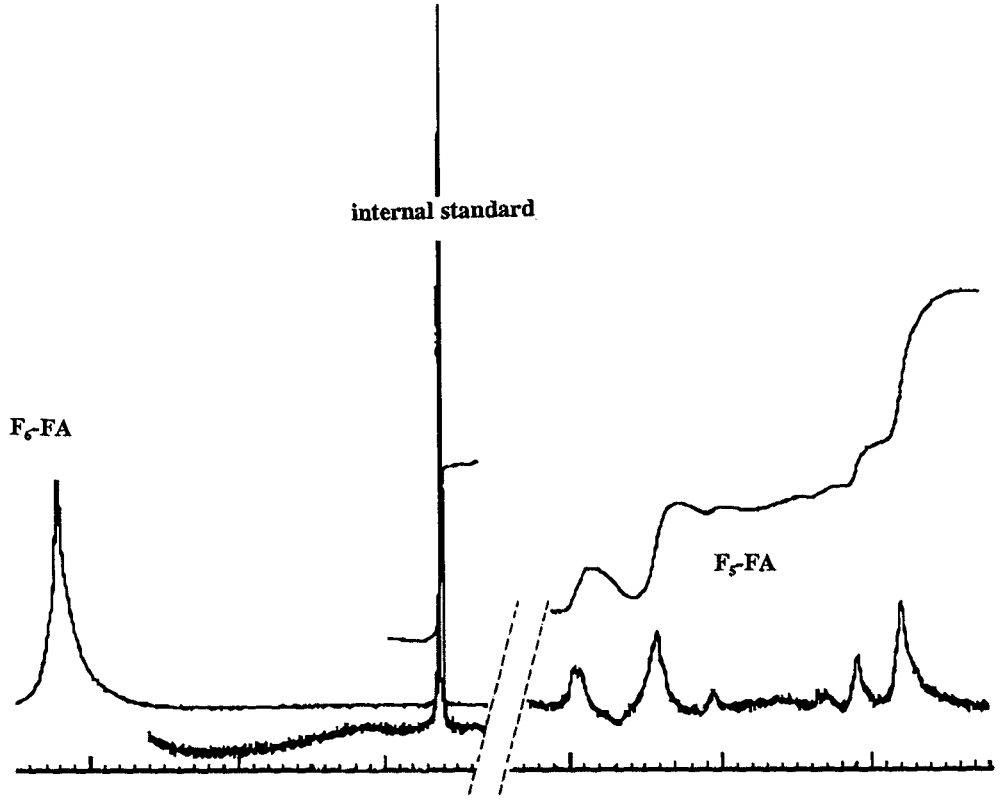

Figure 1. Composite ^{19}F MRS of F_6-FA and F_5-FA, with trifluoro acetic acid (TFA) as internal standard.

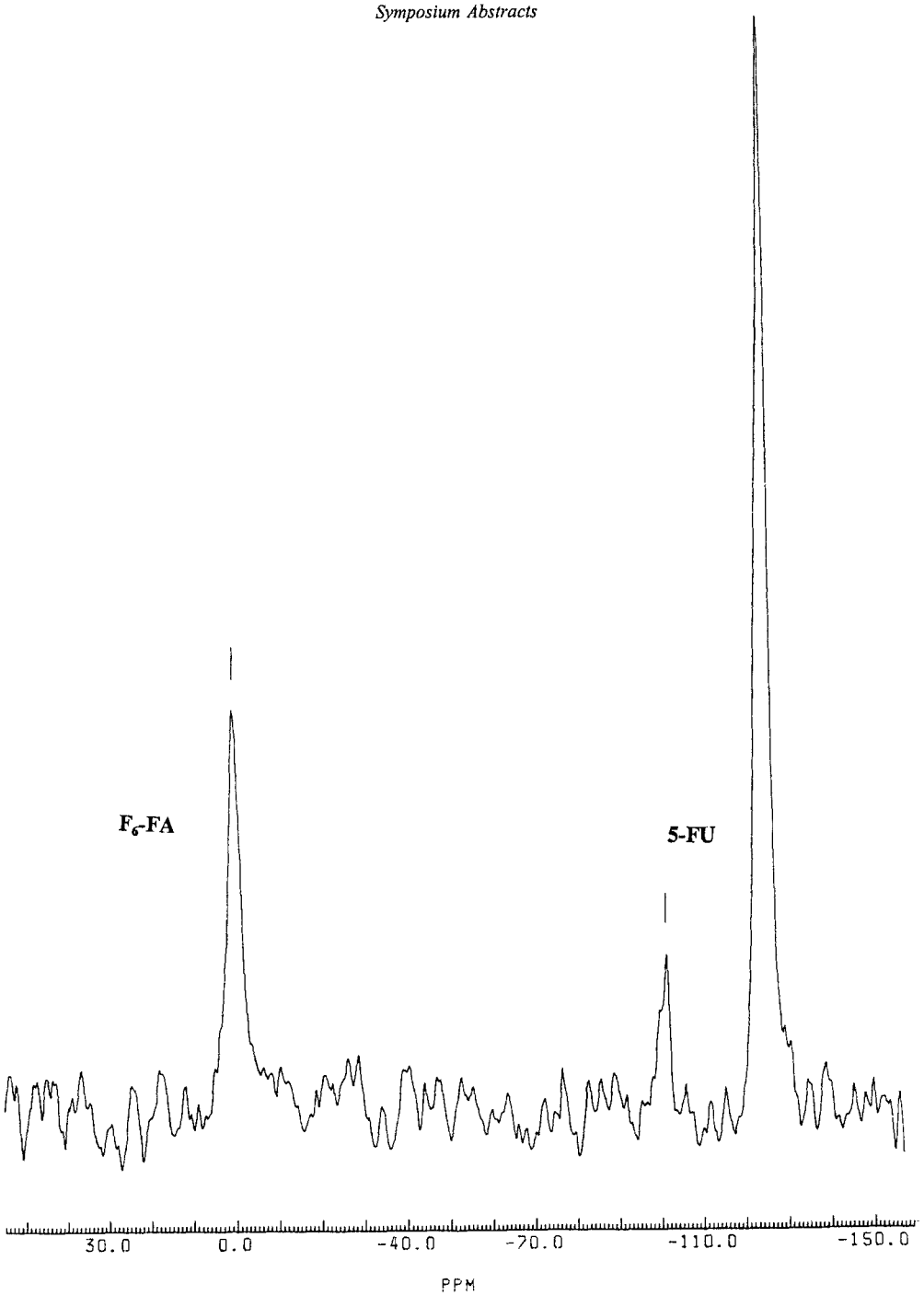

Figure 2. **In vivo ^{19}F MRS of rat liver after injectoin of F_6-FA and 5 fluorouracil (5-FU)**

Estimation of the immunological activity during liver cell proliferation with Fe-coprecipitated ^{67}Ga.

Ohkubo, Y.; Sasayama, A.; Hayashi, A.*; Goto, R.*; Ibuki, Y*. Department of Radiopharmacy, Tohoku College of Pharmacy, 4-4-1, Komatsushima, Aoba-ku, Sendai, 981, Japan. *Laboratory of Radiation Chemistry, Graduate School of Nutritional and environmental Sciences, University of Shizuoka, 52-1, Yada, Shizuoka, 422, Japan.

Gallium-67, which has been used for the detection of various tumors and acute and chronic inflammation, is exclusively bound to transferrin in the blood. Since transferrin is essentially an iron-transport protein, the affinity of gallium for the protein is lower than that of iron. Therefore the binding of ^{67}Ga to transferrin is easily inhibited with iron. We have reported that the administration of Fe^{3+} before the injection of ^{67}Ga decreased the uptake of ^{67}Ga by liver and spleen, but had little effect on the uptake of ^{67}Ga by the inflammatory tissue[1,2]. Moreover, we have found that the simultaneous administration of $FeCl_3$ and ^{67}Ga greatly increased the uptake of ^{67}Ga into liver and spleen as compared with ^{67}Ga alone but decreased those into blood and the inflammatory tissue[1]. Recently we have found that the simultaneous administration of $FeCl_3$ and ^{67}Ga greatly increased the uptake of ^{67}Ga into the bone marrow as well as into the spleen. We thought that iron-colloidal materials might occur in the blood immediately after the administration of $FeCl_3$ and then ^{67}Ga might be coprecipitated with the colloids in blood, since the simultaneous administration of $FeCl_3$ and ^{67}Ga is carried out by the intravenous injection of $FeCl_3$ saline solution containing ^{67}Ga. If Fe-coprecipitated ^{67}Ga is preferentially taken up by spleen and bone marrow, it may be able to use for the estimation of immunological activities of macrophages. It has been reported that the immunosuppressive drug increased the regeneration response in hepatectomized rats[3]. It is very interesting to study a relationship between immunological activities of macrophages and liver cell proliferation. We think that immunological activities of macrophages may decrease when liver cells are proliferating.

In the present study, we attempted to estimate the decrease of immunological activity during liver cell proliferation with the uptake of Fe-coprecipitated ^{67}Ga produced in vitro by spleen and bone marrow. The Fe-coprecipitated ^{67}Ga was produced as follows. Gallium-67 was added into $FeCl_3$ dissolving Tri-HCl buffer (pH 7.4). The mixture solution of $FeCl_3$ and ^{67}Ga was dialyzed against the same buffer (pH7.4) for 15 min, and then occurred brownish colloidal materials were collected by centrifugation. The precipitate, which contained ^{67}Ga coprecipitated with Fe was dissolved into saline. The Fe-coprecipitated ^{67}Ga is abbreviated to ^{67}Ga-Fe Ppt. The model of liver cell proliferation was provided with regenerating liver of rat which was 70% hepatectomized under light ether anesthesis. The hepatectomized rat was intravenously injected with ^{67}Ga-Fe Ppt saline solution in a dose of 37kBq (200 ul). At 4 hrs after the administration, rats were anesthetized with urethane and immediately perfused with cold saline. The spleen, bone marrow, and other tissues were then removed. Radioactivity of various tissues removed was determined with well-type NaI-scintillation counter. The uptake ratios of ^{67}Ga-Fe Ppt in various tissues were expressed in the following formula: Uptake ratio = sample radioactivity (cpm) / sample weight (g) / total radioactivity administered(cpm) / body weight of rat (g).

In normal rats, the uptake of ^{67}Ga-Fe Ppt by liver, spleen, and bone marrow was extremely greater than that of ^{67}Ga alone (Fig.1). These results must indicate that ^{67}Ga-Fe Ppt are taken up kupffer cells and macrophages. In order to ascertain that the uptake of ^{67}Ga-Fe Ppt by spleen and bone marrow reflects the immunological activities of macropharges, rats immunosuppressed with γ-ray exposure were used. Rats were received γ-radiation from ^{137}Cs at a dose of 3.5Gy.

Figure 2 shows the uptake of ^{67}Ga-Fe Ppt by spleen and bone marrow in γ-ray exposed rats. The uptake of ^{67}Ga-Fe Ppt by spleen remarkably decreased at 2 days after γ-ray exposure, and 12 days after the uptake recovered to the level of normal rat. The uptake of ^{67}Ga-Fe Ppt by bone marrow also decreased at 2 days after γ-ray exposure, and then gradually increased but did not recover to the normal level until 12 days after. These results show that γ-ray causes much greater damage for bone marrow than spleen and that the uptake of ^{67}Ga-Fe Ppt reflects the immunological activities of macrophages. Figure 3 shows the uptake of ^{67}Ga-Fe Ppt by spleen and bone marrow at various days after partial hepatectomy. The uptake of ^{67}Ga-Fe Ppt by spleen remarkably decreased at 1 day after partial hepatectomy, and then gradually increased and reached at normal rat level at 4 days after. The uptake pattern of ^{67}Ga-Fe Ppt by bone marrow was completely similar to that by spleen. These results indicate that the immunological activities are suppressed when liver cells are proliferating after partial hepatectomy. There must be a close relationship between immunological activities of macrophages and liver cell proliferation, since macrophages produce interleukin-1β which inhibits liver cell proliferation. In the present study we conclude that Fe-coprecipitated ^{67}Ga produced in vitro is useful for the estimation of immunological activities of macrophages when liver cells are proliferating. Additionally we will show the data obtained from rats treated with CCl_4.

1) Ohkubo,Y.; Araki,S.; Abe,K. et al. The effect of $FeCl_3$ on the accumulation of gallium-67 into inflammatory and normal tissues. Ann.Nucl.Med., 2(2), 59-62 (1988)
2) Ohkubo,Y.; Sawamura,H.; Katoh,S. et al. Study on ^{67}Ga uptake by mouse granuloma tissues. Nucl.Med.Biol., **18**, 205-208 (1991)
3) Francavilla,A.; Barone,M.; Todo,s. et al. Augmentation of rat liver regeneration by FK 506 compared with cyclosporin. T Lancet, **25**, 1248-1249 (1989)

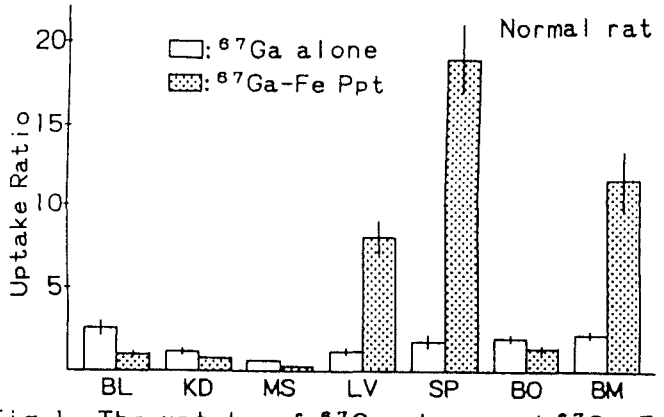

Fig 1. The uptake of ^{67}Ga alone and ^{67}Ga-Fe Ppt by various tissues in normal rats.
BL; Blood, KD; Kidney, MS; Muscle,
LV; Liver, SP; Spleen, BO; Bone,
BM; Bone marrow.

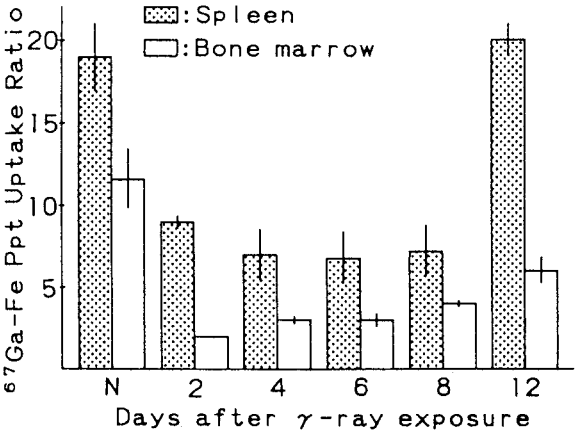

Fig 2. Time course of the uptake of ^{67}Ga-Fe Ppt by spleen and bone marrow after γ-ray exposure(3.5Gy). N; None exporsed rats.

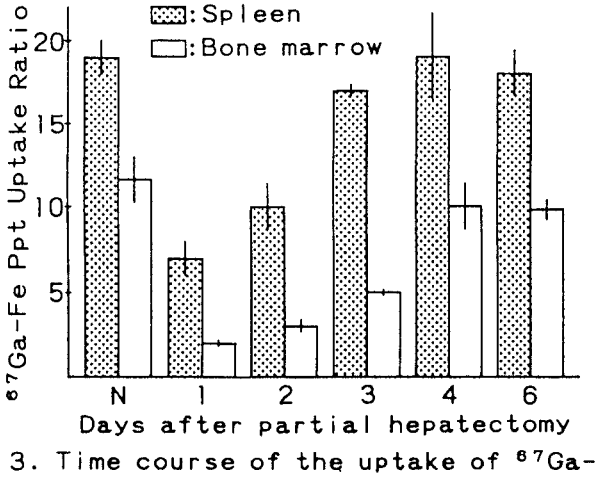

Fig 3. Time course of the uptake of ^{67}Ga-Fe Ppt by spleen and bone marrow after partial hepatectomy. N; None hepatectomized rats.

A β^+-selective radiodetector for capillary electrophoresis

WESTERBERG, G., LUNDQVIST, H., LÅNGSTRÖM, B. Uppsala University PET Centre, UAS S-751 85, Uppsala, Sweden.

In the development of methods for labelling proteins with ^{11}C [1], we required a complement to analytical HPLC for the analysis of the labelled products. High sensitivity, short analysis times and small sample consumption are features making capillary electrophoresis a suitable tool in the analysis of compounds labelled with short-lived radionuclides. Previously, radiodetection in capillary electrophoresis has been reported for both β- and γ-emitting radionuclides such as ^{32}P, ^{14}C and ^{99m}Tc [2 - 5]. In this study [6], a positron radiodetector for use with a high performance capillary electrophoresis system with simultaneous mass- and radiodetection is described. The application of the electrophoresis system for the analysis of labelled proteins is illustrated by isoelectric focusing (IEF) and capillary zone electrophoresis (CZE) experiments.

Fig. 1a

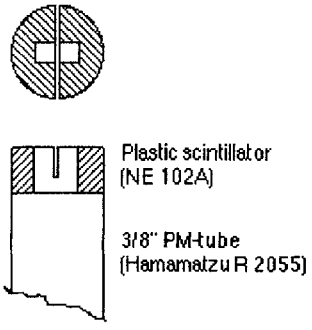

Fig. 1b

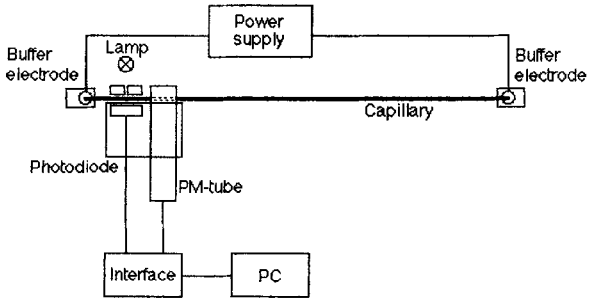

Radiodetector element – The detector element was constructed from a small plastic scintillator (2 x 4 x 4 mm, polyvinyltoluene, Nuclear Enterprise NE 102 A, Nuclear Enterprise, Edinburgh, U.K.) mounted onto a 3/8" photomultiplier tube (Hamamatzu R 2055, Hamamatzu Photonics, Japan). A slit (2 mm long, 0.5 mm wide and 2 mm deep) was made in the plastic scintillator allowing the capillary to be placed centrally in the detector, Fig. 1a. An amplifier and low energy discriminator, developed in-house, was used for the amplification of the photomultiplier tube signals and for the minimization of noise in the measurements. The radiodetector was mounted adjacent to the UV-photodiode-detector at a distance of 24 mm in a cartridge sliding on guiding rods allowing the simultaneous removal of both detectors, Fig. 1b. The distance between the detector cartridge and the end of the capillary was 20 mm. The UV-detector compartment of a BioRad HPE-100 Microsampler Capillary Electrophoresis

apparatus (BioRad, Richmond, Calif., USA) was modified to accomodate the two-detector assembly. The incident light from the UV-lamp was focused through a 0.05 x 1 mm slit facing the capillary. When operating the system, the entire capillary compartment was closed by a removable housing to avoid stray light entering the detectors. Both detectors were interfaced to a personal computer *via* a Beckman AI 406 interface adjusted to accept TTL-pulses from the photomultiplier tube and the analog signal from the UV-photodiode. Data were processed using a Beckman System Gold Chromatography Software Package.

In principle, both the β- and γ-radiation emitted from e.g. ^{11}C or ^{18}F could be used for the detection of the radioactivity. In practice, beta-detection is preferable when considering the spatial resolution of the detector. The plastic scintillator has a high sensitivity for beta-detection (i.e. the full beta-energy of ^{11}C-positrons is absorbed within 2 mm of scintillator plastic) and a low sensitivity for gamma-detection (hence a low background level).

Physical characteristics of the radiodetector – The radiodetector response was found to be linear in the interval 0 - 600 000 counts per second (cps). The plastic scintillator has a very fast response to incident betas, i.e. the pulses are short (10 - 20 ns). The characteristics of the scintillator and the amplifier - discriminator (10 - 20 ns pulses, 100 ns TTL) sets an upper limit for the linearity in the order of 1 Mcps. A simple amplifier and a low-energy discriminator were developed, and found to give satisfactory results. If required, more sofisticated electronics can be used to increase the linear range to about 10 Mcps.

The detector background count rate was determined to be 0.2 cps. During operation, no interference from the UV-lamp or the high-voltage power supply for the electrophoresis electrodes electrodes was observed.

The spatial resolution of the radiodetector was assessed by stepwise movement of a capillary partially filled with radioactivity through the detector. Assuming a gaussian detector response to a point source, the measured data was fitted using the least-squares method. The standard deviation of the detector response function was 1.52 mm corresponding to a full-width-half-maximum value of 2.53 mm. The effective detector width using a line source was calculated to be 2.69 mm, corresponding to an effective detector cell volume of 21 nl when using a 0.1 mm ID capillary. Using the value obtained above for the effective detector volume, the efficiency of the detector (^{11}C) was approximately 85 %. A similar value (87 %) was obtained using ^{18}F.

A capillary zone electropherogram of ^{11}C-albumin is shown in Fig. 2. Electrophoresis buffer; 10mM glutamine, adjusted to pH 9.7 (TEA); capillary, 0.1 mm ID x 180 mm, internally coated with non-crosslinked polyacrylamide; applied voltage 8.0 kV; UV-detection at 280 nm. The sample (70 ng, total activity 12 kBq) was applied as a 0.5 mm long starting zone.
Fig. 3 shows the same sample in an isoelectric focusing experiment. a) Focusing step. Applied voltage 5.0 kV; anolyte 20mM phosphoric, catholyte 20 mM NaOH. b) Mobilization step. Applied voltage 7.0 kV, anolyte 20 mM NaOH. Capillary 0.1 mm ID x 200 mm, internally coated with non-crosslinked polyacrylamide. UV-detection at 280 nm.

Fig. 2

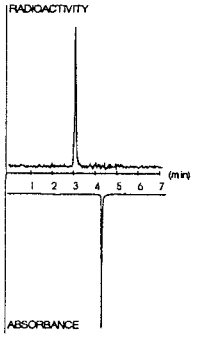

Fig. 3

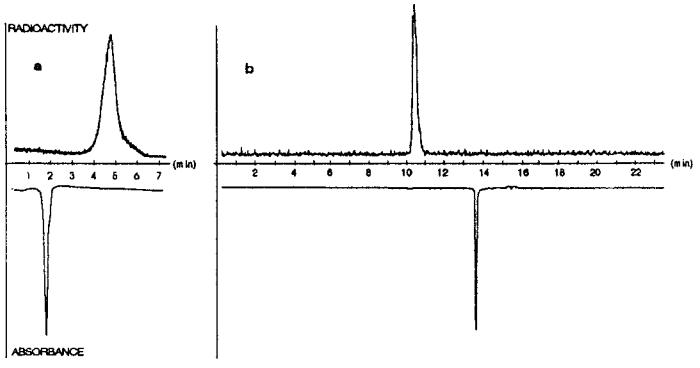

References

1. Westerberg, G. and B. Långström, *J. Biol. Chem. (1993), Submitted.*
2. R.E. Needham, M.F. and Delaney, *Anal. Chem. 55 (1983) 148 - 150.*
3. S.L. Pentoney, R.N. Zare and J.F. Quint, *Anal. Chem. 61 (1989) 1642 - 1647.*
4. D. Kaniansky, P. Rajec, A. Svec, P. Havasi and F. Macásek, *J. Chromatogr. 258 (1983) 238 - 243.*
5. K.D. Altria, C. F. Simpson, A.K. Bharij and A.E. Theobald, *Electrophoresis 11 (1990) 732 - 734.*
6. Westerberg, G., Kilár, F., Lundqvist, H. and Långström, *B. J. Chromatogr., In press.*

Monitoring and Disposal System for Cyclotron Produced Short-Lived Radioactive Gases.
TOCHON-DANGUY, H.J.; MIDGLEY, S.; EGAN, G.F.; SACHINIDIS, J.I.; PHAN, K.S. and CHAN, J.G. Centre for Positron Emission Tomography, Austin Hospital, Heidelberg, 3084, Australia.

The growing demand for medical cyclotrons able to supply positron-emitting radioisotopes within a hospital complex has stimulated efforts to develop reliable and efficient radioactive waste disposal and monitoring systems. Such a system as implemented in our hospital is described and our operational experience is presented.

A Positron Emission Tomography Centre has been established at the Austin Hospital, Melbourne, Australia. The equipment consists of an Ion Beam Application 10/5 MeV cyclotron, a full body Siemens/CTI 951 PET camera and all radiochemistry facilities. The equipment is housed in 500m^2 of new laboratory space adjacent to the Department of Nuclear Medicine. The cyclotron accelerates negatively charged particles (hydrogen and deuteron ions) and allows the production of the four common positron-emitters through the following nuclear reactions: $^{14}N(d,n)^{15}O$; $^{16}O(p,\alpha)^{13}N$; $^{14}N(p,\alpha)^{11}C$; and $^{18}O(p,n)^{18}F$.
Due to their relatively short half-lifes, no major problems exist with the waste disposal of the liquid radioactive forms such as $[^{18}F]F^-$ and $[^{13}N]$ NH_4^+. However, radioactive gas production such as $[^{11}C]CO_2$ or $[^{11}C]CH_4$ needed for hotcell radiosyntheses, as well as $[^{15}O]O_2$, $[^{15}O]CO$ and $[^{15}O]CO_2$ delivered in continuous flow to the scanner suite, require particular attention for their disposal. Compliance with the ICRP #60 radiation protection principles limits the radioactive doses to patients and workers, and radioactivity releases to the environment. Details of the Austin Hospital gas transport and gas storage systems as well as the radiation monitoring network are shown in figure 1.

$[^{11}C]$ Gas production
A 200 litre balloon constructed from MELLIMEX material and shielded with 2 cm of lead plate, is located inside the cyclotron vault. The balloon is inflated and deflated via an in-line pump connected on one side to the waste gas return pipe from the labelling module, and on the other side to the balloon. Security pressure sensors monitor positive and negative pressure in the balloon. An automatic operational procedure deflates the balloon into the vault at the commencement of each working day with a safety interlock of twelve hours delay after the last radioactive gas input.
Assuming that the maximum time duration for a $[^{11}C]$ radiolabelling procedure is approximately 30 minutes (excluding HPLC purification), a dedicated extraction flow rate from the chemistry module of 2 litre/min corresponds to a total volume of 60 litres of radioactive waste gas being deposited into the balloon. Thus up to three consecutive $[^{11}C]$ radiolabelling procedures can be undertaken without radioactive gas releases into the vault.

$[^{15}O]$ Gas production
The return radioactive gas flow rate during a PET gas study, is approximately 8 litre/min, corresponding to the normal breathing rate of an adult. As this flow rate can persist for up to two hours it is unrealistic to store such a large volume of gas in a balloon. However because of the 2 min radioactive half life, $[^{15}O]$ gas can easily be retained through a dedicated delay pipe. For this purpose, 40m of PVC 90mm diameter pipe has been fixed along one wall of the cyclotron vault and connected on one side to the output of the patient gas administration unit and on the other side to an appropriate remotely controlled fan. The delay pipe is designed to retain the waste $[^{15}O]$ gas for at least 30 minutes (corresponding to 15 half-lives) before being discharged into the vault.

Vault Exhaust
The vault itself is exhausted through a remote fan directly to the atmosphere at a flow rate of 200 litre/min.
A radioactive gas detector is continuously sampling the vault air to detect accidental radioactive gas discharges, and any radioactive gas alarm will immediately turn off the vault exhaust fan as well as the cyclotron itself.

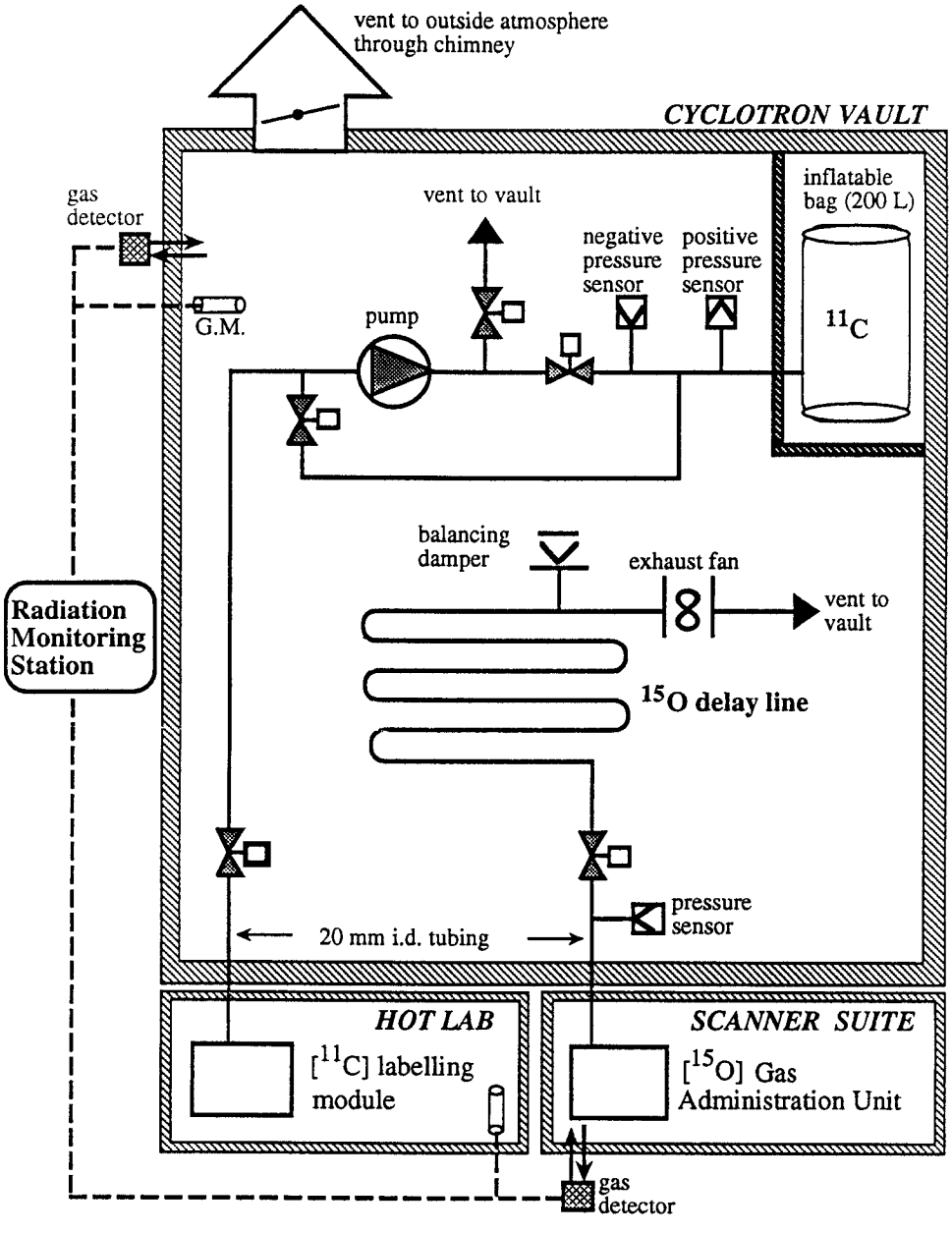

fig 1. Austin Hospital PET Centre Radioactive Waste Gas Monitoring and Disposal System.

Considerations Necessary For Determining Radiation Dosimetry of Positron Emitting Radiopharmaceuticals.

S.W. SCHWARZ, J.O. EICHLING, M.J. WELCH. Mallinckrodt Institute of Radiology, Washington University School of Medicine, St. Louis, MO 63110.

Prior to the human use of all new positron emitting radiopharmaceuticals, calculations of absorbed doses are necessary to evaluate the risks involved in administration of the radiopharmaceuticals to humans. Although the legal requirements may vary from country to country, these calculations necessitate biologic distribution data. The use of radiopharmaceuticals labeled with positron emitting radionuclides in humans involve unique difficulties in determining organ cummulative activities for very short, to short half-life nuclides. In this paper various approaches for determining radiation absorbed dose for positron emitting radionuclides will be discussed.

Traditional asssumptions made in the calculation of internal radiation doses involving longer lived radionuclides are often not accurate when used to calculate absorbed dose due to short-lived isotopes, typically resulting in higher absorbed dose estimates. The use of these conservative estimates is acceptable prior to initiation of clinical trials, since estimated doses can subsequently be refined by analysis of the human imaging and *in vivo* data. Our institution has been involved in development of over 25 new positron emitting radiopharmaceuticals that have proceeded to human use, and the dosimetry estimates have often been refined following human PET imaging. This abstract presents methods which have been used to determine residence times and absorbed doses for ^{68}Ga-citrate in a newborn, and ^{62}Cu-PTSM, ^{18}F-moxestrol, ^{64}Cu-MAb-1A3 and ^{15}O-H_2O in adults.

Different approaches for computing the cumulative activity were used for each radiopharmaceutical: ^{62}Cu-PTSM biodistribution was determined by sacrificing a male cynomologus monkey[1] 10 minutes post iv injection; ^{18}F-Moxestrol and ^{64}Cu-MAb-1A3 biodistributions were determined using Sprague Dawley rats and the data was applied to humans; ^{68}Ga-citrate was assumed to be distributed uniformly within the vascular space of the child after iv injection as ^{68}Ga-citrate. The distribution was calculated mathematically based on the systemic blood in various organs. The cumulative-activity for ^{15}O-water administered by iv bolus injection was calculated using the compartmental model used by Powers[2] for the newborn and was adapted to the 70 kg standard man.[3] Most of the absorbed doses were calculated using the MIRD (Medical Internal Radiation Dose) system. S-factors (absorbed dose per unit cumulated activity) not specified in MIRD Pamphlet 11[4] were calculated independently. Data from several sources were used in these calculations[5,6,7,8]. Limitations of each of these techniques will be discussed.

Following initial human imaging with PET, time-activity curves can be obtained and dosimetry may be refined. Table 1 shows summary data of critical organs for radiopharmaceuticals listed above. It is interesting to note that for ^{62}Cu-PTSM, analysis of human PET imaging data resulted in a kidney self dose of 1.15E-05Gy/MBq and a liver self dose of 1.81E-05 Gy/MBq which is 15% and 50% respectively, of the dose estimated from the animal data.

Dosimetry calculations are essential for each useful radiopharmaceutical developed. We have

Dosimetry calculations are essential for each useful radiopharmaceutical developed. We have shown several approaches which can be used to generate this data.

Radiopharmaceutical	**Primary Critical Organ**	**Estimated Dose Gy/MBq**
^{62}Cu-PTSM	Kidney	7.30E-05
^{18}F-Moxestrol	U.L.Intestine	2.49E-04
^{64}Cu-MAb-1A3	L.L.Intestine	1.4E-04
^{68}Ga-Citrate 2 kg. Infant	Spleen	1.7E-06
^{15}O-Water Adults (iv bolus)	Lungs	2.19E-06

This work has been supported by DOE Grant Number DE-FG-02-87ER60512, NIH Grant Number CA48286, and NIH Grant Number HL13851.

1. Green M.H., Klippenstein D.L., Tennison J.R. *J Nucl Med* 29:1548 (1988).
2. Powers W.J., Stabin M, Howse D, Eichling J.O. *J Nucl Med* 29:1961 (1988).
3. Eichling J.0. Unpublished data.
4. NM/*MIRD* Pamphlet 11. Society of Nuclear Medicine, N.Y., 1975.
5. NM/MIRD Pamphlet 3. Society of Nuclear Medicine, N.Y., 1967.
6. Coffey J., Watson E. HHS Publication FDA 81-8166, 1981.
7. Eckerman K., Christy M., Warner G.G. HHS Publication FDA 81-8166, 1981
8. NM/*MIRD* Pamphlet 5. Society of Nuclear Medicine, N.Y., 1969.

Quality control of purified ^{18}O target water using ^{31}P-NMR.

HULST[2], R., SIERTSEMA[1], H., FRANSSEN[1], E.J.F, ELSINGA[1], P.H., FERINGA[2], B.L., VISSER[1], G.M. and VAALBURG[1], W. [1]PET-Center, University Hospital, P,O. Box 30.001, 9700 RB Groningen, the Netherlands. [2]Department of Organic Chemistry, University of Groningen.

The enrichment of $H_2{}^{18}O$ is an important quality control aspect to assure a reliable ^{18}F-fluoride production for clinical purposes. Since $H_2{}^{18}O$ is scarce and expensive, PET-centers are forced to re-use their ^{18}O-enriched water. After irradiation, $H_2{}^{18}O$ can be recycled following the method of Mangner et al. (1). The purification steps include photochemical combustion, followed by fractional distillation. For a regular and rapid check of the degree of ^{18}O-enrichment of our target water, we have developed a ^{31}P-NMR method. This method is based on (i) the chemical derivatization of $H_2{}^{18}O$ into a phosphorinane system (Fig. 1) and (ii) the chemical shift dispersion of ^{31}P-NMR signals (δ 0,047 ppm) to higher field (2).

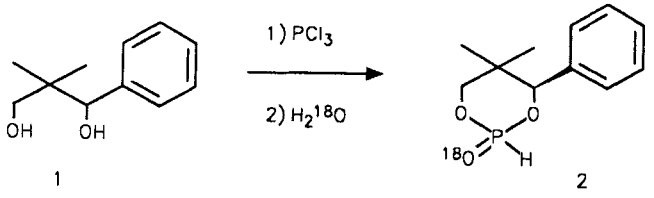

1 2

Fig. 1 The derivatization of $H_2{}^{18}O$ into a phosphorinane structure.

A solution of 0.073 g (0.45 mmol) diol 1 is cooled to 0 °C. Over a 15 min period, 0.061 g (0.45 mmol). PCl_3 is added carefully. The solution is stirred at room temperature for 1 h. Subsequently, 10 μl $H_2{}^{18}O$ is slowly added to the mixture and stirred for 10 min. Evaporation of the solvent yields an oil (compound **2**). A ^{31}P-NMR spectrum of the compound is recorded and the degree of ^{18}O-enrichment is calculated as the ratio of the integrated peaks at δ 3.458 ppm (unlabeled **2**) and δ 3.412 ppm (labeled **2**). A typical example is given in Fig. 2.

A linear calibration curve was obtained, using water samples with known ^{18}O-contents (100%= 95.3 % ^{18}O-enrichment). R^2 was > 0.999. The variation coefficient was estimated to be < 2 %. (Fig. 3). The degree of enrichment of re-used $H_2{}^{18}O$ batches were: 93 % (unpurified), 94 % (recycled and photochemical combustion) and 95 % (recycled, photochemical combustion and fractional distillation).
It was concluded that ^{31}P-NMR of derivatized $H_2{}^{18}O$ affords a rapid, cheap and accurate method to assess the enrichment of $H_2{}^{18}O$. Consequently, it contributes to the validation of recycling and purification methods of $H_2{}^{18}O$.

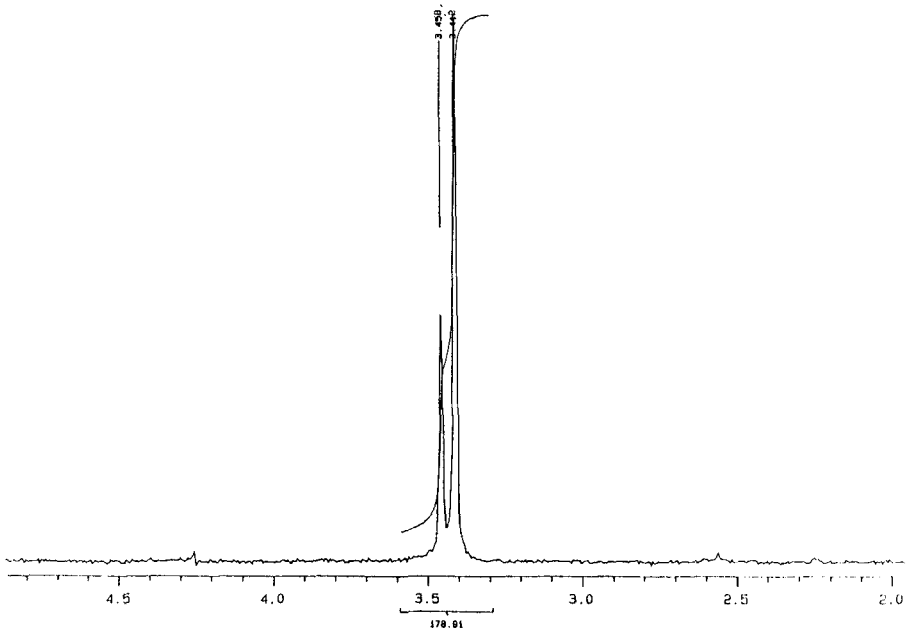

Fig. 2. ^{31}*P-NMR spectrum containing unlabeled 2 (δ 3.458 ppm) and labeled 2 (δ 3.412 ppm). The calculated enrichment was 69.4 %.*

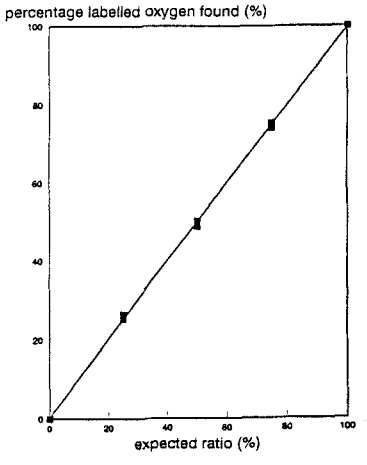

Fig. 3. Percentage labelled oxygen found versus ratio expected.

References

1) Mangner, T.J., Mulholland et al. J. Nucl. Med. 33, 982, (1992).
2) Cohn, M., Hu, A. J. Am. Chem. Soc. 102, 913, (1980).